ABSTRACT

The shell $\delta^{18}O$ of young modern *Aequipecten opercularis* from the southern North Sea provides an essentially faithful record of seasonal variation in seafloor temperature. In this well-mixed setting, *A. opercularis* shell $\delta^{18}O$ also serves as a proxy for seasonal variation in surface temperature. Individuals from less agitated (e.g. deeper) settings in a warm climate would not be expected to record the full seasonal range in surface temperature because of thermal stratification in summer. Such circumstances have been invoked to explain cool isotopic summer temperatures from early Pliocene *A. opercularis* of eastern England. Support for a sub-thermocline setting derives from high-amplitude variation in microgrowth-increment size, which resembles the pattern in sub-thermocline *A. opercularis* from the southern Mediterranean Sea. Here, we present isotope and increment profiles from further sub-thermocline individuals, live-collected from a location in the Adriatic Sea for which we provide modelled values of expected shell $\delta^{18}O$. We also present data from supra-thermocline shells from the English Channel and French Mediterranean coast. The great majority of sub-thermocline *A. opercularis* show high-amplitude variation in increment size, and winter and summer $\delta^{18}O$ values are generally quite close to expectation. However, the relatively warm summer conditions of 2015 are not recorded, in most cases ~~probably~~ due to a break in growth, perhaps caused by hypoxia. The supra-thermocline shells show subdued increment variation and yield isotopic winter and summer temperatures quite close to the local directly measured values. *A. opercularis* shells therefore provide a fairly good isotopic record of ambient temperature (if not always of relatively warm summer conditions below the thermocline) and their hydrographic setting can be determined from increment data. Early Pliocene examples from eastern England can be interpreted as having lived in a setting below the thermocline, with a higher seasonal range in surface temperature than now in the adjacent southern North Sea.

1. Introduction

The $\delta^{18}O$ of skeletal $CaCO_3$ (calcite and aragonite) is very widely used as a proxy for the temperature of the ambient environment; in particular, the $\delta^{18}O$ of marine mollusc shells is used as an indicator of seawater temperature (e.g. Schöne and Surge, 2005; Schöne and Gillikin, 2013; Prendergast et al., 2017; Gillikin et al. 2109). The values obtained are often presented as if they reflect sea-surface temperature, a datum of great interest to climatologists and palaeoclimatologists, but those derived from benthic taxa such as bivalves are of course a record of seafloor temperature (with the additional influence of water $\delta^{18}O$, which must be measured or estimated to enable calculation of temperature from shell $\delta^{18}O$). In agitated settings (where the seafloor is above the fair-weather wave-base, or to somewhat greater depths where tidal currents are strong) stirring of the water is usually sufficient for seafloor temperature to be very similar to surface temperature (Fig. 1A). However, in quieter settings (e.g. at depths below the fair-weather wave-base, in situations where tidal currents are weak), and at latitudes where solar irradiation is significant (i.e. outside the polar regions), seafloor temperature often departs radically from surface temperature in summer (Fig. 1B). This is because the lack of agitation and the lower density of warmed water allows heat to become 'ponded' in a shallow surface layer (commonly extending to 25–30 m in weakly tidal shelf settings), separated from much cooler, deeper waters by a zone of steep temperature change, the thermocline. In the mid-latitudes, where there is significant seasonal variation in insolation, this stratification typically breaks down in autumn because of surface cooling, often aided by storm activity, beginning an equalisation of temperature (Fig. 1B). By the winter months, seafloor temperature is usually about the same as at the surface, to at least mid-shelf depths (e.g. Arthur et al., 1983; Elliott and Li, 1991). Shelf bivalves living below the summer thermocline ('sub-thermocline' individuals) therefore in many cases experience temperatures that are similar to those at the surface in winter (the coldest temperatures

occurring at the same time: February/March in the Northern Hemisphere) but experience temperatures that are cooler than those at the surface in summer (the peak temperature at the surface typically occurring during August/September and the lower peak temperature on the seafloor during October/November in the Northern Hemisphere). Sequential sampling of sub-thermocline shells at high temporal resolution through ontogeny (isotope sclerochronology) will provide $\delta^{18}O$ values corresponding to the ~~coolest~~ coldest winter surface temperature but will not yield values corresponding to the warmest summer surface temperature: this temperature will only be directly recoverable from 'supra-thermocline' individuals (i.e. those that lived above the depth of the summer thermocline).

Fig. 1 about here – double column

Sub-thermocline shells can still be a source of information on summer surface temperature: we can project a likely summer surface value by taking account of the ~~seafloor-surface temperature~~ difference between the maximum seafloor and surface temperature in modern stratified situations. This difference is variable (see Section 2) so sub-thermocline shells can only supply a rough indication of summer surface temperature, and before we add a 'stratification factor' to the warmest $\delta^{18}O$-derived temperature from an individual, we must be sure that it lived in a sub-thermocline setting. Schöne and Fiebig (2009) claimed that sub-thermocline forms of the long-lived bivalve *Arctica islandica* ~~were~~ are recognizable from a saw-tooth $\delta^{18}O$ profile (contrasting with a sinusoidal profile in supra-thermocline shells), but this pattern is ~~shown by~~ also observed in an undoubtedly supra-thermocline individual (6 m depth) from south-west Scotland (Foster et al., 2009). Seafloor temperature variation can be sinusoidal in sub-thermocline settings (Fig. 1B) so under those circumstances the shells of bivalve species which grow throughout the year (e.g. many examples of the short-lived Queen Scallop, *Aequipecten opercularis*, in

100 their first year; Hickson et al. 2000) would provide $\delta^{18}O$ profiles of the same form as supra-thermocline
101 individuals.
102
103 Fig. 2 about here – single column
104
105 Using ~~On the basis of~~ data from modern *Spisula solidissima*, Arthur et al. (1983) suggested that
106 sub- and supra-thermocline bivalves might be distinguishable on the basis of patterns of covariation
107 between $\delta^{13}C$ and $\delta^{18}O$: positive covariation (i.e. in-phase ontogenetic profiles) in the former and
108 negative covariation (i.e. antiphase ontogenetic profiles) in the latter. This notion is superficially
109 appealing because the $\delta^{13}C$ of dissolved inorganic carbon (DIC) increases over spring and summer at
110 shallow depths due to the preferential uptake of ^{12}C by photosynthesizers, and then progressively
111 decreases over the rest of the year, in part as a result of respiratory return of isotopically light carbon
112 to the DIC pool and low photosynthetic uptake (Lorrain et al., 2004). Thus a supra-thermocline
113 bivalve inheriting its shell carbon from DIC would show a pattern of seasonal variation in $\delta^{13}C$
114 opposite to that in $\delta^{18}O$ ~~(low in summer and high in winter because of the inverse correlation between~~
115 ~~shell $\delta^{18}O$ and temperature)~~. By contrast, a sub-thermocline bivalve might be expected to show
116 parallel variation of $\delta^{13}C$ and $\delta^{18}O$ because DIC with a high $\delta^{13}C$ would only be available to it
117 following ~~because of the delayed impact of near-surface photosynthesis, DIC with a high $\delta^{13}C$ only~~
118 ~~being mixed down to the seafloor following~~ the autumn breakdown of stratification and mixing down
119 of surface waters. The problem with this model is that some of the carbon in a bivalve's shell derives
120 from its food (particulate organic carbon), which, being isotopically light (the direct or indirect result
121 of photosynthesis) and typically abundant at shallow depths during summer as a consequence of high
122 primary production, might be expected to cause low shell $\delta^{13}C$ in supra-thermocline individuals
123 during that season (Chauvaud et al., 2011). Low summer $\delta^{13}C$ values have indeed been documented
124 from shallow-water *Pecten maximus* (Chauvaud et al., 2011), contrasting with the data of Arthur et al.

(1983) from shallow-water *S. solidissima* but matching results from other shallow-water examples of *S. soldissima* ~~this species~~ (Krantz et al., 1987, figs 4, 5). Whether the summer $\delta^{13}C$ reduction seen in deeper water (sub-thermocline) *S. solidissima* (Arthur et al., 1983) and also *Placopecten magellanicus* (Krantz et al., 1987, figs 6–9) is due to high incorporation of food-derived carbon into the shell remains unclear (at depth, food availability might be no greater in summer than winter, although feeding rate would probably be higher; cf. Ren et al., 2000). However, whatever the cause, the foregoing examples indicate that summer reduction in shell $\delta^{13}C$ is not limited to sub-thermocline settings. The notion that sub- and supra-thermocline bivalves can be distinguished on the basis of patterns of $\delta^{13}C$ variation in relation to $\delta^{18}O$ is also refuted by data from *A. opercularis*. Modern examples from each setting (Fig. 2A, B) show patterns that are opposite to those recorded by Arthur et al. (1983) from *S. solidissima*, and some early Pliocene specimens of *A. opercularis* simply show a general ontogenetic decline in $\delta^{13}C$ (Fig. 2C).

Fig. 3 about here – double column

Included in Figure 2 are profiles of variation in the size (anatomical height) of microgrowth increments (Fig. 3). Smoothed (5-point average) data from the modern supra-thermocline shell (from the southern North Sea) exhibit a slight long-term fluctuation (broadly seasonal from the rough correspondence to the pattern of seasonal change in $\delta^{18}O$) superimposed on high frequency/low amplitude variation~~, whereas~~. In contrast the modern sub-thermocline shell (from the Gulf of Tunis, southern Mediterranean Sea) shows a much more pronounced long-term fluctuation, and the early Pliocene shell (from the Ramsholt Member, Coralline Crag Formation, Suffolk, eastern England) an essentially identical pattern. Investigation of 18 other *A. opercularis* from the eastern margin of the North Atlantic (including North Sea) revealed limited increment variation in all nine from definitely supra-thermocline settings, as evidenced by a macrotidal regime (hence strong tidal currents) or a

depth of less than 25 m (Johnson et al., 2009, tables 1, 2). ~~All other definite and probable supra-thermocline *A. opercularis* shells investigated to date from the eastern margin of the North Atlantic Ocean, including the North Sea (a further 18 specimens; Johnson et al., 2009), show only slight variation in microgrowth-increment size.~~ By contrast, two of four other investigated sub-thermocline shells from the Gulf of Tunis exhibit pronounced variation (> 0.3 mm between the minimum and maximum of smoothed profiles), as do four of seven other Ramsholt-Member shells (Johnson et al., 2009; Vignols et al., 2019). A sub-thermocline situation for Ramsholt-Member shells is supported by a variety of palaeontological and sedimentological evidence (Johnson et al., 2009), and the modest fluctuations seen in Ramsholt-Member $\delta^{18}O$ profiles (e.g. Fig. 2C) and quite low (cool temperate) peak temperatures calculated from these (contrasting with the warm temperate summer values indicated by the pelagic dinoflagellate assemblage; Head, 1997, 1998) are consistent with this setting (Johnson et al., 2009; Vignols et al., 2019). It cannot be denied, however, that the evidence for hydrographic control of increment-size variation in modern *A. opercularis* is only circumstantial, and that the $\delta^{18}O$ data from the Ramsholt Member could (if from supra-thermocline shells) reflect a low seasonality climate with cool summers. While such an interpretation would be radically at odds with almost all other evidence (Johnson et al., 2009; Vignols et al., 2019), it deserves consideration through further investigation of increment patterns in modern *A. opercularis* in relation to hydrographic setting, and of the closeness of shell $\delta^{18}O$ values to expected values. To this end we studied six further sub-thermocline shells live-collected for the purpose from another location in the Mediterranean Sea (northern Adriatic Sea, Croatia), temporally aligning shell $\delta^{18}O$ values as well as possible with a profile of predicted daily values derived for this location using the extensively validated Regional Ocean Modeling System (ROMS; Janeković et al., 2010, 2014; Vilibić et al., 2016) and a local water $\delta^{18}O$-salinity relationship (Peharda et al., 2019). We also supplemented the already quite large supra-thermocline database with information from two shells collected in the English Channel near Brighton, UK, an area from which data had not previously been obtained. In addition, we acquired

175 isotope data from two probably supra-thermocline shells collected from the shore of the
176 Mediterranean Sea at La Franqui, France. One of these had previously supplied increment data
177 consistent with a supra-thermocline setting but the other (remeasured here) had yielded an anomalous
178 (i.e. sub-thermocline) increment pattern. Since the precise location, depth and time of life of the
179 English Channel and French Mediterranean individuals (museum specimens) was not known, we did
180 not derive profiles of predicted shell $\delta^{18}O$ for comparison with measured values. Instead, we
181 calculated summer and winter temperatures from the latter and compared these with mean seasonal
182 temperatures at each location from direct monitoring.
183
184 Fig. 4 about here – single column
185
186 **2. Material and settings**
187
188 The general provenance of the Adriatic, English Channel and French Mediterranean shells (and
189 those represented in Fig. 2) is illustrated in Figure 4; details of sample locations are supplied below
190 and in Table 1.
191 The Adriatic shells are all left valves: S3A1, S3A3–5, S3A33 and S3A36 = University of Derby,
192 Geological Collections (UD) 53417–53422, respectively. They are amongst the largest (47–51 mm
193 shell height) from a sample of 54 individuals (27–53 mm height; uninvestigated specimens
194 accessioned as UD 53423) live-collected with a dredge on 13th September 2016 by commercial
195 fishermen at 38 m depth in fishing zone A3, 3.5 nautical miles from Pula, Croatia. Specimens were
196 disarticulated and eviscerated shortly after collection. Valves were then matched and inscribed with a
197 code-number (S3A1–54; same for right and left valve of a pair) before dry storage. We chose left
198 valves for investigation because microgrowth increments are usually measurable over a greater range
199 of shell height; the right valve, which lies against the substrate in life, can become significantly

abraded, obscuring increment boundaries. ROMS-derived profiles of daily temperature for the surface and 38 m at the collection location show that the shells are unquestionably from a setting with summer thermal stratification, annual peak temperatures at 38 m being 3.2–9.9°C (mean 7.7°C) below those at the surface over the period 2008–2016 (Fig. 5A). This is a reflection of high heat flux and limited wave-mixing in summer, with tidal current velocities < 0.15 m s^{-1} (Chavanne et al., 2007); geostrophic currents are similarly weak (Djakovac et al., 2015). Surface temperatures are within the warm temperate range (winter > 10°C, summer > 20°C; Vignols et al., 2019).

Fig. 5 about here – single column

The English Channel shells are also left valves: EC1 and EC2 = Natural History Museum, London (NHMUK) 20190467/1 and 20190467/2, respectively. They are examples of similar size (53 and 52 mm height, respectively) to the Adriatic shells, selected from a sample originally formed of seven articulated individuals and five single valves (42–58 mm shell height; uninvestigated specimens accessioned as NHMUK 20190467) collected 'off Brighton' (south coast of the UK) on an unspecified date in 1923 and stored dry (without soft-parts). EC2 still had the right valve attached and EC1 could be matched with a right valve of the same size, so both the individuals concerned were probably alive at or not long before the time of collection. Since water depth is less than 20 m to 10 km offshore from Brighton and the surface velocity of tidal currents in the area exceeds 0.5 m s^{-1} at spring tides (VisitMyHarbour, 2012), it can be confidently assumed that the shells derive from a location where the annual peak temperatures at the seafloor and surface are (and were in the early 20th century) much the same—i.e. a setting without summer stratification. Mean seasonal extreme surface temperatures at Brighton are 8.0°C for winter and 17.4°C for summer (Global Sea Temperature, 2020)—i.e. within the cool temperate range (winter < 10°C, summer < 20°C; Vignols et al., 2019)

224 The French Mediterranean shells are a right valve 51 mm in height and a left valve 60 mm in
225 height: FM1 and FM2 = Muséum National d'Histoire Naturelle, Paris (MNHN) IM-2008-1534 and
226 IM-2008-1535, respectively. These are two of the three single valves from La Franqui (the other a
227 right valve 53 mm in height: FM3 = MNHN-IM-2008-1533) for which increment data were supplied
228 by Johnson et al. (2009, table 2). The three specimens were part of a sample of 35 single but unbroken
229 valves (10–60 mm in height; uninvestigated specimens not given MNHN numbers) collected from the
230 beach north of La Franqui on 25th and 31st October 1987 after a storm and stored dry (without soft-
231 parts). It seems unlikely that a storm would have thrown onto the shore valves from more than a very
232 few tens of metres depth—i.e. they were probably from supra-thermocline individuals. The low
233 increment-size variation of FM1 and FM3 (respectively, 0.22 and 0.26 mm between the maximum and
234 minimum of smoothed profiles) accords with this but FM2 provided a much higher value (0.36 mm),
235 like that of sub-thermocline shells from the Gulf of Tunis (Johnson et al., 2009, table 2). Mean
236 seasonal extreme surface temperatures at La Franqui are about 12°C for winter and 23°C for summer
237 (i.e. within the warm temperate range), but while the cool extreme is the same down to 30 m, the
238 warm extreme declines gradually to about 20°C at 30 m and then somewhat more rapidly to about
239 17°C at 50 m (NOAA, 1994).
240
241 **3. Methods**
242
243 *3.1. Laboratory procedures*
244
245 Shells were coated with a sublimate of ammonium chloride and digitally photographed, then
246 images were inserted into the bespoke software Panopea© (2004, Peinl and Schöne) for the purposes
247 of increment measurement, to the extent that this could be accomplished (increments were usually
248 invisible in the umbonal area, and sometimes elsewhere, due to abrasion). The coating was washed off

with tap-water and most shells then underwent the further cleaning procedure adopted by Valentine et al. (2011) for removal of any surficial organic material prior to isotopic sampling. One Adriatic shell (S3A4) and the French Mediterranean shells were sampled before it was decided to implement this procedure. Samples for isotope analysis were obtained by drilling a dorsal to ventral series of shallow (< 1 mm deep) commarginal grooves into the outer surface of the outer (calcite) shell layer, with the sample sites more closely spaced towards the ventral margin in an attempt to maintain temporal resolution in the context of declining growth rate with age. Details of the measurement and sampling methods used, including the adjustment procedure employed where it was impossible to measure or sample along the dorso-ventral (height) axis, are given in Johnson et al. (2019) with respect to another scallop species. All the increment measurements were made by the same person (AMV) to achieve as uniform an approach as possible, given that increment identification can locally be a subjective matter. Increments are commonly difficult to define between the plicae ('ribs') on left valves (Fig. 3B, C); measurements were made on the plicae in such circumstances. Growth breaks were identified as minor, moderate or major (the last two classes subsequently combined) dependent on the size of the characteristic 'step' in the shell profile, which marks a near or total cessation of extensional growth but not of shell thickening. Minor growth breaks are subtle features (Fig. 3A, B), sometimes only observable by tilting the shell to various angles. The height of growth breaks was therefore determined on the shells themselves (with a ruler) rather than on digital images.

In cool temperate representatives of *A. opercularis*, such as those from around the UK, prominent growth breaks typically occur in winter and appear to represent intervals of a month or two (e.g. Broom and Mason, 1978). However, in other scallop species they may occur at any time of year (e.g. Johnson et al., 2019), presumably reflecting disturbance in some cases, and intervals approaching six months may be represented (Krantz et al., 1984). No assumptions can therefore be made about the timing or duration of growth breaks in warm temperate *A. opercularis*, such as Adriatic individuals, to guide general alignment of shell $\delta^{18}O$ values with predicted values. However, from isotopic evidence

of growth slowdown or cessation for several summer months in Adriatic *Pecten jacobaeus*, and of the same for several winter months in Adriatic *Glycymeris pilosa* (Peharda et al., 2019), it is reasonable to expect some attenuation of growth in Adriatic *A. opercularis* during one or both seasons, and to use evidence of this in the form of growth breaks to refine alignments based on identification of annual $\delta^{18}O$ cycles (see Section 3.2).

Table 1 about here - ? single column

Stable oxygen and carbon isotope analysis (given as $\delta^{18}O$ and $\delta^{13}C$) were carried out either at the stable isotope facility, British Geological Survey, Keyworth, UK, or at the Institute of Geosciences, University of Mainz, Germany. At Keyworth samples were analysed using an Isoprime dual inlet mass spectrometer coupled to a Multiprep system; powder samples were dissolved with concentrated phosphoric acid in borosilicate Wheaton vials at 90°C. At Mainz samples were analysed using a Thermo Finnigan MAT 253 continuous flow-isotope ratio mass spectrometer coupled to a Gasbench II; powder samples were dissolved with water-free phosphoric acid in helium-flushed borosilicate exetainers at 72°C. Both laboratories calculated $\delta^{13}C$ and $\delta^{18}O$ against VPDB and calibrated data against NBS-19 (preferred values: +1.95‰ for $\delta^{13}C$, –2.20‰ for $\delta^{18}O$) and their own Carrara Marble standard (Keyworth: +2.00‰ for $\delta^{13}C$, –1.73‰ for $\delta^{18}O$; Mainz: +2.01‰ for $\delta^{13}C$, –1.91‰ for $\delta^{18}O$). Values were consistently within ± 0.05‰ of the values for $\delta^{18}O$ and $\delta^{13}C$ in NBS-19. Reproducibility was checked by duplicate analysis of some samples, and in the case of seemingly aberrant initial results, repeat sampling and analysis was undertaken. The profiles in Figures 7–9 link singleton values and the means of multiple values. In two cases where results from repeat analysis differed greatly (S3A5, height 46.5 mm; EC2, height 16.5 mm) the more credible data have been used for the profiles and suspect data omitted. Otherwise, all the isotope results obtained are plotted in Figures 7–9.

The full set of raw isotope and increment data, together with modelled values of temperature, salinity and expected shell $\delta^{18}O$ (Section 3.2), is available online (see Appendix A). A summary of the isotope data is provided in Table 1.

3.2. Calculations of temperature and expected shell $\delta^{18}O$

In earlier isotope studies of modern and fossil *A. opercularis* (Hickson et al., 1999, 2000; Johnson et al., 2000, 2009; Valentine et al., 2011; Vignols et al., 2019) the calcite equation of O'Neil et al. (1969) was used to calculate temperatures from shell $\delta^{18}O$ or to calculate expected shell $\delta^{18}O$ values from known temperatures, in each case with an adjustment (most recently –0.27‰, following Gonfiantini et al., 1995) to convert water $\delta^{18}O$ values from the VSMOW scale to the VPDB scale used for calcite. In isotope work on *P. jacobaeus* from the northern Adriatic, Peharda et al. (2019) used the more recent calcite equation of Kim and O'Neil (1997), also widely employed in studies of other calcitic taxa. The equation of Kim and O'Neil (1997) yields temperatures about 2°C lower than that of O'Neil et al. (1969) so the choice of equation is a significant matter. Other calcite equations exist, one of which—the LL (low light) equation of Bemis et al. (1998)—was used by Austin et al. (2006, fig. 6) to derive expected values for calcite $\delta^{18}O$ over a year from monthly data on bottom temperature and water $\delta^{18}O$ for the same latitude (53°N) in the southern North Sea as the *A. opercularis* shell represented in Figure 2A. We used the data of Austin et al. (2006) to also derive expected values of shell $\delta^{18}O$ using the equations of O'Neil et al. (1969) and Kim and O'Neil (1997), and then replicated the three sets of values to produce multi-year profiles (Fig. 6) for comparison with the data from the southern North Sea *A. opercularis* specimen. The most suitable equation was judged by temporally aligning the shell data as well as possible with each profile (i.e. minimising the overall difference between measured and expected shell values within a three-year period, as specified by the number of $\delta^{18}O$ cycles), and then reviewing the closeness of each fit. During early ontogeny, growth of *A.*

323 *opercularis* may be rapid and continuous through summer and winter in the southern North Sea
324 (Johnson et al., 2009). From the long 'wavelength' of the first $\delta^{18}O$ cycle (measured versus shell
325 height) and the absence of visible growth breaks associated with the lowest and highest values (Fig.
326 2A), it is evident that the present specimen did grow rapidly and without interruption during early
327 ontogeny. The most extreme $\delta^{18}O$ values measured over the first cycle can therefore be taken to
328 represent the most extreme temperatures experienced, and the equation yielding predicted $\delta^{18}O$ values
329 closest to those measured can be regarded as the best descriptor of the relationship between
330 temperature and shell $\delta^{18}O$. The LL equation of Bemis et al (1998) provides the closest values (Fig.
331 6), the equation of Kim and O'Neil (1997) yielding values that are somewhat lower than the lowest
332 measured value from the first summer and the equation of O'Neil et al. (1969) yielding values that are
333 somewhat higher than the highest measured value from the first winter. For this reason we used the
334 LL equation of Bemis et al. (1998) to derive expected values of shell $\delta^{18}O$ and to calculate
335 temperatures from the other *A. opercularis* shells investigated herein.
336
337 Fig. 6 about here – single column
338
339 ROMS-derived daily salinity values (Fig. 5B) and the salinity-water $\delta^{18}O$ relationship established
340 by Peharda et al. (2019) for adjacent sites were used to calculate daily water $\delta^{18}O$ values (Fig. 5B) for
341 the location and depth of the Adriatic shells. These values and the modelled daily seafloor
342 temperatures (Fig. 5A) were then used in the equation of Bemis et al. (1998) to calculate values of
343 expected shell $\delta^{18}O$ (Fig. 5C) for comparison with data from *A. opercularis*. This mirrors the approach
344 of Peharda et al. (2019) for other locations and depths in the northern Adriatic, except that they
345 employed the equation of Kim and O'Neil (1997) to derive expected values of shell $\delta^{18}O$ for
346 comparison with data from *P. jacobaeus*.

In view of the inadequate contextual information we did not attempt to derive expected daily values of shell $\delta^{18}O$ for comparison with data from the French Mediterranean and English Channel shells. Instead we compared local summer and winter temperatures (Section 2) with the warmest and coolest temperatures calculated from shell $\delta^{18}O$, using the LL equation of Bemis et al. (1998) and a representative single value of water $\delta^{18}O$ from measurements made nearby: +1.3‰ for La Franqui based on measurements at 4–25 m depth in the north-western Mediterranean (site 1B of Pierre, 1990); +0.2‰ for the English Channel near Brighton based on measurements in the North Sea (Mook and Vogel, 1968).

4. Results

4.1. Adriatic shells (Fig. 7)

Fig. 7 about here – double column

All $\delta^{18}O$ profiles show between one and two major cycles, the amplitude and (in most cases) wavelength ~~(in terms of shell height) and amplitude~~ decreasing in the second cycle, where present. By contrast, $\delta^{13}C$ profiles show little variation, values tending to decrease slightly over the course of ontogeny (e.g. Fig. 7F) and occasionally increasing over short intervals in association with decreasing $\delta^{18}O$ (Fig. 7C, E), but otherwise showing no relation to this parameter. In that the isotope data from S3A4 (Fig. 7C) are closely comparable with those from other shells, it appears that omission of the procedure to remove surficial organic material from the shell had little or no effect (cf. Schöne et al., 2017). In all cases apart from S3A1 (Fig. 7A) the smoothed increment profiles exhibit one more-or-less clear major cycle, with a difference of more than 0.30 mm between the maximum and minimum values. The absence of such features from the S3A1 profile could be because it is the shortest of the

six. Amongst the five individuals showing marked variation in increment size, the maximum size is ~~shown~~ observed in mid-ontogeny, and occurs in an interval of decreasing or low $\delta^{18}O$ in four specimens (S3A3, S3A4, S3A5, S3A33) and of increasing $\delta^{18}O$ in one (S3A36). The minimum size is shown in early or late ontogeny and occurs in an interval of decreasing or low $\delta^{18}O$ in four specimens (S3A3, S3A4, S3A5, S3A36) and of high $\delta^{18}O$ in one (S3A33). Growth breaks are concentrated in late ontogeny and are commonly associated with the highest and lowest ~~values of~~ $\delta^{18}O$ values in this interval. Figure 3B illustrates growth breaks and the pattern and scale of increment variation in S3A4.

4.2. English Channel shells (Fig. 8)

Fig. 8 about here – double column

Both the $\delta^{18}O$ and $\delta^{13}C$ profiles of the English Channel shells are very similar in their general features to those from the (similarly sized) Adriatic shells. However, the $\delta^{18}O$ profiles of the former differ by including lower values and the $\delta^{13}C$ profiles by their consistently higher values at all stages of ontogeny (see also Fig. 11), with instances of positive (rather than negative) correlation with $\delta^{18}O$ (early ontogeny of EC1—Fig. 8A; late ontogeny of EC2—Fig. 8B). Smoothed increment profiles show a much smaller range of variation (well below 0.30 mm) than is seen in most Adriatic shells. Minimum values are much the same as in Adriatic shells but maximum values are less than ~~from most of these~~ in most Adriatic shells. Growth breaks are concentrated in late ontogeny; examples are associated with the $\delta^{18}O$ maxima (but not with the minima) in this interval in the two shells~~, and in some cases associated with the highest $\delta^{18}O$ values in this interval but not with the lowest~~. Figure 3C illustrates the subdued increment variation in EC1.

4.3. French Mediterranean shells (Fig. 9)

Fig. 9 about here – double column

The $\delta^{18}O$ profiles are again very similar in their general features to profiles from Adriatic shells, spanning also a comparable range of values. However, in FM1, in which 1.5 cycles are identifiable, the amplitude (and wavelength) is greater in the second (incomplete) cycle~~, but with the second cycle extending to lower values than the first and also (at least in FM1) occupying a larger height interval~~. The $\delta^{13}C$ profiles are also quite similar in their general features to those from Adriatic shells, but with higher values at most stages of ontogeny (although not generally as high as from English Channel shells; see also Fig. 11) and instances of positive correlation with $\delta^{18}O$ (mid-ontogeny of FM1—Fig. 9A; late ontogeny of FM2—Fig. 9B), although there are also some intervals of negative correlation in FM1. In view of the evidence from Adriatic shell S3A4 it may be assumed that omission of the procedure to remove surficial organic material had no effect on the isotope data from the French Mediterranean shells. The smoothed increment profiles show variation of less than 0.30 mm (remeasurement of FM2 revealed that the anomalously high variation recorded previously was down to a single, very inaccurate value in the raw data). As in the English Channel shells, minimum ~~values~~ increment sizes are much like those from Adriatic shells and maximum ~~values~~ sizes are less than from ~~most of the latter~~ most Adriatic shells. Growth breaks are more frequent in early ontogeny than in the Adriatic and English Channel shells; examples are associated with the $\delta^{18}O$ maxima (but not with the minima) in the two shells ~~some are associated with the highest values of $\delta^{18}O$ but none with the lowest~~.

5. Interpretation

5.1. $\delta^{18}O$ data

The number of $\delta^{18}O$ cycles (one to two) in the profiles illustrated in Figures 7–9 is the same as in most profiles up to the same shell height from other modern (and fossil) *A. opercularis* (Hickson et al., 1999, 2000; Heilmayer et al., 2004; Johnson et al., 2009; Valentine et al., 2011; Vignols et al., 2019). Taking the cycles essentially to reflect seasonal variation in water temperature (cf. Section 3.2), and their generally declining wavelength to reflect declining growth rate, the implied ages and rates of growth-rate decline are consistent with growth statistics for *A. opercularis* obtained by other means (e.g. Taylor and Venn, 1978; Richardson et al., 1982; Heilmayer et al., 2004). It is thus clear that none of the shells were more than three years old. In the case of the Adriatic specimens, we can use this information to guide temporal alignment of measured $\delta^{18}O$ values with predicted values, following the same approach as for the southern North Sea specimen discussed in Section 3.2. We consider details of the alignment of Adriatic data immediately below, proceeding to evaluate the extent to which shell $\delta^{18}O$ profiles from this area reflect ambient temperature. We then discuss $\delta^{18}O$-derived temperatures from English Channel and French Mediterranean shells in more general terms—i.e. the fidelity of summer and winter values to mean seasonal temperatures.

Fig. 10 about here - double column

5.1.1. Adriatic shells

Figure 10 shows predicted shell $\delta^{18}O$ for a period spanning the lives of the Adriatic shells (i.e. from late 2016 as far back as 2013), accompanied by aligned measured values from each shell. It has been assumed that growth breaks adjacent to the locations of maxima and minima in measured values relate to extreme winter and summer temperatures—i.e. the maximum/minimum $\delta^{18}O$ values concerned have been positioned so that the adjacent growth break includes the time of inflection in the curve of predicted values (cf. Section 3.1).

447 General positioning of values (i.e. assignment to years) was largely unproblematic except in the
448 case of S3A1, where two significantly different 'solutions' emerged: one with most values assigned to
449 2015, and another with most values assigned to 2014. The latter achieves an alignment that is slightly
450 more precise overall but leaves a gap of 188 days in summer 2015. Unlike the similarly long gaps in
451 summer 2015 in S3A4 (187 days) and S3A36 (174 days) there is no growth break to explain this gap
452 so the former alignment (which leaves a gap of 49 days, unaccompanied by a growth break, in
453 summer 2015) has been used in Figure 10A. Adoption of the alternative alignment for S3A1 would
454 not have affected the argument below. The long gaps (> 100 days; identified by grey bars) in other
455 records are unavoidable; alternative arrangements to reduce them result in larger, inexplicable gaps
456 elsewhere. Some of them are associated with growth breaks but not the winter 2014 gaps in S3A5 and
457 S3A36, and the gaps from spring (or even late winter) 2016 to the date of collection shown by all
458 shells except S3A1 (in which there is nevertheless a shorter gap). The winter 2014 gaps relate to the
459 abraded umbonal areas of the shells concerned, where it was impossible to obtain growth-increment
460 data, and evidence of growth breaks may ~~also~~ therefore have been lost. The 2016 gaps probably reflect
461 the culmination of ontogenetic decline in growth rate, with the last sample from each shell (taken at or
462 very close to the shell edge) including a significant amount of material deposited early in the year. The
463 long gaps can therefore be explained by time-averaging of sample material and provide no grounds for
464 suspecting serious misalignment—i.e. with the wrong year.
465 Multiple, similar values within a short time interval (e.g. S3A5 and S3A33, mid-summer 2015)
466 might be regarded as evidence of serious misalignment because they demand very rapid growth.
467 However, the rates required are not unreasonable. In the examples cited the height intervals between
468 the first and last values are 6.0 and 5.5 mm, respectively (Fig. 7D, E), amounts of size increase that
469 have been shown through experiment to be achievable by *A. opercularis* in a month or somewhat less
470 under warm conditions (Broom and Mason, 1978, table 2). This period is comparable to the time
471 interval of 20 days spanned in each case by the mid-summer 2015 values from S3A5 and S3A33, as

positioned in Figure 10. In S3A33 a period of 10 days in spring 2015 is represented by a series of five $\delta^{18}O$ values, which align perfectly with the plot of predicted values and cover a height interval of 9.5 mm (Fig. 7E), confirming ~~that~~ the plausibility of a size increase of 5.5 mm in 20 days during the succeeding summer ~~is entirely plausible~~.

While it appears that the $\delta^{18}O$ values from all shells have been associated with the correct year, not every value can be precisely aligned with the curve of predicted values. Small (unavoidable) discrepancies can be considered to reflect the known analytical and modelling errors. Moderate departures (< 0.5‰) from predicted values, for example in summer 2014 (S3A3, S3A4, S3A36; all negative) and winter 2016 (S3A33, S3A36; both positive), seem likely to reflect inaccuracy in the shell record of ambient conditions (i.e. non-equilibrium isotope incorporation), and are discussed further below. Large departures (> 0.5‰; open symbols) from predicted values in summer 2014 (S3A5; positive), winter 2015 (S3A3, S3A4, S3A5, S3A33; all negative) and spring 2016 (S3A1; positive) are unlikely to have this cause, given the quite close correspondence of measured to predicted values in *A. opercularis* from the southern North Sea (Fig. 6). Contamination by material from other sample positions can be ruled out because all the significantly discrepant values were checked by resampling, either at the place of the initial sample or very close by. That four shells show a confirmed, large discrepancy of the same sign in winter 2015 (and that S3A36 shows a smaller discrepancy of the same sign) suggests that the departure from expectation is a function of inaccurate modelling—i.e. that this failed to take into account some environmental event in winter 2015. While in theory the observed negative excursion could reflect a brief warming episode, a winter influx of (isotopically light) freshwater is a more plausible event. The River Po is the likeliest source, given its large supply of freshwater to the northern Adriatic in general (Vilibić et al., 2016, table 1). The confirmed, large, positive departures are difficult to account for, particularly the summer 2014 excursion in S3A5, which could exceed 1.0‰, dependent on precise timing. Being isolated instances,

these departures perhaps reflect incorporation of carbonate from some small, unnoticed encrusting organism.

Of those (moderate) departures from predicted values which seem likely to reflect non-equilibrium isotope incorporation, the largest in summer 2014 (0.31‰) is from S3A3 and the largest in winter 2016 (0.28‰) is from S3A33. The former departure translates into a temperature overestimate of 1.5°C and the latter into an underestimate of 1.3°C. While these figures give a good indication of the extent by which seasonal temperatures calculated from *A. opercularis* shell $\delta^{18}O$ might be exaggerations of the temperature extremes experienced, they do not represent amounts which can be routinely combined with isotopic summer and winter temperatures to determine actual seasonal extremes. This is because the extreme measured values of shell $\delta^{18}O$ are often not as low in summer and not as high in winter as the extreme predicted values. Thus, in addition to the large gaps referred to above, there are smaller gaps in the shell records (winter 2015 in S3A36; summer 2015 in S3A1, S3A3, S3A5 and S3A33) which omit values corresponding to the relevant predicted extremes. In the case of winter 2015 in S3A36 the discrepancy between measured and predicted extreme values is fairly small (0.29‰; equivalent to a temperature overestimate of 1.4°C). However, in the summer 2015 cases the discrepancies are substantial (largest 0.98‰ in S3A3; equivalent to a temperature underestimate of 4.7°C). In most cases there are associated growth breaks (possible environmental cause discussed in Section 5.4), so it is no surprise that the shell records are incomplete. However, the magnitude of the discrepancies with the predicted $\delta^{18}O$ extreme for summer 2015 ~~(especially low because of relatively warm conditions; Fig. 5)~~, within datasets for that season which are otherwise fairly complete, is a salutary demonstration of the potential for misinterpretation of summer temperatures from *A. opercularis* shell $\delta^{18}O$. Of the four individuals alive in summer 2014 as well as summer 2015 (S3A3, S3A4, S3A5, S3A36) only S3A5 shows a lower minimum $\delta^{18}O$ value for 2015 than for 2014, despite the predicted minimum for summer 2015 (–0.21‰) being much lower than for 2014 (+0.37‰) as a consequence of the unusually warm conditions (Fig. 5). This suggests that the

incompleteness of the summer 2015 records from these shells might be a function of their age and consequent slower growth, leading to greater time-averaging within samples (cf. Fig. 6). However, the summer 2015 records from S3A1 and S3A33, individuals which were not alive in summer 2014, are similarly incomplete. In S3A33 a growth break is associated with the lowest measured value of $\delta^{18}O$ for summer 2015, providing a hint that the individual experienced warmer temperatures than are recorded in its $\delta^{18}O$ profile. However, the discrepancy between the measured and predicted extremes (0.83‰; equivalent to a temperature underestimate of 3.9°C) is not much less than in the ontogenetically older shell S3A3 (see above), and the discrepancy in S3A1 (0.97‰; equivalent to a temperature underestimate of 4.6°C), a shell which shows no growth break in summer 2015, is very nearly the same as in S3A3. It therefore appears that neither restricting sampling to early ontogeny nor examining specimens for the existence of growth breaks are strategies which could lead to accurate estimation of summer temperature every year in the Adriatic from the shell $\delta^{18}O$ of *A. opercularis*. There is potential for serious underestimation of the peak temperature in warm years (evidenced by the data for 2015), although in cooler years (evidenced by the data for 2014) $\delta^{18}O$ records are fairly accurate, tending to provide just a slight overestimate (< 1.5°C) of the warmest temperature. The situation is otherwise for winter temperature, conditions in both 2015 and 2016 being fairly accurately represented by at least some shells, these providing a slight overestimate (1.4°C) of the coolest temperature for the former year and a slight underestimate (< 1.3°C) for the latter. Turning these findings into guidelines for interpreting $\delta^{18}O$ records from sub-thermocline *A. opercularis* in general, one should only regard minimum $\delta^{18}O$ values as an indication of seafloor temperature in relatively cool summers. Maximum $\delta^{18}O$ values can, however, be regarded as an indication of average winter seafloor temperature, provided that data are available from at least a few shells, and anomalously low values associated with growth breaks are excluded from consideration.

5.1.2. English Channel and French Mediterranean shells

Summer and winter inflections can be recognised in the English Channel and French Mediterranean $\delta^{18}O$ profiles (Figs 8, 9) at the following shell heights. EC1— winter 1: 5.5 mm, summer 1: 38.0 mm, winter 2: 49.5 mm; EC2—summer 1: 16.5 mm, winter 1: 39.0 mm; summer 2: 49.0 mm; FM1—summer 1: 9.0 mm, winter 1: 25.0 mm, summer 2: 48.0 mm; FM2—winter 1: 29.0 mm, summer 1: 41.5 mm. While there are no growth breaks associated with $\delta^{18}O$ minima to suggest truncation of summer records, the association of growth breaks with almost all $\delta^{18}O$ maxima (winter 1 in EC1 is the sole exception) suggests possible truncation of winter records. However, given the lengthy upward and downward trends on either side of each $\delta^{18}O$ maximum, which can be taken to span the preceding autumn and succeeding spring periods, any truncation is likely to have been minor.

The summer 1 isotopic temperatures (from $\delta^{18}O$ minima) ~~Isotopic summer temperatures for year 1~~ in the English Channel shells (EC1: 18.2°C; EC2: 18.8°C) are similar to the local average warm extreme (17.4°C), but consistently a little warmer ~~higher~~. The rather cool summer 2 temperature ~~for year 2~~ in EC2 (14.8°C) could reflect sampling at inadequate resolution (i.e. closer sampling later in ontogeny failed to compensate for declining growth rate; cf. Fig. 6). All the winter temperatures (from $\delta^{18}O$ maxima) in EC1 (winter 1: 6.1°C; winter 2: 7.2°C) and EC2 (winter 1: 7.2°C) are similar to the local average cool extreme (8.0°C), but consistently a little cooler. As growth breaks are associated with the two warmer (7.2°C) recorded extremes it is possible that the records are a little truncated—i.e. that the actual minimum temperatures in the winters concerned were similar to the cooler (6.1°C) recorded extreme. Like the winter temperatures from the English Channel shells, those from the French Mediterranean shells (FM1, winter 1: 12.9°C; FM2, winter 1: 10.3°C;) are similar to the local average cool extreme (*c.* 12°C), but while one is a little cooler, the other is a little warmer. As growth breaks are associated with both recorded extremes, the actual minimum temperatures in the winters concerned may have been a little lower. All the summer temperatures in FM1 (summer 1: 21.2°C; summer 2: 21.7°C) and FM2 (summer 1: 19.9°C) are cooler than the local average warm extreme at the surface (*c.* 23°C). This seems likely to reflect life-positions near the base of the mixed layer, at

depths down to 30 m, where the average peak temperature is 20°C. This would not be inconsistent with transport to the shore during a storm.

To summarize and conclude, winter temperatures calculated from the $\delta^{18}O$ of the English Channel and French Mediterranean shells are quite close to expectation; values cooler than the local average (the ~~slight~~ majority) might represent underestimates of actual winter temperatures due to disequilibrium, but could be essentially accurate, reflecting relatively cool winters. Summer temperatures are in some cases quite close to expectation but in others several degrees cooler; the latter instances might also represent disequilibrium but seem more likely to be effects of growth-rate decline with age or life in relatively deep (but not sub-thermocline) settings. The English Channel and French Mediterranean shells therefore provide a fairly accurate indication of average winter temperatures, like the Adriatic shells, but unlike the latter they also provide (or would be capable of providing if suitably sampled) a fairly accurate indication of average summer benthic temperatures.

5.2. $\delta^{13}C$ data

Of the three sets of shells, only the French Mediterranean specimens show any sign of the pattern of $\delta^{13}C$-$\delta^{18}O$ covariation predicted for their hydrographic setting from the data and arguments of Arthur et al. (1983). The intervals of negative correlation in FM1 are consistent with the evidence of relatively warm summer temperature from this shell indicating a supra-thermocline setting. However, the interval of positive correlation is inconsistent. The interval of positive correlation in FM2 is consistent with the evidence of relatively cool summer temperature from this shell suggesting a life-position a little below the mixed layer, although only an intra- rather than truly sub-thermocline setting is permissible from the temperature evidence. Far from showing the predicted positive correlation between $\delta^{13}C$ and $\delta^{18}O$ (i.e. in-phase variation), some of the Adriatic (sub-thermocline) shells show instances of negative correlation. Likewise, instead of showing a negative correlation (i.e.

antiphase variation), both of the English Channel (supra-thermocline) shells show instances of positive correlation.

Fig. 11 about here – single column

The widely exhibited ontogenetic decline in $\delta^{13}C$ values is as seen in many bivalves and may well reflect greater use of carbon released by the organism's respiration (isotopically light) for shell formation with increasing age (Lorrain et al., 2004; McConnaughey and Gillikin, 2008; Chauvaud et al., 2011). The geographic differences in $\delta^{13}C$ values (Adriatic < French Mediterranean < English Channel; Fig. 11) resemble those revealed by Chauvaud et al. (2011, fig. 3) in *Pecten maximus* from coastal locations in the eastern North Atlantic (Spain < France < Norway). Those in *P. maximus* probably relate in part to variation in the amount of respiratory carbon used for shell formation as determined by temperature, but differences in the amount of food consumed, and its carbon isotopic composition, also influence $\delta^{13}C$ in this species (Marchais et al., 2015). While the Adriatic *A. opercularis* certainly lived and grew under warmer winter conditions than the English Channel individuals, the French Mediterranean individuals did so under much the same winter temperatures, and actually grew under warmer summer conditions than the Adriatic shells. Differences in shell $\delta^{13}C$ are not therefore matched by temperature differences and probably relate mainly to nutrition.

5.3. Microgrowth-increment data

The variation in (smoothed) increment size of more than 0.30 mm shown by five of the six Adriatic shells is as predicted for their sub-thermocline setting, and the variation of less than 0.30 mm shown by both English Channel shells is as predicted for their supra-thermocline setting. Viewed as essentially supra-thermocline (i.e. including uppermost intra-thermocline settings but no deeper), the

variation in increment size of less than 0.30 mm shown by the French Mediterranean shells is also as predicted.

The large increments in mid-ontogeny that account for the greater size variation in sub-thermocline Adriatic shells are associated with declining, low or increasing $\delta^{18}O$ values—i.e. with times in the spring–autumn period. They seem likely to reflect high food availability then in the form of phytoplankton. The small increments in early and late ontogeny, often also associated with declining or low $\delta^{18}O$ values, may reflect overriding age effects. The lack of large increments in supra-thermocline English Channel and French Mediterranean shells cannot be attributed to a lack of phytoplankton in the spring–autumn period. Possibly these individuals subsisted largely on resuspended detritus (cf. Johnson et al., 2009). The availability of this throughout the year as a result of wave and current action would account for the minimal variation in increment size, and its low nutritive value would explain the small absolute size of increments.

5.4. Synthesis

It is clear from the foregoing evidence that the pattern of variation in $\delta^{13}C$ relative to $\delta^{18}O$ cannot be used to distinguish sub- from supra-thermocline examples of *A. opercularis*, but that the pattern of variation in (smoothed) microgrowth-increment height can, at least if a number of specimens are examined to allow for occasional departures from the norm of large-amplitude (> 0.30 mm) variation over the course of ontogeny in sub-thermocline forms. One qualification is necessary: while the increment results from Adriatic sub-thermocline individuals agree with those obtained previously from Gulf of Tunis specimens, it should be recognised that both sets derive from warm temperate environments. Almost all the available increment information from modern cool temperate shells (Johnson et al., 2009, tables 1, 2) is definitely or probably from supra-thermocline settings, and the two specimens that most likely derive from sub-thermocline settings (mesotidal but *c.*110 m depth in

the Firth of Clyde, Scotland and Western Approaches, Ireland/England) actually exhibit little variation in increment height. It is possible therefore that the large-amplitude variation seen in a high proportion of Mediterranean (warm temperate) sub-thermocline *A. opercularis* is not characteristic of cool temperate sub-thermocline forms.

Winter temperatures are quite accurately registered (to within 2°C) by the $\delta^{18}O$ of ~~modern~~ sub-thermocline shells from the Adriatic, as seemingly by English Channel and French Mediterranean supra- and intra-thermocline shells. However, while English Channel and French Mediterranean shells probably provide (or could provide) a fairly accurate record of summer benthic temperatures, Adriatic shells present a biased picture: they provide a fairly accurate estimate (to within 2°C) of the peak temperature in relatively cool years but a serious underestimate in warm years. Thus the warmest modelled seafloor temperature for the warm summer of 2015 is 23.3°C (Fig. 5A; Table 2) but the warmest isotopic temperature for 2015 (from S3A5) is 20.0°C, well short of this figure. However, the warmest isotopic temperature from the Gulf of Tunis sub-thermocline shell represented in Figure 2B is very close (22.7°C; calculated using a water $\delta^{18}O$ value of +1.35‰, measured at 50 m depth at an adjacent location—site 8 of Pierre, 1990). Hence *A. opercularis* is capable of recording temperatures similar to those reached in warm summers in the Adriatic but for some reason failed to do so there in 2015. Most shells suffered an interruption of growth in summer 2015, suggesting some unfavourable environmental condition. This might have been low quantity or quality of food (cf. Johnson et al., 2009), but hypoxia seems the likeliest cause, given its known effect on growth in bivalves (Gobler et al., 2014; Gobler and Baumann, 2016) and fairly common summer occurrence in the northern Adriatic area (Djakovac et al., 2015). Such evidence of summer benthic oxygen levels as exists in relation to the sample site near Pula (for the summers of 1972, 1977, 1983, 1989, 2003, 2006; Djakovac et al., 2015, fig. 2) indicates or strongly suggests full saturation. However, Kralj et al. (2019) recorded hypoxic events in the Bay of Trieste (*c*. 85 km north of Pula) during the exceptionally warm summers of 2015 and 2016, reversing a 30-year trend to increasing benthic oxygenation, so it is possible that

hypoxia extended to the Pula area then. It would certainly be worth measuring benthic oxygen levels in the Pula area during future exceptionally warm summers, and documenting the growth of *A. opercularis* over these intervals. ~~The influence of this factor, and its association with warm summer conditions, would certainly be worth investigating further.~~ It would also be worth investigating the diet of sub- and supra-thermocline *A. opercularis* to see if, as speculated, this differs ~~is different~~ in sub- and supra-thermocline forms and provides an explanation for the high variation in increment size over the course of ontogeny in the former and low variation in the latter.

Table 2 about here - ? single column

6. Application to the early Pliocene Ramsholt Member

Our results from modern shells confirm that the occurrence of high-amplitude increment variation amongst examples of *A. opercularis* from the early Pliocene Ramsholt Member of eastern England is an indication of a sub-thermocline setting, as also suggested by other evidence. Therefore, while isotopic minimum temperatures can be read as surface minima, isotopic maximum temperatures cannot be read as surface maxima. The amount by which the peak in benthic temperature obtained from $\delta^{18}O$ data underestimates the surface maximum temperature is a matter of some uncertainty. Vignols et al. (2019) suggested a stratification factor of 5°C for the Ramsholt Member on the basis of modern temperature data from the Gulf of Tunis. However, as noted earlier, the difference between annual seafloor and surface temperature maxima in the northern Adriatic varies considerably, from 3.2–9.9°C over the nine years from 2008–2016. Adding the mean difference (7.7°C) to the seafloor maximum in each year yields, of course, an accurate figure for the mean surface maximum over this period (27.6°C; Table 2). However, while 7.7°C serves as an accurate average stratification factor for the interval, for the two individual years with the highest seafloor temperature maxima (2015: 23.3°C;

696 2016: 23.5°C), it provides significant overestimates of the respective surface maxima (by 1.5°C and
697 4.5°C), because the difference between the surface and seafloor maxima is least in these years (surface
698 maximum 6.2°C higher than seafloor in 2015 and 3.2°C higher than seafloor in 2016; Table 2). We
699 know, however, that while *A. opercularis* shell $\delta^{18}O$ provides a fairly accurate estimate of maximum
700 seafloor temperature in years of relatively cool seafloor conditions (at least in 2014), it provides a
701 3−4°C underestimate in unusually warm years (at least in 2015). Adjusting the maximum (modelled)
702 seafloor temperatures for 2015 and 2016 downward by an amount (3.5°C) reflecting this, then
703 recalculating the mean surface maximum for 2008−2016 assuming the same stratification factor
704 (7.7°C), yields a value of 26.8°C, only 0.8°C below the actual figure (Table 2). Thus, armed with a
705 knowledge of water $\delta^{18}O$ and of the average stratification factor, we should be able to reconstruct the
706 mean surface maximum temperature for any given period quite accurately from *A. opercularis* shell
707 $\delta^{18}O$, irrespective of whether the period includes unusually warm years.

708 Water $\delta^{18}O$ and the average stratification factor cannot be precisely specified in 'fossil' situations,
709 but they may be constrained. Before providing approximations for the Ramsholt Member, it is worth
710 noting the effect of using incorrect, but plausible stratification factors in calculation of Adriatic
711 surface temperature. If, instead of 7.7°C, we add 9.9°C (the largest difference between annual seafloor
712 and surface maxima in the 2008−2016 period) to all the seafloor temperature values used previously,
713 we obtain a figure of 29.0°C for mean surface maximum temperature, just 1.4°C above the actual
714 figure; by contrast, if we add 3.2°C (the smallest difference between annual seafloor and surface
715 maxima in the 2008−2016 period), we obtain a figure of 22.3°C, 5.3°C below the actual figure (Table
716 2). Thus what can be regarded as maximum and minimum stratification factors yield, respectively, a
717 slight overestimate and a significant underestimate of the actual mean surface maximum
718 temperature—i.e. in 'fossil' situations, we should favour estimates of surface maximum temperature
719 based on stratification factors in the upper part of the 'plausible range'. What therefore might be this
720 range for the Ramsholt Member? The lower limit must surely be above 2.6°C, the figure for the

721 difference between the surface (13.7°C) and seafloor (11.1°C) maxima at the stratified North Sea site
722 represented in Figure 1B. The surface maximum at this site (57°N), over 500 km north of the
723 Ramsholt Member's location (*c.* 52°N), is far below the summer surface temperature of at least 20°C
724 implied by the warm temperate pelagic dinoflagellate assemblage of the Ramsholt Member (Head,
725 1997, 1998). There has been a long history of also interpreting the Ramsholt Member's benthic biota
726 as of warm-water aspect, and specifically 'Mediterranean' in the case of the Mollusca (Long and
727 Zalasiewicz, 2011; Vignols et al., 2019). While shell $\delta^{18}O$ evidence argues strongly against warm
728 temperate seafloor conditions, it is entirely consistent (assuming stratification) with summer surface
729 temperatures in the warm temperate range (Johnson et al., 2009; Vignols et al. 2019). Stratification
730 factors under such a climatic regime are therefore the best indication of the plausible range for the
731 Ramsholt Member, and the 3.2−9.9°C northern Adriatic range, discussed above, may well be an
732 appropriate choice. Given the more northerly location than the northern Adriatic (*c.* 45°N) it is
733 difficult to believe that summer insolation during Ramsholt Member deposition would have been
734 sufficient to achieve temperatures as high as those typical of the northern Adriatic (25−30°C; Fig.
735 5A), which are higher than the mean summer surface temperature at the more southerly (*c.* 43°N) La
736 Franqui location (Section 2). On the other hand, even 'generous' interpretations of seafloor
737 temperature from Ramsholt-Member shell $\delta^{18}O$ data (using a water $\delta^{18}O$ of +0.5‰; Johnson et al.,
738 2009; Vignols et al., 2019) provide few indications of benthic temperature maxima like those in the
739 northern Adriatic, which are rarely much below and sometimes above 20°C (Fig. 5A). The difference
740 between annual surface and seafloor temperature maxima during Ramsholt Member deposition was
741 therefore probably much the same as now in the northern Adriatic, and by the same token, there was
742 probably about the same range of variation in this parameter (stratification factor).
743 Adopting the northern Adriatic range and favouring values in the upper part on the basis of the
744 argument made earlier, 5, 7 and 9°C are sensible choices for stratification factors to use in calculation
745 of a selection of surface temperature estimates for the Ramsholt Member. We need of course also to

identify suitable values for water $\delta^{18}O$, and indeed the most appropriate $\delta^{18}O$-temperature equation. In previous work on Ramsholt-Member *A. opercularis* (Johnson et al., 2009; Vignols et al., 2019), water values of −0.5, −0.2, +0.1 and +0.5‰ were used in conjunction with the calcite equation of O'Neil et al. (1969). The first two water values are minimum and maximum estimates of the Pliocene global seawater average (Buchardt and Simonarson, 2003) and are doubtfully appropriate for a shelf basin somewhat isolated from the North Atlantic (e.g. Dearing Crampton-Flood et al., 2020, fig. 1). The last two are minimum and maximum modelled values for seawater in the Pliocene at the specific location of the Ramsholt Member (Johnson et al., 2009). The minimum modelled value yields temperatures from the co-occurring bivalve *Arctica islandica* that are all below the upper tolerance limit of modern *A. islandica* in the North Sea (16°C; Witbaard and Bergman, 2003), while the maximum modelled value yields a temperature above this from one shell (Vignols et al., 2019). Of the four values previously considered, +0.1‰ is therefore the most credible and adopted here. It is worth noting that this value is almost identical to modern seafloor values in the western part of the southern North Sea (i.e. adjacent to the location of the Ramsholt Member), and that more centrally, within the area of influence of the rivers Rhine, Meuse and Scheldt, values are only 0.2‰ lower (Harwood et al., 2008). In both the western and central southern North Sea seasonal variation in salinity is only about 0.25 PSU (Howarth et al. 1993), which translates to a seasonal variation in water $\delta^{18}O$ of just 0.07‰ using the salinity-water $\delta^{18}O$ relationship for the North Sea of Harwood et al. (2008). It seems doubtful that the additional supply of freshwater from the Baltic region in the Pliocene (e.g. Dearing Crampton-Flood et al., 2020, fig. 1) would have had much effect on salinity, and hence water $\delta^{18}O$, at the location of the Ramsholt Member.

Table 3 about here - ? single column

We argued ~~earlier~~ in Section 3.2 that the LL calcite equation of Bemis et al. (1998) is more appropriate than the calcite equation of O'Neil et al. (1969) for calculation of temperatures from *A. opercularis* shell $\delta^{18}O$. Using the former in conjunction with the minimum shell $\delta^{18}O$ values from the 10 Ramsholt-Member *A. opercularis* analysed to date, together with the water $\delta^{18}O$ value and (for surface temperatures) stratification factors identified above, yields the summer seafloor and surface temperature estimates set out in Table 3. All surface estimates with a stratification factor of 9°C are in the warm temperate summer range (20°C or above), as are six with a stratification factor of 7°C, and four with a stratification factor of 5°C. These temperatures are consistent with the dinoflagellate evidence referred to above. Included in Table 3 are winter seafloor temperatures calculated from maximum shell $\delta^{18}O$~~,~~ all well within the cool temperate winter range (below 10°C). Contrary to earlier speculation (Vignols et al., 2019) it is unlikely that surface temperatures were lower, since at present in the North Sea winter seafloor and surface temperatures are identical (Fig. 1). Nevertheless, these firmly cool temperate estimates for winter, combined with the warm temperate surface estimates for summer, indicate that during Ramsholt Member deposition seasonal variation in surface temperature (perhaps > 15°C) was higher than at present in the adjacent southern North Sea (12.4°C; Fig. 1A) and much higher than in the central North Sea (7.5°C; Fig. 1B). As it is not significantly affected by assumptions about water $\delta^{18}O$, this is a robust inference, with implications in its own right for the early Pliocene climatology of NW Europe—e.g. possibly reduced oceanic heat supply (Johnson, 2009; Vignols et al., 2019). It would be desirable, however, to obtain firm estimates of absolute seasonal temperatures. The carbonate clumped isotope (Δ_{47}) technique provides a means of determining water $\delta^{18}O$ and hence of translating shell $\delta^{18}O$ values into reliable temperatures (e.g. Winkelstern et al., 2017; de Winter et al., 2018; Peral et al., 2020). Application of the technique to early and also late Pliocene marine shells from NW Europe that have already supplied $\delta^{18}O$ data (Johnson et al. 2009; Valentine et al., 2011; Vignols et al., 2019) should serve to settle current conflicts over absolute seasonal temperatures in the marine realm and enable accurate comparison

with terrestrial absolute temperatures, which are presently at odds with marine temperatures over some intervals (Dearing Crampton-Flood, 2018, 2020). Such an improvement in the marine database would also assist evaluation of the roles of oceanic heat supply and radiative heating in determining regional climate.

7. Conclusions

Modern *A. opercularis* individuals from (warm temperate) sub-thermocline settings are characterised by high-amplitude variation in microgrowth-increment size over the course of ontogeny; those from supra- (and intra-) thermocline settings show much less variation. In neither sub- nor supra-thermocline settings is there a characteristic pattern of ontogenetic variation in $\delta^{13}C$ relative to $\delta^{18}O$. Shell $\delta^{18}O$ affords a fairly accurate record of winter temperature in both settings and of summer benthic temperature in supra-thermocline settings. It affords a fairly accurate record of summer benthic temperature in sub-thermocline settings during relatively cool years, but in relatively warm years temperature may be seriously underestimated.

On the basis of the findings from modern *A. opercularis*, early Pliocene specimens from the Ramsholt Member of the Coralline Crag Formation (UK) can be interpreted as sub-thermocline individuals by the evidence of their increment patterns. Subject to the accuracy of estimates of water $\delta^{18}O$ and (for summer) the difference between maximum seafloor and surface temperatures, their shell $\delta^{18}O$ indicates winter surface temperatures within the cool temperate range and summer surface temperatures at least sometimes in the warm temperate range. There can be little doubt that the seasonal range in surface temperature was higher than now in the area.

Acknowledgements

We thank L. Iveša and D. Skoko for collecting the set of Adriatic shells alongside their commercial fishing activities, and M. Peharda (Institute of Oceanography and Fisheries, Split, Croatia) for processing and forwarding the shells for investigation. S. Gofas and V. Héros kindly facilitated the loan of French Mediterranean shells from the Muséum National d'Histoire Naturelle, Paris, and T. White and J. Perera did likewise for English Channel shells from the Natural History Museum, London. W. Austin (University of St Andrews) generously retrieved and supplied precise location and depth information relating to the data in Figure 1. We are grateful to M. Maus for assistance with isotopic analysis at the Institute of Geosciences, University of Mainz, and to the Alexander von Humboldt Foundation for support of work there by ALAJ. We also appreciate the assistance of S. Berry (College of Engineering and Technology, University of Derby) in rearranging the temperature-$\delta^{18}O$ equation of O'Neil et al. (1969) to enable derivation of expected shell $\delta^{18}O$ values for given temperatures and water $\delta^{18}O$ values. We thank the two anonymous reviewers for their close reading of the ~~original~~ manuscript and constructive comments, which led to significant improvements in the final version.

Appendix A. Supplementary data

Supplementary data to this article can be found online at https://doi.org/……

References

Arthur, M.A., Williams, D.F., Jones, D.S., 1983. Seasonal temperature-salinity changes and thermocline development in the mid-Atlantic Bight as recorded by the isotopic composition of bivalves. Geol. 11, 655–659. https://doi.org/10.1130/0091-7613(1983)11<655:STCATD>2.0.CO;2.

Austin, W.E.N., Cage, A.G., Scourse, J.D. 2006. Mid-latitude shelf seas: a NW European perspective on the seasonal dynamics of temperature, salinity and oxygen isotopes. The Holocene 16, 937–947. https://doi.org/10.1177/0959683606hl985rp.

Bemis, B.E., Spero, H.J., Bijma, J., Lea, D.W., 1998. Reevaluation of the oxygen isotopic composition of planktonic foraminifera: Experimental results and revised paleotemperature equations. Paleoceanogr. 13, 150–160. https://doi.org/10.1029/98PA00070.

Broom, M.J., Mason, J., 1978. Growth and spawning in the pectinid *Chlamys opercularis* in relation to temperature and phytoplankton concentration. Mar. Biol. 47, 277–285. https://doi.org/10.1007/BF00541005.

Buchardt, B., Simonarson, L.A., 2003. Isotopic palaeotemperatiures from the Tjörnes Beds in Iceland: evidence of Pliocene cooling. Palaeogeogr. Palaeoclimatol. Palaeoecol. 189, 71–95. https://doi.org/10.1016/S0031-0182(02)00594-1.

Chauvaud, L., Thébault, J., Clavier, J., Lorrain, A., Strand, Ø., 2011. What's hiding behind ontogenetic $\delta^{13}C$ variations in mollusk shells? New Insights from the Great Scallop (*Pecten maximus*). Estuaries and Coasts 34, 20111–220. https://doi.org/10.1007/s12237-010-9267-4.

Chavanne, C., Janeković, I., Flament, P., Poulain, P.-M., Kuzmić, M., Gurgel, K.-W., 2007. Tidal currents in the northwestern Adriatic: High- frequency radio observations and numerical model predictions. J. Geophys. Res.—Oceans 112, eC03S21. https://doi.org/10.1029/2006JC003523.

Dearing Crampton-Flood, E., Peterse, F., Munsterman, D., Sinninghe Damsté, J. S., 2018. Using tetraether lipids archived in North Sea Basin sediments to extract North Western European Pliocene continental air temperatures. Earth Planet. Sci. Lett. 490, 193–205. https://doi.org/10.1016/j.epsl.2018.03.030.

868 Dearing Crampton-Flood, E., Noorbergen, L.J., Smits, D., Boschman, R.C., Donders, T.H., Muns,
869 D.K., 2020. A new age model for the Pliocene of the southern North Sea basin: a multi-proxy
870 climate reconstruction. Clim. Past 16, 523–541. https://doi.org/10.5194/cp-16-523-2020.
871 De Winter, N.J., Vellekoop, J., Vorsselmans, R., Golreihan, A., Soete, J., Petersen, S.V., Meyer,
872 K.W., Casadio, S., Speijer, R.P., Claeys, P., 2018. An assessment of latest Cretaceous
873 *Pycnodonte vesicularis* (Lamarck, 1806) shells as records for palaeoseasonality: a multi-proxy
874 investigation. Clim. Past 14, 725–749. https://doi.org/10.5194/cp-14-725-2018.
875 Djakovac, T., Supić, N., Bernardi Aubry, F., Degobbis, D., Giani, M., 2015. Mechanisms of hypoxia
876 frequency changes in the northern Adriatic Sea during the period 1972–2012. J. Mar. Syst.
877 141, 179–189. https://doi.org/10.1016/j.jmarsys.2014.08.001.
878 Elliott, A.J., Li, Z., 1991. Thermocline depths and water temperature at selected sites in the N.W.
879 European shelf seas. Mar. Pollut. Bull., 22, 282−286. https://doi.org/10.1016/0025-
880 326X(91)90805-3.
881 Foster, L.C., Allison, N., Finch, A.A., Andersson, C., Ninnemann, U.S., 2009. Controls on $\delta^{18}O$ and
882 $\delta^{13}C$ profiles within the aragonite bivalve *Arctica islandica*. The Holocene 19, 549–558,
883 https://doi.org/10.1177/0959683609104028.
884 Gillikin, D.P., Wanamaker, A.D., Andrus, F.T., 2019. Chemical sclerochronology. Chem. Geol. 526,
885 1–6. https://doi.org/10.1016/j.chemgeo.2019.06.016.
886 Global Sea Temperature, 2020. Brighton sea temperature.
887 https://www.seatemperature.org/europe/united-kingdom/brighton.htm (accessed 26 March
888 2020).
889 Gobler, C.J., Baumann H., 2016. Hypoxia and acidification in ocean ecosystems: coupled dynamics
890 and effects on marine life. Biol. Lett. 12, e20150976. https://doi.org/10.1098/rsbl.2015.0976.

Gobler, C.J., DePasquale, E.L., Griffith, A.W., Baumann, H., 2014. Hypoxia and acidification have additive and synergistic negative effects on the growth, survival, and metamorphosis of early life stage bivalves. PLoS ONE 9, e83648. https://doi.org/10.1371/journal.pone.0083648.

Gonfiantini, R., Stichler, W., Rozanski,, K. 1995 Standards and intercomparison materials distributed by the International Atomic Energy Agency for stable isotope measurements, in: International Atomic Energy Agency, Reference and Intercomparison Materials for Stable Isotopes of Light Elements: IAEA-TECDOC-825, Vienna, Austria, pp. 13–29.

Harwood, A.J.P., Dennis, P.F., Marca, A.D., Pilling, G.M., Millner, R.S., 2008. The oxygen isotope composition of water masses within the North Sea. Estuar. Coast. Shelf Sci. 78, 353-359. https://doi.org/10.1016/j.ecss.2007.12.010.

Head, M.J., 1997. Thermophilic dinoflagellate assemblages from the Mid-Pliocene of eastern England. J. Paleontol. 71, 165–193. https://doi.org/10.1017/S0022336000039123.

Head, M.J., 1998. New goniodomacean dinoflagellates with a compound hypotractal archeopyle from the late Cenozoic: Capisocysta Warny and Wrenn, emend. J. Paleontol. 72, 797–809. https://doi.org/10.1017/S0022336000027153.

Heilmayer, O., Brey, T., Storch, D., Mackensen, A., Arntz, W.E., 2004. Population dynamics and metabolism of *Aequipecten opercularis* (L.) from the western English Channel (Roscoff, France). J. Sea Res. 52, 33–44. https://doi.org/10.1016/j.seares.2003.07.005.

Hickson, J.A., Johnson, A.L.A., Heaton, T.H.E., Balson, P.S., 1999. The shell of the Queen Scallop *Aequipecten opercularis* (L.) as a promising tool for palaeoenvironmental reconstruction: evidence and reasons for equilibrium stable-isotope incorporation. Palaeogeogr. Palaeoclimatol. Palaeoecol. 154, 325–337. https://doi.org/10.1016/S0031-0182(99)00120-0.

Hickson, J.A., Johnson, A.L.A., Heaton, T.H.E., Balson, P.S., 2000. Late Holocene environment of the southern North Sea from the stable isotopic composition of Queen Scallop shells.

915 Palaeontolog. Electron. 3, iss. 2, art. 3, 11 pp. http://palaeo-
916 electronica.org/2000_2/scallop/issue2_00.htm.
917 Howarth, M.J., Dyer, K.R., Joint, I.R., Hydes, D.J., Purdie, D.A., Edmunds, H., Jones, J.E., Lowry,
918 R.K., Moffat, T.J., Pomroy, A.J., Proctor, R. 1993. Seasonal cycles and their variability.
919 Philosophical Transactions R. Soc. A, 343, 383−403. https://doi.org/10.1098/rsta.1993.0054.
920 Janeković, I., Dutour Sikirić, M., Tomažić, I., Kuzmić, M., 2010. Hindcasting the Adriatic Sea surface
921 temperature and salinity: A recent modeling experience. Geofizika 27, 85–100.
922 Janeković, I., Mihanović, H., Vilibić, I., Tudor, M., 2014. Extreme cooling and dense water formation
923 estimates in open and coastal regions of the Adriatic Sea during the winter of 2012. J.
924 Geophys. Res.—Oceans 119, 3200–3218. https://doi.org/10.1002/2014JC009865.
925 Johnson, A.L.A., Hickson, J.A., Bird, A., Schöne, B.R., Balson, P.S., Heaton, T.H.E., Williams, M.,
926 2009. Comparative sclerochronology of modern and mid-Pliocene (c. 3.5 Ma) *Aequipecten*
927 *opercularis* (Mollusca, Bivalvia): an insight into past and future climate change in the north-
928 east Atlantic region. Palaeogeogr. Palaeoclimatol. Palaeoecol. 284, 164–179.
929 https://doi.org/10.1016/j.palaeo.2009.09.022.
930 Johnson, A.L.A., Valentine, A., Leng, M.J., Sloane, H.J., Schöne, B.R., Balson, P.S., 2017. Isotopic
931 temperatures from the Early and Mid-Pliocene of the US Middle Atlantic Coastal Plain, and
932 their implications for the cause of regional marine climate change. Palaios 32, 250–269.
933 https://doi.org/10.2110/palo.2016.080.
934 Johnson, A.L.A., Valentine, A.M., Leng, M.J., Schöne, B.R., Sloane, H.J., 2019. Life history,
935 environment and extinction of the scallop *Carolinapecten eboreus* (Conrad) in the Plio-
936 Pleistocene of the US eastern seaboard. Palaios 34, 49–70.
937 https://doi.org/10.2110/palo.2018.056.

938 Kim, S.-T., O'Neil, J.R., 1997. Equilibrium and nonequilibrium oxygen isotope effects in synthetic
939 carbonates. Geochim. Cosmochim. Acta 61, 3461–3475. https://doi.org/10.1016/S0016-
940 7037(97)00169-5.
941 Kralj, M., Lipizer, M., Čermelj, B., Celio, M., Fabbro, C., Brunetti, F., Francé, J., Mozetič, P., Giani,
942 M., 2019. Hypoxia and dissolved oxygen trends in the northeastern Adriatic Sea (Gulf of
943 Trieste). Deep Sea Res. Part II: Topical Stud. Oceanography, 164, 74−88.
944 https://doi.org/10.1016/j.dsr2.2019.06.002.
945 Krantz, D.E., 1990. Mollusk-isotope records of Plio-Pleistocene marine paleoclimate, U.S. Middle
946 Atlantic Coastal Plain. Palaios 5, 317–335. https://doi.org/10.2307/3514888.
947 Krantz, D.E., Jones, D.S., Williams, D.F., 1984. Growth rates of the sea scallop, *Placopecten*
948 *magellanicus*, determined from the $^{18}O/^{16}O$ record in shell calcite. Biol. Bull. 167, 186–199.
949 https://doi.org/10.2307/1541347.
950 Krantz, D.E., Williams, D.F., Jones, D.S., 1987. Ecological and paleoenvironmental information using
951 stable isotope profiles from living and fossil molluscs: Palaeogeogr. Palaeoclimatol.
952 Palaeoecol. 58, 249–266. https://doi.org/10.1016/0031-0182(87)90064-2.
953 Long, P.E., Zalasiewicz, J.A., 2011. The molluscan fauna of the Coralline Crag (Pliocene, Zanclean)
954 at Raydon Hall, Suffolk, UK: Palaeoecological significance reassessed. Palaeogeogr.
955 Palaeoclimatol. Palaeoecol. 309, 53–72. http://dx.doi.org/10.1016/j.palaeo.2011.05.039.
956 Lorrain, A., Paulet, Y.M., Chauvaud, L., Dunbar, R., Mucciarone, D., Fontugne, M., 2004. $\delta^{13}C$
957 variation in scallop shells: Increasing metabolic carbon contribution with body size?
958 Geochim.Cosmochim. Acta 68, 3509–3519. https://doi.org/10.1016/j.gca.2004.01.025.
959 Marchais, V., Richard, J., Jolivet, A., Flye-Sainte-Marie, J., Thébault, J., Jean, F., Richard, P., Paulet,
960 Y.-M., Clavier, J., Chauvaud, L., 2015. Coupling experimental and field-based approaches to
961 decipher carbon sources in the shell of the great scallop, *Pecten maximus* (L.). Geoch.
962 Cosmochim. Acta 168, 58–69. https://doi.org/10.1016/j.gca.2015.07.010.

963 McConnaughey, T.A., Gillikin, D.P., 2008. Carbon isotopes in mollusk shell carbonates. Geo-Mar.
964 Lett. 28, 287–299. https://doi.org/10.1007/s00367-008-0116-4.
965 Mook, W.G., Vogel, J.C., 1968. Isotopic equilibrium between shells and their environment. Science
966 159, 874–875. https://doi.org/10.1126/science.159.3817.874.
967 NOAA (US Department of Commerce, National Oceanic and Atmospheric Administration, 1994.
968 NODC (Levitus) World Ocean Atlas: Ocean Temperature: Monthly Long Term Mean.
969 https://www.esrl.noaa.gov/psd/cgi-
970 bin/db_search/DBSearch.pl?Dataset=NODC+(Levitus)+World+Ocean+Atlas&Variable=Ocea
971 n+temperature (accessed 25 March 2020).
972 O'Neil, J.R., Clayton, R.N., Mayeda, T.K., 1969. Oxygen isotope fractionation in divalent metal
973 carbonates. J. Chem. Phys. 51, 5547–5558. https://doi.org/10.1063/1.1671982.
974 Owen, R., Richardson, C., Kennedy, H., 2002. The influence of shell growth rate on striae deposition
975 in the scallop *Pecten maximus.* J. Mar. Biol. Assoc. U. K. 82, 621–623.
976 https://doi.org/10.1017/S0025315402005969.
977 Peharda, M., Thébault, J., Markulin, K., Schöne, B.R., Janeković, I., Chauvaud, L., 2019. Contrasting
978 shell growth strategies in two Mediterranean bivalves revealed by oxygen-isotope ratio
979 geochemistry: The case of *Pecten jacobaeus* and *Glycymeris pilosa*. Chem. Geol. 526, 23–35.
980 https://doi.org/10.1016/j.chemgeo.2017.09.029.
981 Peral, M., Blamart, D., Bassinot, F., Daëron, M., Dewilde, F., Rebaubier, H, Nomade, S., Girone, A,
982 Marino, M., Maiorano, P, Ciaranfi, N., 2020. Changes in temperature and oxygen isotopic
983 composition of Mediterranean water during the Mid-Pleistocene transition in the Montalbano
984 Jonico section (southern Italy) using the clumped-isotope thermometer. Palaeogeogr.
985 Palaeoclimatol. Palaeoecol. 544, https://doi.org/10.1016/j.palaeo.2020.109603.
986 Pierre, C., 1999. The oxygen and carbon isotope distribution in the Mediterranean water masses. Mar.
987 Geol. 153, 41–55. https://doi.org/10.1016/S0025-3227(98)00090-5.

Prendergast, A.L., Versteegh, E.A.A., Schöne, B.R., 2017. New research on the development of high-resolution palaeoenvironmental proxies from geochemical properties of biogenic carbonates. Palaeogeogr. Palaeoclimatol. Palaeoecol. 484, 1–6. https://doi.org/10.1016/j.palaeo.2017.05.032.

Ren, J.S., Ross, A.H.. Schiel, D.R., 2000. Functional descriptions of feeding and energetics of the Pacific oyster *Crassostrea gigas* in New Zealand. Mar. Ecol., Prog. Series 208, 119–130. https://doi.org/10.3354/meps208119.

Schöne, B.R., Surge, D., 2005. Looking back over skeletal diaries — High-resolution environmental reconstructions from accretionary hard parts of aquatic organisms. Palaeogeogr. Palaeoclimatol. Palaeoecol. 228, 1–3. https://doi.org/10.1016/j.palaeo.2005.03.043.

Schöne, B.R., Fiebig, J., 2009. Seasonality in the North Sea during the Allerød and Late Medieval Climate Optimum using bivalve sclerochronology. Int. J. Earth Sci. 98, 83–98. https://doi.org/10.1007/s00531-008-0363-7.

Schöne, B.R., Gillikin, D.P., 2013. Unravelling environmental histories from skeletal diaries—Advances in sclerochronology. Palaeogeogr. Palaeoclimatol. Palaeoecol. 373, 1–5. https://doi.org/10.1016/j.palaeo.2012.11.026.

Schöne, B.R., Freyre Castro, A.D., Fiebig, J., Houk, S.D., Oschmann, W., Kröncke, I., 2004. Sea surface water temperatures over the period 1884–1983 reconstructed from oxygen isotope ratios of a bivalve mollusc shell (*Arctica islandica*, southern North Sea). Palaeogeogr. Palaeoclimatol. Palaeoecol. 212, 215–232. https://doi.org/10.1016/j.palaeo.2004.05.024.

Schöne, B.R., Houk, S.D., Freyre Castro, A.D., Fiebig, J., Kröncke, I., Dreyer, W., Oschmann, W., 2005a. Daily growth rates in shells of *Arctica islandica*: assessing subseasonal environmental controls on a long-lived bivalve mollusk. Palaios 20, 78–92. https://doi.org/10.2110/palo.2003.p03-101.

1012 Schöne, B.R., Fiebig, J., Pfeiffer, M., Gleß, R., Hickson, J., Johnson, A.L.A., Dreyer, W., Oschmann,
1013 W., 2005b. Climate records from a bivalved Methuselah (*Arctica islandica*, Mollusca;
1014 Iceland). Palaeogeogr. Palaeoclimatol. Palaeoecol. 228, 130–148.
1015 https://doi.org/10.1016/j.palaeo.2005.03.049.
1016 Schöne, B.R., Schmitt, K., Maus, M., 2017. Effects of sample pretreatment and external
1017 contamination on bivalve shell and Carrara marble $\delta^{18}O$ and $\delta^{13}C$ signatures. Palaeogeogr.
1018 Palaeoclimatol. Palaeoecol. 484, 22–32. https://doi.org/10.1016/j.palaeo.2016.10.026.
1019 Stenni, B., Nichetto, P., Bregant, D., Scarazzato, P., Longinelli, A., 1995. The $\delta^{18}O$ signal of the
1020 northward flow of Mediterranean waters in the Adriatic Sea. Oceanol. Acta 18, 319–328.
1021 Taylor, A.C., Venn, T.J., 1978. Growth of the queen scallop, *Chlamys opercularis*, from the Clyde
1022 Sea area. J. Mar. Biol. Assoc. U. K. 58, 687–700.
1023 https://doi.org/10.1017/S0025315400041333.
1024 Valentine, A., Johnson, A.L.A., Leng, M.J., Sloane, H.J., Balson, P.S., 2011. Isotopic evidence of
1025 cool winter conditions in the mid-Piacenzian (Pliocene) of the southern North Sea Basin.
1026 Palaeogeogr. Palaeoclimatol. Palaeoecol. 309, 9–16.
1027 https://doi.org/10.1016/j.palaeo.2011.05.015.
1028 van Leeuwen, S., Tett, P., Mills, D., van der Molen, J., 2015. Stratified and nonstratified areas in the
1029 North Sea: Long-term variability and biological and policy implications, J. Geophys. Res.—
1030 Oceans 120, 4670–4686. https://doi.org/10.1002/2014JC010485.
1031 Vignols, R.M., Valentine, A.M., Finlayson, A.G., Harper, E.M., Schöne, B.R., Leng, M.J., Sloane,
1032 H.J., Johnson, A.L.A., 2019. Marine climate and hydrography of the Coralline Crag (early
1033 Pliocene, UK): isotopic evidence from 16 benthic invertebrate taxa. Chem. Geol. 536, 62–83.
1034 https://doi.org/doi:10.1016/j.chemgeo.2018.05.034.

VisitMyHarbour, 2012. Hourly tidal streams, English Channel East. https://www.visitmyharbour.com/articles/3173/hourly-tidal-streams-english-channel-east/ (accessed 26 March 2020).

Vilibić, I., Mihanović, H., Janeković, I., Šepić, J., 2016. Modelling the formation of dense water in the northern Adriatic: Sensitivity studies. Ocean Model. 101, 17–29. http://dx.doi.org/10.1016/j.ocemod.2016.03.001.

Winkelstern, I. Z., Rowe, M.P., Lohmann, K.C., Defliese, W.F., Petersen, S.V., Brewer , A.W., 2017. Meltwater pulse recorded in Last Interglacial mollusk shells from Bermuda. Paleoceanogr. 32. https://doi.org/10.1002/2016PA003014.

Witbaard, R., Bergman, M.J.N., 2003. The distribution and population structure of the bivalve *Arctica islandica* L. in the North Sea: what possible factors are involved? J. Sea Res. 50, 11–25. http://dx.doi.org/10.1016/S1385-1101(03)00039-X.

FIGURE CAPTIONS

Fig. 1. Profiles of monthly average surface (red line) and seafloor (blue line; red where identical with surface) temperature for locations in the southern (A) and central (B) North Sea (data from Austin et al., 2006, fig. 8). Note the almost identical summer surface and seafloor temperatures at the shallow (well-mixed) southern location and the strongly divergent summer temperatures at the deeper (seasonally stratified) northern location (see also Elliott and Li, 1991; van Leeuwen et al., 2015). Summer and winter surface temperatures are within the respective cool temperate ranges (< 20°C, < 10°C; Vignols et al., 2019) at both locations.

Fig. 2. Profiles of ontogenetic variation in $\delta^{13}C$ (grey), $\delta^{18}O$ (pink) and microgrowth-increment height (green; thicker, continuous line connects 5-point moving averages) in *Aequipecten opercularis* from:

1060 (A) a supra-thermocline setting in the UK sector of the southern North Sea (macrotidal); (B) a sub-
1061 thermocline setting in the Gulf of Tunis, southern Mediterranean Sea (microtidal, 50 m depth); (C) the
1062 Ramsholt Member of the Coralline Crag Formation (early Pliocene), Suffolk, eastern England.
1063 Specimens represented are, respectively, British Geological Survey (BGS) Zt 9957, Muséum National
1064 d'Histoire Naturelle, Paris (MNHN), IM-2008-1537, and University of Derby, Geological Collections
1065 (UD) 52795 (illustrated in Fig. 3A). Data from Johnson et al. (2009), where further background
1066 information can be found. Specific location for BGS Zt 9957 given in Hickson et al. (2000); general
1067 location for all shells shown in Fig. 4. The isotopic axis has been reversed in each part so that lower
1068 values of shell $\delta^{18}O$ (corresponding to higher temperatures) plot towards the top. Note that data for
1069 BGS Zt 9957, a specimen from which the dorsal part had been broken off, are here correctly plotted
1070 (as by Hickson et al., 2000, fig. 4) in relation to height from the ventral margin, unlike in plots by
1071 Johnson et al. (2009, fig 4D; 2017, fig. 5B). Open triangles indicate the position of minor growth
1072 breaks. Value shown for variation in increment height is the difference between the maximum and
1073 minimum of smoothed (5-point moving average) data.
1074
1075 **Fig. 3.** Microgrowth increments in *Aequipecten opercularis.* A: the early Pliocene specimen (right
1076 valve) from which the measurements in Fig. 2C were obtained; B: the modern Adriatic specimen
1077 S3A4 (left valve) from which the measurements in Fig. 7C were obtained; C: the modern English
1078 Channel specimen EC1 (left valve) from which the measurements in Fig. 8A were obtained. Note the
1079 substantial variation in increment size in A and B, and the much more uniform increment size in C.
1080 Triangles indicate the positions of minor (open) and moderate–major (filled) growth breaks within the
1081 area of the enlargements. Scale bars = 10 mm; vertical for full-shell images, horizontal for
1082 enlargements. Microgrowth increments have been described as 'striae' in work on this and other
1083 scallop species (e.g. Broom and Mason, 1978; Owen et al., 2002; Peharda et al., 2019). They are
1084 bounded by commarginal lamellae, which on left valves (e.g. B, C) are commonly discontinuous

between the plicae ('ribs'), making it difficult to define increments there. In such circumstances measurements were made on the plicae.

Fig. 4. Collection locations of the Adriatic (1), English Channel (2) and French Mediterranean (3) shells, and of the shells represented in Fig. 2A (4), Fig. 2B (5) and Fig. 2C (6). See Section 2 and Table 1 for details.

Fig. 5. A: Profiles of daily temperature from 2008–2016 for the surface (red line) and seafloor (38 m depth; blue line) at the location of the Adriatic specimens, derived using the numerical ocean model ROMS. B: Profiles of daily salinity and water $\delta^{18}O$ at the seafloor for the same location and interval; salinity derived using ROMS and water $\delta^{18}O$ derived using the salinity-water $\delta^{18}O$ relationship of Peharda et al. (2019), based on the data of Stenni et al. (1995) from adjacent sites in the northern Adriatic. C: Predicted shell (calcite) $\delta^{18}O$ for the location and depth of the Adriatic specimens, derived using the seafloor temperature and water $\delta^{18}O$ data in A and B, and the LL equation of Bemis et al. (1998). Note that the $\delta^{18}O$ axis has been reversed in C (see Fig. 2 for explanation). Error estimates have been excluded for the sake of clarity but are included in the shorter profile of predicted shell $\delta^{18}O$ (2013–2016) in Fig. 10. All data available online (see Appendix A).

Fig. 6. Shell $\delta^{18}O$ values (filled circles) from Fig. 2A (supra-thermocline *A. opercularis* from 53°N in the North Sea) temporally aligned with a curve (pink line) of expected monthly shell (calcite) $\delta^{18}O$ for 53°N in the North Sea, derived using the LL equation of Bemis et al. (1998) and the monthly average seafloor temperature and water $\delta^{18}O$ data of Austin et al. (2006, fig. 8), replicated over four years (note that the $\delta^{18}O$ axis has been reversed; see Fig. 2 for explanation). Also included are curves based on the same data but derived using the calcite equations of O'Neil et al. (1969; lavender) and Kim and O'Neil (1997; gold). Minor growth breaks (open triangles) inserted in accordance with their position

relative to measured $\delta^{18}O$ values (Fig. 2A). The decreasing completeness of the measured record over time probably reflects increasing time-averaging within samples due to ontogenetic decline in growth rate.

Fig. 7. Isotope and increment data for Adriatic shells S3A1 (A), S3A3 (B), S3A4 (C), S3A5 (D), S3A33 (E) and S3A36 (F), plotted as in Fig. 2, with a pale green background used to correspond with Fig. 2B (data also from a sub-thermocline setting). Isotope profiles link singleton or mean values (crosses indicate the values from which these were derived). Open and filled triangles indicate the position of minor and moderate–major growth breaks, respectively. S3A4 is illustrated in Fig. 3B.

Fig. 8. Isotope and increment data for English Channel shells EC1 (A) and EC2 (B), plotted as in Fig. 2, with a pale blue background used to correspond with Fig. 2A (data also from a supra-thermocline setting). Isotope profiles link singleton or mean values (crosses indicate the values from which these were derived). Open and filled triangles indicate the position of minor and moderate–major growth breaks, respectively. EC1 is illustrated in Fig. 3C.

Fig. 9. Isotope and increment data for French Mediterranean shells FM1 (A) and FM2 (B), plotted as in Fig. 2, with a pale blue background used to correspond with Fig. 2A (data also from a supra-thermocline setting). Increment data from 55–60 mm height in FM2 have been excluded in the interests of clarity and comparability with other datasets; inclusion of these data (available online; see Appendix A) would not have increased the range of variation recorded. Open and filled triangles indicate the position of minor and moderate–major growth breaks, respectively.

Fig. 10. Values of $\delta^{18}O$ (circles; open for anomalous values) from Adriatic shells S3A1 (A), S3A3 (B), S3A4 (C), S3A5 (D), S3A33 (E) and S3A36 (F), aligned with a curve of predicted daily values.

Note that the $\delta^{18}O$ axis has been reversed (see Fig. 2 for explanation). Measured values from Fig. 7 (individual values contributing to means excluded); predicted values from Fig. 5C, with added error estimates (dotted lines) based on 1σ values for modelled temperature and salinity. Minor and moderate–major growth breaks (open and filled triangles, respectively) inserted in accordance with their position relative to measured $\delta^{18}O$ values (Fig. 7). Vertical grey bars signify gaps of > 100 days in the sequence of measured $\delta^{18}O$ values. References in the text to winters in specific calendar years refer to the cold period (i.e. the interval of high $\delta^{18}O$) at the start of the year stated.

Fig. 11. Scatterplot showing the relatively low $\delta^{13}C$ values from Adriatic shells (open orange diamonds), the relatively high values from English Channel shells (filled teal diamonds), and the intermediate values from French Mediterranean shells (black crosses), independent of $\delta^{18}O$. Data from the profiles in Figs 7–9.

TABLE CAPTIONS

Table 1

Locational information and descriptive statistics for shell $\delta^{13}C$ and $\delta^{18}O$

Table 2

Modelled annual surface and seafloor temperature maxima in the northern Adriatic (Fig. 5A; Appendix A), and inferred surface maxima from accurate and underestimated (2015, 2016) seafloor data, using various stratification factors (see text for explanation of underestimation and stratification factors)

Table 3

1160 Seasonal seafloor and surface temperatures from $\delta^{18}O$ of Ramsholt Member *A. opercularis*, calculated

1161 using the LL equation of Bemis et al. (1998) and water $\delta^{18}O$ of +0.1‰

1162

Highlights

- Sub- and supra-thermocline *A. opercularis* differ in their increment patterns
- Seasonal ambient temperatures are generally recorded quite accurately by shell $\delta^{18}O$
- Relatively warm summer conditions are not registered by sub-thermocline forms
- Individuals from the early Pliocene of eastern England lived below the thermocline
- The seasonal range in sea-surface temperature was higher then than now in the area

Growth-increment characteristics and isotopic ($\delta^{18}O$) temperature record of sub-thermocline *Aequipecten opercularis* (Mollusca:Bivalvia): evidence from modern Adriatic forms and an application to early Pliocene examples from eastern England

Andrew L.A. Johnson[a,*], Annemarie M. Valentine[b], Bernd R. Schöne[c], Melanie J. Leng[d], Hilary J. Sloane[d], Ivica Janeković[e]

[a] *School of Environmental Sciences, University of Derby, Derby DE22 1GB, UK*

[b] *School of Geography and Environmental Science, Nottingham Trent University, Southwell NG25 0QF, UK, drmitzyvalentine@gmail.com*

[c] *Institute of Geosciences, University of Mainz, 55128 Mainz, Germany, schoeneb@uni-mainz.de*

[d] *National Environmental Isotope Facility, British Geological Survey, Keyworth NG12 5GG, UK, mjl@bgs.ac.uk*

[e] *UWA Oceans Institute, University of Western Australia, Crawley, WA 6009, Australia, ivica.janekovic@uwa.edu.au*

* Corresponding author.

E-mail address: a.l.a.johnson@derby.ac.uk (A.L.A. Johnson).

Keywords: Sclerochronology; Bivalve; Marine climate; Hydrography; Pliocene

ABSTRACT

The shell $\delta^{18}O$ of young modern *Aequipecten opercularis* from the southern North Sea provides an essentially faithful record of seasonal variation in seafloor temperature. In this well-mixed setting, *A. opercularis* shell $\delta^{18}O$ also serves as a proxy for seasonal variation in surface temperature. Individuals from less agitated (e.g. deeper) settings in a warm climate would not be expected to record the full seasonal range in surface temperature because of thermal stratification in summer. Such circumstances have been invoked to explain cool isotopic summer temperatures from early Pliocene *A. opercularis* of eastern England. Support for a sub-thermocline setting derives from high-amplitude variation in microgrowth-increment size, which resembles the pattern in sub-thermocline *A. opercularis* from the southern Mediterranean Sea. Here, we present isotope and increment profiles from further sub-thermocline individuals, live-collected from a location in the Adriatic Sea for which we provide modelled values of expected shell $\delta^{18}O$. We also present data from supra-thermocline shells from the English Channel and French Mediterranean coast. The great majority of sub-thermocline *A. opercularis* show high-amplitude variation in increment size, and winter and summer $\delta^{18}O$ values are generally quite close to expectation. However, the relatively warm summer conditions of 2015 are not recorded, in most cases due to a break in growth, perhaps caused by hypoxia. The supra-thermocline shells show subdued increment variation and yield isotopic winter and summer temperatures quite close to the local directly measured values. *A. opercularis* shells therefore provide a fairly good isotopic record of ambient temperature (if not always of relatively warm summer conditions below the thermocline) and their hydrographic setting can be determined from increment data. Early Pliocene examples from eastern England can be interpreted as having lived in a setting below the thermocline, with a higher seasonal range in surface temperature than now in the adjacent southern North Sea.

1. Introduction

The $\delta^{18}O$ of skeletal $CaCO_3$ (calcite and aragonite) is very widely used as a proxy for the temperature of the ambient environment; in particular, the $\delta^{18}O$ of marine mollusc shells is used as an indicator of seawater temperature (e.g. Schöne and Surge, 2005; Schöne and Gillikin, 2013; Prendergast et al., 2017; Gillikin et al., 2109). The values obtained are often presented as if they reflect sea-surface temperature, a datum of great interest to climatologists and palaeoclimatologists, but those derived from benthic taxa such as bivalves are of course a record of seafloor temperature (with the additional influence of water $\delta^{18}O$, which must be measured or estimated to enable calculation of temperature from shell $\delta^{18}O$). In agitated settings (where the seafloor is above the fair-weather wave-base, or to somewhat greater depths where tidal currents are strong) stirring of the water is usually sufficient for seafloor temperature to be very similar to surface temperature (Fig. 1A). However, in quieter settings (e.g. at depths below the fair-weather wave-base, in situations where tidal currents are weak), and at latitudes where solar irradiation is significant (i.e. outside the polar regions), seafloor temperature often departs radically from surface temperature in summer (Fig. 1B). This is because the lack of agitation and the lower density of warmed water allows heat to become 'ponded' in a shallow surface layer (commonly extending to 25–30 m in weakly tidal shelf settings), separated from much cooler, deeper waters by a zone of steep temperature change, the thermocline. In the mid-latitudes, where there is significant seasonal variation in insolation, this stratification typically breaks down in autumn because of surface cooling, often aided by storm activity, beginning an equalisation of temperature (Fig. 1B). By the winter months, seafloor temperature is usually about the same as at the surface, to at least mid-shelf depths (e.g. Arthur et al., 1983; Elliott and Li, 1991). Shelf bivalves living below the summer thermocline ('sub-thermocline' individuals) therefore in many cases experience temperatures that are similar to those at the surface in winter (the coldest temperatures occurring at the same time: February/March in the Northern Hemisphere) but experience temperatures that are cooler than those at the surface in summer (the peak temperature at the surface typically

occurring during August/September and the lower peak temperature on the seafloor during October/November in the Northern Hemisphere). Sequential sampling of sub-thermocline shells at high temporal resolution through ontogeny (isotope sclerochronology) will provide $\delta^{18}O$ values corresponding to the coldest winter surface temperature but will not yield values corresponding to the warmest summer surface temperature: this temperature will only be directly recoverable from 'supra-thermocline' individuals (i.e. those that lived above the depth of the summer thermocline).

Fig. 1 about here – double column

Sub-thermocline shells can still be a source of information on summer surface temperature: we can project a likely summer surface value by taking account of the difference between the maximum seafloor and surface temperature in modern stratified situations. This difference is variable (see Section 2) so sub-thermocline shells can only supply a rough indication of summer surface temperature, and before we add a 'stratification factor' to the warmest $\delta^{18}O$-derived temperature from an individual, we must be sure that it lived in a sub-thermocline setting. Schöne and Fiebig (2009) claimed that sub-thermocline forms of the long-lived bivalve *Arctica islandica* are recognizable from a saw-tooth $\delta^{18}O$ profile (contrasting with a sinusoidal profile in supra-thermocline shells), but this pattern is also observed in an undoubtedly supra-thermocline individual (6 m depth) from south-west Scotland (Foster et al., 2009). Seafloor temperature variation can be sinusoidal in sub-thermocline settings (Fig. 1B) so under those circumstances the shells of bivalve species which grow throughout the year (e.g. many examples of the short-lived Queen Scallop, *Aequipecten opercularis*, in their first year; Hickson et al., 2000) would provide $\delta^{18}O$ profiles of the same form as supra-thermocline individuals.

Fig. 2 about here – single column

Using data from modern *Spisula solidissima*, Arthur et al. (1983) suggested that sub- and supra-thermocline bivalves might be distinguishable on the basis of patterns of covariation between $\delta^{13}C$ and $\delta^{18}O$: positive covariation (i.e. in-phase ontogenetic profiles) in the former and negative covariation (i.e. antiphase ontogenetic profiles) in the latter. This notion is superficially appealing because the $\delta^{13}C$ of dissolved inorganic carbon (DIC) increases over spring and summer at shallow depths due to the preferential uptake of ^{12}C by photosynthesizers, and then progressively decreases over the rest of the year, in part as a result of respiratory return of isotopically light carbon to the DIC pool and low photosynthetic uptake (Lorrain et al., 2004). Thus a supra-thermocline bivalve inheriting its shell carbon from DIC would show a pattern of seasonal variation in $\delta^{13}C$ opposite to that in $\delta^{18}O$. By contrast, a sub-thermocline bivalve might be expected to show parallel variation of $\delta^{13}C$ and $\delta^{18}O$ because DIC with a high $\delta^{13}C$ would only be available to it following the autumn breakdown of stratification and mixing down of surface waters. The problem with this model is that some of the carbon in a bivalve's shell derives from its food (particulate organic carbon), which, being isotopically light (the direct or indirect result of photosynthesis) and typically abundant at shallow depths during summer as a consequence of high primary production, might be expected to cause low shell $\delta^{13}C$ in supra-thermocline individuals during that season (Chauvaud et al., 2011). Low summer $\delta^{13}C$ values have indeed been documented from shallow-water *Pecten maximus* (Chauvaud et al., 2011), contrasting with the data of Arthur et al. (1983) from shallow-water *S. solidissima* but matching results from other shallow-water examples of *S. soldissima* (Krantz et al., 1987, figs 4, 5). Whether the summer $\delta^{13}C$ reduction seen in deeper water (sub-thermocline) *S. solidissima* (Arthur et al., 1983) and also *Placopecten magellanicus* (Krantz et al., 1987, figs 6–9) is due to high incorporation of food-derived carbon into the shell remains unclear (at depth, food availability might be no greater in summer than winter, although feeding rate would probably be higher; cf. Ren et al., 2000). However, whatever the cause, the foregoing examples indicate that summer reduction in shell $\delta^{13}C$ is not limited to sub-thermocline settings. The notion that sub- and supra-thermocline bivalves can be distinguished

126 on the basis of patterns of $\delta^{13}C$ variation in relation to $\delta^{18}O$ is also refuted by data from *A. opercularis*.
127 Modern examples from each setting (Fig. 2A, B) show patterns that are opposite to those recorded by
128 Arthur et al. (1983) from *S. solidissima*, and some early Pliocene specimens of *A. opercularis* simply
129 show a general ontogenetic decline in $\delta^{13}C$ (Fig. 2C).
130
131 Fig. 3 about here – double column
132
133 Included in Figure 2 are profiles of variation in the size (anatomical height) of microgrowth
134 increments (Fig. 3). Smoothed (5-point average) data from the modern supra-thermocline shell (from
135 the southern North Sea) exhibit a slight long-term fluctuation (broadly seasonal from the rough
136 correspondence to the pattern of seasonal change in $\delta^{18}O$) superimposed on high frequency/low
137 amplitude variation. In contrast the modern sub-thermocline shell (from the Gulf of Tunis, southern
138 Mediterranean Sea) shows a much more pronounced long-term fluctuation, and the early Pliocene
139 shell (from the Ramsholt Member, Coralline Crag Formation, Suffolk, eastern England) an essentially
140 identical pattern. Investigation of 18 other *A. opercularis* from the eastern margin of the North
141 Atlantic (including North Sea) revealed limited increment variation in all nine from definitely supra-
142 thermocline settings, as evidenced by a macrotidal regime (hence strong tidal currents) or a depth of
143 less than 25 m (Johnson et al., 2009, tables 1, 2). By contrast, two of four other investigated sub-
144 thermocline shells from the Gulf of Tunis exhibit pronounced variation (> 0.30 mm between the
145 minimum and maximum of smoothed profiles), as do four of seven other Ramsholt-Member shells
146 (Johnson et al., 2009; Vignols et al., 2019). A sub-thermocline situation for Ramsholt-Member shells
147 is supported by a variety of palaeontological and sedimentological evidence (Johnson et al., 2009),
148 and the modest fluctuations seen in Ramsholt-Member $\delta^{18}O$ profiles (e.g. Fig. 2C) and quite low (cool
149 temperate) peak temperatures calculated from these (contrasting with the warm temperate summer
150 values indicated by the pelagic dinoflagellate assemblage; Head, 1997, 1998) are consistent with this

151 setting (Johnson et al., 2009; Vignols et al., 2019). It cannot be denied, however, that the evidence for
152 hydrographic control of increment-size variation in modern *A. opercularis* is only circumstantial, and
153 that the $\delta^{18}O$ data from the Ramsholt Member could (if from supra-thermocline shells) reflect a low
154 seasonality climate with cool summers. While such an interpretation would be radically at odds with
155 almost all other evidence (Johnson et al., 2009; Vignols et al., 2019), it deserves consideration through
156 further investigation of increment patterns in modern *A. opercularis* in relation to hydrographic
157 setting, and of the closeness of shell $\delta^{18}O$ values to expected values. To this end we studied six further
158 sub-thermocline shells live-collected for the purpose from another location in the Mediterranean Sea
159 (northern Adriatic Sea, Croatia), temporally aligning shell $\delta^{18}O$ values as well as possible with a
160 profile of predicted daily values derived for this location using the extensively validated Regional
161 Ocean Modeling System (ROMS; Janeković et al., 2010, 2014; Vilibić et al., 2016) and a local water
162 $\delta^{18}O$-salinity relationship (Peharda et al., 2019). We also supplemented the already quite large supra-
163 thermocline database with information from two shells collected in the English Channel near
164 Brighton, UK, an area from which data had not previously been obtained. In addition, we acquired
165 isotope data from two probably supra-thermocline shells collected from the shore of the
166 Mediterranean Sea at La Franqui, France. One of these had previously supplied increment data
167 consistent with a supra-thermocline setting but the other (remeasured here) had yielded an anomalous
168 (i.e. sub-thermocline) increment pattern. Since the precise location, depth and time of life of the
169 English Channel and French Mediterranean individuals (museum specimens) was not known, we did
170 not derive profiles of predicted shell $\delta^{18}O$ for comparison with measured values. Instead, we
171 calculated summer and winter temperatures from the latter and compared these with mean seasonal
172 temperatures at each location from direct monitoring.
173
174 Fig. 4 about here – single column
175

2. Material and settings

The general provenance of the Adriatic, English Channel and French Mediterranean shells (and those represented in Fig. 2) is illustrated in Figure 4; details of sample locations are supplied below and in Table 1.

The Adriatic shells are all left valves: S3A1, S3A3–5, S3A33 and S3A36 = University of Derby, Geological Collections (UD) 53417–53422, respectively. They are amongst the largest (47–51 mm shell height) from a sample of 54 individuals (27–53 mm height; uninvestigated specimens accessioned as UD 53423) live-collected with a dredge on 13th September 2016 by commercial fishermen at 38 m depth in fishing zone A3, 3.5 nautical miles from Pula, Croatia. Specimens were disarticulated and eviscerated shortly after collection. Valves were then matched and inscribed with a code-number (S3A1–54; same for right and left valve of a pair) before dry storage. We chose left valves for investigation because microgrowth increments are usually measurable over a greater range of shell height; the right valve, which lies against the substrate in life, can become significantly abraded, obscuring increment boundaries. ROMS-derived profiles of daily temperature for the surface and 38 m at the collection location show that the shells are unquestionably from a setting with summer thermal stratification, annual peak temperatures at 38 m being 3.2–9.9°C (mean 7.7°C) below those at the surface over the period 2008–2016 (Fig. 5A). This is a reflection of high heat flux and limited wave-mixing in summer, with tidal current velocities < 0.15 m s^{-1} (Chavanne et al., 2007); geostrophic currents are similarly weak (Djakovac et al., 2015). Surface temperatures are within the warm temperate range (winter > 10°C, summer > 20°C; Vignols et al., 2019).

Fig. 5 about here – single column

The English Channel shells are also left valves: EC1 and EC2 = Natural History Museum, London (NHMUK) 20190467/1 and 20190467/2, respectively. They are examples of similar size (53 and 52 mm height, respectively) to the Adriatic shells, selected from a sample originally formed of seven articulated individuals and five single valves (42–58 mm shell height; uninvestigated specimens accessioned as NHMUK 20190467) collected 'off Brighton' (south coast of the UK) on an unspecified date in 1923 and stored dry (without soft-parts). EC2 still had the right valve attached and EC1 could be matched with a right valve of the same size, so both the individuals concerned were probably alive at or not long before the time of collection. Since water depth is less than 20 m to 10 km offshore from Brighton and the surface velocity of tidal currents in the area exceeds 0.5 m s^{-1} at spring tides (VisitMyHarbour, 2012), it can be confidently assumed that the shells derive from a location where the annual peak temperatures at the seafloor and surface are (and were in the early 20th century) much the same—i.e. a setting without summer stratification. Mean seasonal extreme surface temperatures at Brighton are 8.0°C for winter and 17.4°C for summer (Global Sea Temperature, 2020)—i.e. within the cool temperate range (winter < 10°C, summer < 20°C; Vignols et al., 2019).

The French Mediterranean shells are a right valve 51 mm in height and a left valve 60 mm in height: FM1 and FM2 = Muséum National d'Histoire Naturelle, Paris (MNHN) IM-2008-1534 and IM-2008-1535, respectively. These are two of the three single valves from La Franqui (the other a right valve 53 mm in height: FM3 = MNHN-IM-2008-1533) for which increment data were supplied by Johnson et al. (2009, table 2). The three specimens were part of a sample of 35 single but unbroken valves (10–60 mm in height; uninvestigated specimens not given MNHN numbers) collected from the beach north of La Franqui on 25th and 31st October 1987 after a storm and stored dry (without soft-parts). It seems unlikely that a storm would have thrown onto the shore valves from more than a very few tens of metres depth—i.e. they were probably from supra-thermocline individuals. The low increment-size variation of FM1 and FM3 (respectively, 0.22 and 0.26 mm between the maximum and minimum of smoothed profiles) accords with this but FM2 provided a much higher value (0.36 mm),

like that of sub-thermocline shells from the Gulf of Tunis (Johnson et al., 2009, table 2). Mean seasonal extreme surface temperatures at La Franqui are about 12°C for winter and 23°C for summer (i.e. within the warm temperate range), but while the cool extreme is the same down to 30 m, the warm extreme declines gradually to about 20°C at 30 m and then somewhat more rapidly to about 17°C at 50 m (NOAA, 1994).

3. Methods

3.1. Laboratory procedures

Shells were coated with a sublimate of ammonium chloride and digitally photographed, then images were inserted into the bespoke software Panopea© (2004, Peinl and Schöne) for the purposes of increment measurement, to the extent that this could be accomplished (increments were usually invisible in the umbonal area, and sometimes elsewhere, due to abrasion). The coating was washed off with tap-water and most shells then underwent the further cleaning procedure adopted by Valentine et al. (2011) for removal of any surficial organic material prior to isotopic sampling. One Adriatic shell (S3A4) and the French Mediterranean shells were sampled before it was decided to implement this procedure. Samples for isotope analysis were obtained by drilling a dorsal to ventral series of shallow (< 1 mm deep) commarginal grooves into the outer surface of the outer (calcite) shell layer, with the sample sites more closely spaced towards the ventral margin in an attempt to maintain temporal resolution in the context of declining growth rate with age. Details of the measurement and sampling methods used, including the adjustment procedure employed where it was impossible to measure or sample along the dorso-ventral (height) axis, are given in Johnson et al. (2019) with respect to another scallop species. All the increment measurements were made by the same person (AMV) to achieve as uniform an approach as possible, given that increment identification can locally be a subjective matter.

Increments are commonly difficult to define between the plicae ('ribs') on left valves (Fig. 3B, C); measurements were made on the plicae in such circumstances. Growth breaks were identified as minor, moderate or major (the last two classes subsequently combined) dependent on the size of the characteristic 'step' in the shell profile, which marks a near or total cessation of extensional growth but not of shell thickening. Minor growth breaks are subtle features (Fig. 3A, B), sometimes only observable by tilting the shell to various angles. The height of growth breaks was therefore determined on the shells themselves (with a ruler) rather than on digital images.

In cool temperate representatives of *A. opercularis*, such as those from around the UK, prominent growth breaks typically occur in winter and appear to represent intervals of a month or two (e.g. Broom and Mason, 1978). However, in other scallop species they may occur at any time of year (e.g. Johnson et al., 2019), presumably reflecting disturbance in some cases, and intervals approaching six months may be represented (Krantz et al., 1984). No assumptions can therefore be made about the timing or duration of growth breaks in warm temperate *A. opercularis*, such as Adriatic individuals, to guide general alignment of shell $\delta^{18}O$ values with predicted values. However, from isotopic evidence of growth slowdown or cessation for several summer months in Adriatic *Pecten jacobaeus*, and of the same for several winter months in Adriatic *Glycymeris pilosa* (Peharda et al., 2019), it is reasonable to expect some attenuation of growth in Adriatic *A. opercularis* during one or both seasons, and to use evidence of this in the form of growth breaks to refine alignments based on identification of annual $\delta^{18}O$ cycles (see Section 3.2).

Table 1 about here - ? single column

Stable oxygen and carbon isotope analysis (given as $\delta^{18}O$ and $\delta^{13}C$) were carried out either at the stable isotope facility, British Geological Survey, Keyworth, UK, or at the Institute of Geosciences, University of Mainz, Germany. At Keyworth samples were analysed using an Isoprime dual inlet

mass spectrometer coupled to a Multiprep system; powder samples were dissolved with concentrated phosphoric acid in borosilicate Wheaton vials at 90°C. At Mainz samples were analysed using a Thermo Finnigan MAT 253 continuous flow-isotope ratio mass spectrometer coupled to a Gasbench II; powder samples were dissolved with water-free phosphoric acid in helium-flushed borosilicate exetainers at 72°C. Both laboratories calculated $\delta^{13}C$ and $\delta^{18}O$ against VPDB and calibrated data against NBS-19 (preferred values: +1.95‰ for $\delta^{13}C$, –2.20‰ for $\delta^{18}O$) and their own Carrara Marble standard (Keyworth: +2.00‰ for $\delta^{13}C$, –1.73‰ for $\delta^{18}O$; Mainz: +2.01‰ for $\delta^{13}C$, –1.91‰ for $\delta^{18}O$). Values were consistently within ± 0.05‰ of the values for $\delta^{18}O$ and $\delta^{13}C$ in NBS-19. Reproducibility was checked by duplicate analysis of some samples, and in the case of seemingly aberrant initial results, repeat sampling and analysis was undertaken. The profiles in Figures 7–9 link singleton values and the means of multiple values. In two cases where results from repeat analysis differed greatly (S3A5, height 46.5 mm; EC2, height 16.5 mm) the more credible data have been used for the profiles and suspect data omitted. Otherwise, all the isotope results obtained are plotted in Figures 7–9.

The full set of raw isotope and increment data, together with modelled values of temperature, salinity and expected shell $\delta^{18}O$ (Section 3.2), is available online (see Appendix A). A summary of the isotope data is provided in Table 1.

3.2. Calculations of temperature and expected shell $\delta^{18}O$

In earlier isotope studies of modern and fossil *A. opercularis* (Hickson et al., 1999, 2000; Johnson et al., 2000, 2009; Valentine et al., 2011; Vignols et al., 2019) the calcite equation of O'Neil et al. (1969) was used to calculate temperatures from shell $\delta^{18}O$ or to calculate expected shell $\delta^{18}O$ values from known temperatures, in each case with an adjustment (most recently –0.27‰, following Gonfiantini et al., 1995) to convert water $\delta^{18}O$ values from the VSMOW scale to the VPDB scale used for calcite. In isotope work on *P. jacobaeus* from the northern Adriatic, Peharda et al. (2019) used the

300 more recent calcite equation of Kim and O'Neil (1997), also widely employed in studies of other
301 calcitic taxa. The equation of Kim and O'Neil (1997) yields temperatures about 2°C lower than that of
302 O'Neil et al. (1969) so the choice of equation is a significant matter. Other calcite equations exist, one
303 of which—the LL (low light) equation of Bemis et al. (1998)—was used by Austin et al. (2006, fig. 6)
304 to derive expected values for calcite $\delta^{18}O$ over a year from monthly data on bottom temperature and
305 water $\delta^{18}O$ for the same latitude (53°N) in the southern North Sea as the *A. opercularis* shell
306 represented in Figure 2A. We used the data of Austin et al. (2006) to also derive expected values of
307 shell $\delta^{18}O$ using the equations of O'Neil et al. (1969) and Kim and O'Neil (1997), and then replicated
308 the three sets of values to produce multi-year profiles (Fig. 6) for comparison with the data from the
309 southern North Sea *A. opercularis* specimen. The most suitable equation was judged by temporally
310 aligning the shell data as well as possible with each profile (i.e. minimising the overall difference
311 between measured and expected shell values within a three-year period, as specified by the number of
312 $\delta^{18}O$ cycles), and then reviewing the closeness of each fit. During early ontogeny, growth of *A.*
313 *opercularis* may be rapid and continuous through summer and winter in the southern North Sea
314 (Johnson et al., 2009). From the long 'wavelength' of the first $\delta^{18}O$ cycle (measured versus shell
315 height) and the absence of visible growth breaks associated with the lowest and highest values (Fig.
316 2A), it is evident that the present specimen did grow rapidly and without interruption during early
317 ontogeny. The most extreme $\delta^{18}O$ values measured over the first cycle can therefore be taken to
318 represent the most extreme temperatures experienced, and the equation yielding predicted $\delta^{18}O$ values
319 closest to those measured can be regarded as the best descriptor of the relationship between
320 temperature and shell $\delta^{18}O$. The LL equation of Bemis et al (1998) provides the closest values (Fig.
321 6), the equation of Kim and O'Neil (1997) yielding values that are somewhat lower than the lowest
322 measured value from the first summer and the equation of O'Neil et al. (1969) yielding values that are
323 somewhat higher than the highest measured value from the first winter. For this reason we used the

LL equation of Bemis et al. (1998) to derive expected values of shell $\delta^{18}O$ and to calculate temperatures from the other *A. opercularis* shells investigated herein.

Fig. 6 about here – single column

ROMS-derived daily salinity values (Fig. 5B) and the salinity-water $\delta^{18}O$ relationship established by Peharda et al. (2019) for adjacent sites were used to calculate daily water $\delta^{18}O$ values (Fig. 5B) for the location and depth of the Adriatic shells. These values and the modelled daily seafloor temperatures (Fig. 5A) were then used in the equation of Bemis et al. (1998) to calculate values of expected shell $\delta^{18}O$ (Fig. 5C) for comparison with data from *A. opercularis*. This mirrors the approach of Peharda et al. (2019) for other locations and depths in the northern Adriatic, except that they employed the equation of Kim and O'Neil (1997) to derive expected values of shell $\delta^{18}O$ for comparison with data from *P. jacobaeus*.

In view of the inadequate contextual information we did not attempt to derive expected daily values of shell $\delta^{18}O$ for comparison with data from the French Mediterranean and English Channel shells. Instead we compared local summer and winter temperatures (Section 2) with the warmest and coolest temperatures calculated from shell $\delta^{18}O$, using the LL equation of Bemis et al. (1998) and a representative single value of water $\delta^{18}O$ from measurements made nearby: +1.3‰ for La Franqui, based on measurements at 4–25 m depth in the north-western Mediterranean (site 1B of Pierre, 1990); +0.2‰ for the English Channel near Brighton, based on measurements in the North Sea (Mook and Vogel, 1968).

4. Results

4.1. Adriatic shells (Fig. 7)

Fig. 7 about here – double column

All $\delta^{18}O$ profiles show between one and two major cycles, the amplitude and (in most cases) wavelength decreasing in the second cycle, where present. By contrast, $\delta^{13}C$ profiles show little variation, values tending to decrease slightly over the course of ontogeny (e.g. Fig. 7F) and occasionally increasing over short intervals in association with decreasing $\delta^{18}O$ (Fig. 7C, E), but otherwise showing no relation to this parameter. In that the isotope data from S3A4 (Fig. 7C) are closely comparable with those from other shells, it appears that omission of the procedure to remove surficial organic material from the shell had little or no effect (cf. Schöne et al., 2017). In all cases apart from S3A1 (Fig. 7A) the smoothed increment profiles exhibit one more-or-less clear major cycle, with a difference of more than 0.30 mm between the maximum and minimum values. The absence of such features from the S3A1 profile could be because it is the shortest of the six. Amongst the five individuals showing marked variation in increment size, the maximum size is observed in mid-ontogeny, and occurs in an interval of decreasing or low $\delta^{18}O$ in four specimens (S3A3, S3A4, S3A5, S3A33) and of increasing $\delta^{18}O$ in one (S3A36). The minimum size is shown in early or late ontogeny and occurs in an interval of decreasing or low $\delta^{18}O$ in four specimens (S3A3, S3A4, S3A5, S3A36) and of high $\delta^{18}O$ in one (S3A33). Growth breaks are concentrated in late ontogeny and are commonly associated with the highest and lowest $\delta^{18}O$ values in this interval. Figure 3B illustrates growth breaks and the pattern and scale of increment variation in S3A4.

4.2. English Channel shells (Fig. 8)

Fig. 8 about here – double column

374 Both the $\delta^{18}O$ and $\delta^{13}C$ profiles of the English Channel shells are very similar in their general
375 features to those from the (similarly sized) Adriatic shells. However, the $\delta^{18}O$ profiles of the former
376 differ by including lower values and the $\delta^{13}C$ profiles by their consistently higher values at all stages
377 of ontogeny (see also Fig. 11), with instances of positive (rather than negative) correlation with $\delta^{18}O$
378 (early ontogeny of EC1—Fig. 8A; late ontogeny of EC2—Fig. 8B). Smoothed increment profiles
379 show a much smaller range of variation (well below 0.30 mm) than is seen in most Adriatic shells.
380 Minimum values are much the same as in Adriatic shells but maximum values are less than in most
381 Adriatic shells. Growth breaks are concentrated in late ontogeny; examples are associated with the
382 $\delta^{18}O$ maxima (but not with the minima) in this interval in the two shells. Figure 3C illustrates the
383 subdued increment variation in EC1.
384
385 *4.3. French Mediterranean shells (Fig. 9)*
386
387 Fig. 9 about here – double column
388
389 The $\delta^{18}O$ profiles are again very similar in their general features to profiles from Adriatic shells,
390 spanning also a comparable range of values. However, in FM1, in which 1.5 cycles are identifiable,
391 the amplitude (and wavelength) is greater in the second (incomplete) cycle. The $\delta^{13}C$ profiles are also
392 quite similar in their general features to those from Adriatic shells, but with higher values at most
393 stages of ontogeny (although not generally as high as from English Channel shells; see also Fig. 11)
394 and instances of positive correlation with $\delta^{18}O$ (mid-ontogeny of FM1—Fig. 9A; late ontogeny of
395 FM2—Fig. 9B), although there are also some intervals of negative correlation in FM1. In view of the
396 evidence from Adriatic shell S3A4 it may be assumed that omission of the procedure to remove
397 surficial organic material had no effect on the isotope data from the French Mediterranean shells. The
398 smoothed increment profiles show variation of less than 0.30 mm (remeasurement of FM2 revealed

399 that the anomalously high variation recorded previously was down to a single, very inaccurate value in
400 the raw data). As in the English Channel shells, minimum increment sizes are much like those from
401 Adriatic shells and maximum sizes are less than from most Adriatic shells. Growth breaks are more
402 frequent in early ontogeny than in the Adriatic and English Channel shells; examples are associated
403 with the $\delta^{18}O$ maxima (but not with the minima) in the two shells.
404
405 **5. Interpretation**
406
407 *5.1. $\delta^{18}O$ data*
408
409 The number of $\delta^{18}O$ cycles (one to two) in the profiles illustrated in Figures 7–9 is the same as in
410 most profiles up to the same shell height from other modern (and fossil) *A. opercularis* (Hickson et
411 al., 1999, 2000; Heilmayer et al., 2004; Johnson et al., 2009; Valentine et al., 2011; Vignols et al.,
412 2019). Taking the cycles essentially to reflect seasonal variation in water temperature (cf. Section 3.2),
413 and their generally declining wavelength to reflect declining growth rate, the implied ages and rates of
414 growth-rate decline are consistent with growth statistics for *A. opercularis* obtained by other means
415 (e.g. Taylor and Venn, 1978; Richardson et al., 1982; Heilmayer et al., 2004). It is thus clear that none
416 of the shells were more than three years old. In the case of the Adriatic specimens, we can use this
417 information to guide temporal alignment of measured $\delta^{18}O$ values with predicted values, following the
418 same approach as for the southern North Sea specimen discussed in Section 3.2. We consider details
419 of the alignment of Adriatic data immediately below, proceeding to evaluate the extent to which shell
420 $\delta^{18}O$ profiles from this area reflect ambient temperature. We then discuss $\delta^{18}O$-derived temperatures
421 from English Channel and French Mediterranean shells in more general terms—i.e. the fidelity of
422 summer and winter values to mean seasonal temperatures.
423

Fig. 10 about here - double column

5.1.1. Adriatic shells

Figure 10 shows predicted shell $\delta^{18}O$ for a period spanning the lives of the Adriatic shells (i.e. from late 2016 as far back as 2013), accompanied by aligned measured values from each shell. It has been assumed that growth breaks adjacent to the locations of maxima and minima in measured values relate to extreme winter and summer temperatures—i.e. the maximum/minimum $\delta^{18}O$ values concerned have been positioned so that the adjacent growth break includes the time of inflection in the curve of predicted values (cf. Section 3.1).

General positioning of values (i.e. assignment to years) was largely unproblematic except in the case of S3A1, where two significantly different 'solutions' emerged: one with most values assigned to 2015, and another with most values assigned to 2014. The latter achieves an alignment that is slightly more precise overall but leaves a gap of 188 days in summer 2015. Unlike the similarly long gaps in summer 2015 in S3A4 (187 days) and S3A36 (174 days) there is no growth break to explain this gap so the former alignment (which leaves a gap of 49 days, unaccompanied by a growth break, in summer 2015) has been used in Figure 10A. Adoption of the alternative alignment for S3A1 would not have affected the argument below. The long gaps (> 100 days; identified by grey bars) in other records are unavoidable; alternative arrangements to reduce them result in larger, inexplicable gaps elsewhere. Some of them are associated with growth breaks but not the winter 2014 gaps in S3A5 and S3A36, and the gaps from spring (or even late winter) 2016 to the date of collection shown by all shells except S3A1 (in which there is nevertheless a shorter gap). The winter 2014 gaps relate to the abraded umbonal areas of the shells concerned, where it was impossible to obtain growth-increment data, and evidence of growth breaks may therefore have been lost. The 2016 gaps probably reflect the culmination of ontogenetic decline in growth rate, with the last sample from each shell (taken at or very close to the shell edge) including a significant amount of material deposited early in the year. The

449 long gaps can therefore be explained by time-averaging of sample material and provide no grounds for
450 suspecting serious misalignment—i.e. with the wrong year.

451 Multiple, similar values within a short time interval (e.g. S3A5 and S3A33, mid-summer 2015)
452 might be regarded as evidence of serious misalignment because they demand very rapid growth.
453 However, the rates required are not unreasonable. In the examples cited the height intervals between
454 the first and last values are 6.0 and 5.5 mm, respectively (Fig. 7D, E), amounts of size increase that
455 have been shown through experiment to be achievable by *A. opercularis* in a month or somewhat less
456 under warm conditions (Broom and Mason, 1978, table 2). This period is comparable to the time
457 interval of 20 days spanned in each case by the mid-summer 2015 values from S3A5 and S3A33, as
458 positioned in Figure 10. In S3A33 a period of 10 days in spring 2015 is represented by a series of five
459 $\delta^{18}O$ values, which align perfectly with the plot of predicted values and cover a height interval of 9.5
460 mm (Fig. 7E), confirming the plausibility of a size increase of 5.5 mm in 20 days during the
461 succeeding summer.

462 While it appears that the $\delta^{18}O$ values from all shells have been associated with the correct year, not
463 every value can be precisely aligned with the curve of predicted values. Small (unavoidable)
464 discrepancies can be considered to reflect the known analytical and modelling errors. Moderate
465 departures (< 0.5‰) from predicted values, for example in summer 2014 (S3A3, S3A4, S3A36; all
466 negative) and winter 2016 (S3A33, S3A36; both positive), seem likely to reflect inaccuracy in the
467 shell record of ambient conditions (i.e. non-equilibrium isotope incorporation), and are discussed
468 further below. Large departures (> 0.5‰; open symbols) from predicted values in summer 2014
469 (S3A5; positive), winter 2015 (S3A3, S3A4, S3A5, S3A33; all negative) and spring 2016 (S3A1;
470 positive) are unlikely to have this cause, given the quite close correspondence of measured to
471 predicted values in *A. opercularis* from the southern North Sea (Fig. 6). Contamination by material
472 from other sample positions can be ruled out because all the significantly discrepant values were
473 checked by resampling, either at the place of the initial sample or very close by. That four shells show

a confirmed, large discrepancy of the same sign in winter 2015 (and that S3A36 shows a smaller discrepancy of the same sign) suggests that the departure from expectation is a function of inaccurate modelling—i.e. that this failed to take into account some environmental event in winter 2015. While in theory the observed negative excursion could reflect a brief warming episode, a winter influx of (isotopically light) freshwater is a more plausible event. The River Po is the likeliest source, given its large supply of freshwater to the northern Adriatic in general (Vilibić et al., 2016, table 1). The confirmed, large, positive departures are difficult to account for, particularly the summer 2014 excursion in S3A5, which could exceed 1.0‰, dependent on precise timing. Being isolated instances, these departures perhaps reflect incorporation of carbonate from some small, unnoticed encrusting organism.

Of those (moderate) departures from predicted values which seem likely to reflect non-equilibrium isotope incorporation, the largest in summer 2014 (0.31‰) is from S3A3 and the largest in winter 2016 (0.28‰) is from S3A33. The former departure translates into a temperature overestimate of 1.5°C and the latter into an underestimate of 1.3°C. While these figures give a good indication of the extent by which seasonal temperatures calculated from *A. opercularis* shell $\delta^{18}O$ might be exaggerations of the temperature extremes experienced, they do not represent amounts which can be routinely combined with isotopic summer and winter temperatures to determine actual seasonal extremes. This is because the extreme measured values of shell $\delta^{18}O$ are often not as low in summer and not as high in winter as the extreme predicted values. Thus, in addition to the large gaps referred to above, there are smaller gaps in the shell records (winter 2015 in S3A36; summer 2015 in S3A1, S3A3, S3A5 and S3A33) which omit values corresponding to the relevant predicted extremes. In the case of winter 2015 in S3A36 the discrepancy between measured and predicted extreme values is fairly small (0.29‰; equivalent to a temperature overestimate of 1.4°C). However, in the summer 2015 cases the discrepancies are substantial (largest 0.98‰ in S3A3; equivalent to a temperature underestimate of 4.7°C). In most cases there are associated growth breaks (possible environmental

cause discussed in Section 5.4), so it is no surprise that the shell records are incomplete. However, the magnitude of the discrepancies with the predicted $\delta^{18}O$ extreme for summer 2015, within datasets for that season which are otherwise fairly complete, is a salutary demonstration of the potential for misinterpretation of summer temperatures from *A. opercularis* shell $\delta^{18}O$. Of the four individuals alive in summer 2014 as well as summer 2015 (S3A3, S3A4, S3A5, S3A36) only S3A5 shows a lower minimum $\delta^{18}O$ value for 2015 than for 2014, despite the predicted minimum for summer 2015 (–0.21‰) being much lower than for 2014 (+0.37‰) as a consequence of the unusually warm conditions (Fig. 5). This suggests that the incompleteness of the summer 2015 records from these shells might be a function of their age and consequent slower growth, leading to greater time-averaging within samples (cf. Fig. 6). However, the summer 2015 records from S3A1 and S3A33, individuals which were not alive in summer 2014, are similarly incomplete. In S3A33 a growth break is associated with the lowest measured value of $\delta^{18}O$ for summer 2015, providing a hint that the individual experienced warmer temperatures than are recorded in its $\delta^{18}O$ profile. However, the discrepancy between the measured and predicted extremes (0.83‰; equivalent to a temperature underestimate of 3.9°C) is not much less than in the ontogenetically older shell S3A3 (see above), and the discrepancy in S3A1 (0.97‰; equivalent to a temperature underestimate of 4.6°C), a shell which shows no growth break in summer 2015, is very nearly the same as in S3A3. It therefore appears that neither restricting sampling to early ontogeny nor examining specimens for the existence of growth breaks are strategies which could lead to accurate estimation of summer temperature every year in the Adriatic from the shell $\delta^{18}O$ of *A. opercularis*. There is potential for serious underestimation of the peak temperature in warm years (evidenced by the data for 2015), although in cooler years (evidenced by the data for 2014) $\delta^{18}O$ records are fairly accurate, tending to provide just a slight overestimate (< 1.5°C) of the warmest temperature. The situation is otherwise for winter temperature, conditions in both 2015 and 2016 being fairly accurately represented by at least some shells, these providing a slight overestimate (1.4°C) of the coolest temperature for the former year and a slight underestimate

(< 1.3°C) for the latter. Turning these findings into guidelines for interpreting $\delta^{18}O$ records from sub-thermocline *A. opercularis* in general, one should only regard minimum $\delta^{18}O$ values as an indication of seafloor temperature in relatively cool summers. Maximum $\delta^{18}O$ values can, however, be regarded as an indication of average winter seafloor temperature, provided that data are available from at least a few shells, and anomalously low values associated with growth breaks are excluded from consideration.

5.1.2. English Channel and French Mediterranean shells

Summer and winter inflections can be recognised in the English Channel and French Mediterranean $\delta^{18}O$ profiles (Figs 8, 9) at the following shell heights. EC1— winter 1: 5.5 mm, summer 1: 38.0 mm, winter 2: 49.5 mm; EC2—summer 1: 16.5 mm, winter 1: 39.0 mm; summer 2: 49.0 mm; FM1—summer 1: 9.0 mm, winter 1: 25.0 mm, summer 2: 48.0 mm; FM2—winter 1: 29.0 mm, summer 1: 41.5 mm. While there are no growth breaks associated with $\delta^{18}O$ minima to suggest truncation of summer records, the association of growth breaks with almost all $\delta^{18}O$ maxima (winter 1 in EC1 is the sole exception) suggests possible truncation of winter records. However, given the lengthy upward and downward trends on either side of each $\delta^{18}O$ maximum, which can be taken to span the preceding autumn and succeeding spring periods, any truncation is likely to have been minor.

The summer 1 isotopic temperatures (from $\delta^{18}O$ minima) in the English Channel shells (EC1: 18.2°C; EC2: 18.8°C) are similar to the local average warm extreme (17.4°C), but consistently a little warmer. The rather cool summer 2 temperature in EC2 (14.8°C) could reflect sampling at inadequate resolution (i.e. closer sampling later in ontogeny failed to compensate for declining growth rate; cf. Fig. 6). All the winter temperatures (from $\delta^{18}O$ maxima) in EC1 (winter 1: 6.1°C; winter 2: 7.2°C) and EC2 (winter 1: 7.2°C) are similar to the local average cool extreme (8.0°C), but consistently a little cooler. As growth breaks are associated with the two warmer (7.2°C) recorded extremes it is possible that the records are a little truncated—i.e. that the actual minimum temperatures in the winters

549 concerned were similar to the cooler (6.1°C) recorded extreme. Like the winter temperatures from the
550 English Channel shells, those from the French Mediterranean shells (FM1, winter 1: 12.9°C; FM2,
551 winter 1: 10.3°C;) are similar to the local average cool extreme (*c.* 12°C), but while one is a little
552 cooler, the other is a little warmer. As growth breaks are associated with both recorded extremes, the
553 actual minimum temperatures in the winters concerned may have been a little lower. All the summer
554 temperatures in FM1 (summer 1: 21.2°C; summer 2: 21.7°C) and FM2 (summer 1: 19.9°C) are cooler
555 than the local average warm extreme at the surface (*c.* 23°C). This seems likely to reflect life-
556 positions near the base of the mixed layer, at depths down to 30 m, where the average peak
557 temperature is 20°C. This would not be inconsistent with transport to the shore during a storm.
558 To summarize and conclude, winter temperatures calculated from the $\delta^{18}O$ of the English Channel
559 and French Mediterranean shells are quite close to expectation; values cooler than the local average
560 (the majority) might represent underestimates of actual winter temperatures due to disequilibrium, but
561 could be essentially accurate, reflecting relatively cool winters. Summer temperatures are in some
562 cases quite close to expectation but in others several degrees cooler; the latter instances might also
563 represent disequilibrium but seem more likely to be effects of growth-rate decline with age or life in
564 relatively deep (but not sub-thermocline) settings. The English Channel and French Mediterranean
565 shells therefore provide a fairly accurate indication of average winter temperatures, like the Adriatic
566 shells, but unlike the latter they also provide (or would be capable of providing if suitably sampled) a
567 fairly accurate indication of average summer benthic temperatures.
568
569 *5.2. $\delta^{13}C$ data*
570
571 Of the three sets of shells, only the French Mediterranean specimens show any sign of the pattern
572 of $\delta^{13}C$-$\delta^{18}O$ covariation predicted for their hydrographic setting from the data and arguments of
573 Arthur et al. (1983). The intervals of negative correlation in FM1 are consistent with the evidence of

574 relatively warm summer temperature from this shell indicating a supra-thermocline setting. However,
575 the interval of positive correlation is inconsistent. The interval of positive correlation in FM2 is
576 consistent with the evidence of relatively cool summer temperature from this shell suggesting a life-
577 position a little below the mixed layer, although only an intra- rather than truly sub-thermocline
578 setting is permissible from the temperature evidence. Far from showing the predicted positive
579 correlation between $\delta^{13}C$ and $\delta^{18}O$ (i.e. in-phase variation), some of the Adriatic (sub-thermocline)
580 shells show instances of negative correlation. Likewise, instead of showing a negative correlation (i.e.
581 antiphase variation), both of the English Channel (supra-thermocline) shells show instances of
582 positive correlation.
583
584 Fig. 11 about here – single column
585
586 The widely exhibited ontogenetic decline in $\delta^{13}C$ values is as seen in many bivalves and may well
587 reflect greater use of carbon released by the organism's respiration (isotopically light) for shell
588 formation with increasing age (Lorrain et al., 2004; McConnaughey and Gillikin, 2008; Chauvaud et
589 al., 2011). The geographic differences in $\delta^{13}C$ values (Adriatic < French Mediterranean < English
590 Channel; Fig. 11) resemble those revealed by Chauvaud et al. (2011, fig. 3) in *Pecten maximus* from
591 coastal locations in the eastern North Atlantic (Spain < France < Norway). Those in *P. maximus*
592 probably relate in part to variation in the amount of respiratory carbon used for shell formation as
593 determined by temperature, but differences in the amount of food consumed, and its carbon isotopic
594 composition, also influence $\delta^{13}C$ in this species (Marchais et al., 2015). While the Adriatic *A.*
595 *opercularis* certainly lived and grew under warmer winter conditions than the English Channel
596 individuals, the French Mediterranean individuals did so under much the same winter temperatures,
597 and actually grew under warmer summer conditions than the Adriatic shells. Differences in shell $\delta^{13}C$
598 are not therefore matched by temperature differences and probably relate mainly to nutrition.

599

600 *5.3. Microgrowth-increment data*

601

602 The variation in (smoothed) increment size of more than 0.30 mm shown by five of the six Adriatic
603 shells is as predicted for their sub-thermocline setting, and the variation of less than 0.30 mm shown
604 by both English Channel shells is as predicted for their supra-thermocline setting. Viewed as
605 essentially supra-thermocline (i.e. including uppermost intra-thermocline settings but no deeper), the
606 variation in increment size of less than 0.30 mm shown by the French Mediterranean shells is also as
607 predicted.

608 The large increments in mid-ontogeny that account for the greater size variation in sub-thermocline
609 Adriatic shells are associated with declining, low or increasing $\delta^{18}O$ values—i.e. with times in the
610 spring–autumn period. They seem likely to reflect high food availability then in the form of
611 phytoplankton. The small increments in early and late ontogeny, often also associated with declining
612 or low $\delta^{18}O$ values, may reflect overriding age effects. The lack of large increments in supra-
613 thermocline English Channel and French Mediterranean shells cannot be attributed to a lack of
614 phytoplankton in the spring–autumn period. Possibly these individuals subsisted largely on
615 resuspended detritus (cf. Johnson et al., 2009). The availability of this throughout the year as a result
616 of wave and current action would account for the minimal variation in increment size, and its low
617 nutritive value would explain the small absolute size of increments.

618

619 *5.4. Synthesis*

620

621 It is clear from the foregoing evidence that the pattern of variation in $\delta^{13}C$ relative to $\delta^{18}O$ cannot
622 be used to distinguish sub- from supra-thermocline examples of *A. opercularis*, but that the pattern of
623 variation in (smoothed) microgrowth-increment height can, at least if a number of specimens are

examined to allow for occasional departures from the norm of large-amplitude (> 0.30 mm) variation over the course of ontogeny in sub-thermocline forms. One qualification is necessary: while the increment results from Adriatic sub-thermocline individuals agree with those obtained previously from Gulf of Tunis specimens, it should be recognised that both sets derive from warm temperate environments. Almost all the available increment information from modern cool temperate shells (Johnson et al., 2009, tables 1, 2) is definitely or probably from supra-thermocline settings, and the two specimens that most likely derive from sub-thermocline settings (mesotidal but *c.*110 m depth in the Firth of Clyde, Scotland and Western Approaches, Ireland/England) actually exhibit little variation in increment height. It is possible therefore that the large-amplitude variation seen in a high proportion of Mediterranean (warm temperate) sub-thermocline *A. opercularis* is not characteristic of cool temperate sub-thermocline forms.

Winter temperatures are quite accurately registered (to within 2°C) by the $\delta^{18}O$ of sub-thermocline shells from the Adriatic, as seemingly by English Channel and French Mediterranean supra- and intra-thermocline shells. However, while English Channel and French Mediterranean shells probably provide (or could provide) a fairly accurate record of summer benthic temperatures, Adriatic shells present a biased picture: they provide a fairly accurate estimate (to within 2°C) of the peak temperature in relatively cool years but a serious underestimate in warm years. Thus the warmest modelled seafloor temperature for the warm summer of 2015 is 23.3°C (Fig. 5A; Table 2) but the warmest isotopic temperature for 2015 (from S3A5) is 20.0°C, well short of this figure. However, the warmest isotopic temperature from the Gulf of Tunis sub-thermocline shell represented in Figure 2B is very close (22.7°C; calculated using a water $\delta^{18}O$ value of +1.35‰, measured at 50 m depth at an adjacent location—site 8 of Pierre, 1990). Hence *A. opercularis* is capable of recording temperatures similar to those reached in warm summers in the Adriatic but for some reason failed to do so there in 2015. Most shells suffered an interruption of growth in summer 2015, suggesting some unfavourable environmental condition. This might have been low quantity or quality of food (cf. Johnson et al.,

649 2009), but hypoxia seems the likeliest cause, given its known effect on growth in bivalves (Gobler et
650 al., 2014; Gobler and Baumann, 2016) and fairly common summer occurrence in the northern Adriatic
651 area (Djakovac et al., 2015). Such evidence of summer benthic oxygen levels as exists in relation to
652 the sample site near Pula (for the summers of 1972, 1977, 1983, 1989, 2003, 2006; Djakovac et al.,
653 2015, fig. 2) indicates or strongly suggests full saturation. However, Kralj et al. (2019) recorded
654 hypoxic events in the Bay of Trieste (*c*. 85 km north of Pula) during the exceptionally warm summers
655 of 2015 and 2016, reversing a 30-year trend to increasing benthic oxygenation, so it is possible that
656 hypoxia extended to the Pula area then. It would certainly be worth measuring benthic oxygen levels
657 in the Pula area during future exceptionally warm summers, and documenting the growth of *A.*
658 *opercularis* over these intervals. It would also be worth investigating the diet of sub- and supra-
659 thermocline *A. opercularis* to see if, as speculated, this differs in sub- and supra-thermocline forms
660 and provides an explanation for the high variation in increment size over the course of ontogeny in the
661 former and low variation in the latter.
662
663 Table 2 about here - ? single column
664
665 **6. Application to the early Pliocene Ramsholt Member**
666
667 Our results from modern shells confirm that the occurrence of high-amplitude increment variation
668 amongst examples of *A. opercularis* from the early Pliocene Ramsholt Member of eastern England is
669 an indication of a sub-thermocline setting, as also suggested by other evidence. Therefore, while
670 isotopic minimum temperatures can be read as surface minima, isotopic maximum temperatures
671 cannot be read as surface maxima. The amount by which the peak in benthic temperature obtained
672 from $\delta^{18}O$ data underestimates the surface maximum temperature is a matter of some uncertainty.
673 Vignols et al. (2019) suggested a stratification factor of 5°C for the Ramsholt Member on the basis of

674 modern temperature data from the Gulf of Tunis. However, as noted earlier, the difference between
675 annual seafloor and surface temperature maxima in the northern Adriatic varies considerably, from
676 3.2−9.9°C over the nine years from 2008−2016. Adding the mean difference (7.7°C) to the seafloor
677 maximum in each year yields, of course, an accurate figure for the mean surface maximum over this
678 period (27.6°C; Table 2). However, while 7.7°C serves as an accurate average stratification factor for
679 the interval, for the two individual years with the highest seafloor temperature maxima (2015: 23.3°C;
680 2016: 23.5°C), it provides significant overestimates of the respective surface maxima (by 1.5°C and
681 4.5°C), because the difference between the surface and seafloor maxima is least in these years (surface
682 maximum 6.2°C higher than seafloor in 2015 and 3.2°C higher than seafloor in 2016; Table 2). We
683 know, however, that while *A. opercularis* shell $\delta^{18}O$ provides a fairly accurate estimate of maximum
684 seafloor temperature in years of relatively cool seafloor conditions (at least in 2014), it provides a
685 3−4°C underestimate in unusually warm years (at least in 2015). Adjusting the maximum (modelled)
686 seafloor temperatures for 2015 and 2016 downward by an amount (3.5°C) reflecting this, then
687 recalculating the mean surface maximum for 2008−2016 assuming the same stratification factor
688 (7.7°C), yields a value of 26.8°C, only 0.8°C below the actual figure (Table 2). Thus, armed with a
689 knowledge of water $\delta^{18}O$ and of the average stratification factor, we should be able to reconstruct the
690 mean surface maximum temperature for any given period quite accurately from *A. opercularis* shell
691 $\delta^{18}O$, irrespective of whether the period includes unusually warm years.

692 Water $\delta^{18}O$ and the average stratification factor cannot be precisely specified in 'fossil' situations,
693 but they may be constrained. Before providing approximations for the Ramsholt Member, it is worth
694 noting the effect of using incorrect, but plausible stratification factors in calculation of Adriatic
695 surface temperature. If, instead of 7.7°C, we add 9.9°C (the largest difference between annual seafloor
696 and surface maxima in the 2008−2016 period) to all the seafloor temperature values used previously,
697 we obtain a figure of 29.0°C for mean surface maximum temperature, just 1.4°C above the actual
698 figure; by contrast, if we add 3.2°C (the smallest difference between annual seafloor and surface

699 maxima in the 2008−2016 period), we obtain a figure of 22.3°C, 5.3°C below the actual figure (Table
700 2). Thus what can be regarded as maximum and minimum stratification factors yield, respectively, a
701 slight overestimate and a significant underestimate of the actual mean surface maximum
702 temperature—i.e. in 'fossil' situations, we should favour estimates of surface maximum temperature
703 based on stratification factors in the upper part of the 'plausible range'. What therefore might be this
704 range for the Ramsholt Member? The lower limit must surely be above 2.6°C, the figure for the
705 difference between the surface (13.7°C) and seafloor (11.1°C) maxima at the stratified North Sea site
706 represented in Figure 1B. The surface maximum at this site (57°N), over 500 km north of the
707 Ramsholt Member's location (*c.* 52°N), is far below the summer surface temperature of at least 20°C
708 implied by the warm temperate pelagic dinoflagellate assemblage of the Ramsholt Member (Head,
709 1997, 1998). There has been a long history of also interpreting the Ramsholt Member's benthic biota
710 as of warm-water aspect, and specifically 'Mediterranean' in the case of the Mollusca (Long and
711 Zalasiewicz, 2011; Vignols et al., 2019). While shell $\delta^{18}O$ evidence argues strongly against warm
712 temperate seafloor conditions, it is entirely consistent (assuming stratification) with summer surface
713 temperatures in the warm temperate range (Johnson et al., 2009; Vignols et al. 2019). Stratification
714 factors under such a climatic regime are therefore the best indication of the plausible range for the
715 Ramsholt Member, and the 3.2−9.9°C northern Adriatic range, discussed above, may well be an
716 appropriate choice. Given the more northerly location than the northern Adriatic (*c*. 45°N) it is
717 difficult to believe that summer insolation during Ramsholt Member deposition would have been
718 sufficient to achieve temperatures as high as those typical of the northern Adriatic (25−30°C; Fig.
719 5A), which are higher than the mean summer surface temperature at the more southerly (*c.* 43°N) La
720 Franqui location (Section 2). On the other hand, even 'generous' interpretations of seafloor
721 temperature from Ramsholt-Member shell $\delta^{18}O$ data (using a water $\delta^{18}O$ of +0.5‰; Johnson et al.,
722 2009; Vignols et al., 2019) provide few indications of benthic temperature maxima like those in the
723 northern Adriatic, which are rarely much below and sometimes above 20°C (Fig. 5A). The difference

between annual surface and seafloor temperature maxima during Ramsholt Member deposition was therefore probably much the same as now in the northern Adriatic, and by the same token, there was probably about the same range of variation in this parameter (stratification factor).

Adopting the northern Adriatic range and favouring values in the upper part on the basis of the argument made earlier, 5, 7 and 9°C are sensible choices for stratification factors to use in calculation of a selection of surface temperature estimates for the Ramsholt Member. We need of course also to identify suitable values for water $\delta^{18}O$, and indeed the most appropriate $\delta^{18}O$-temperature equation. In previous work on Ramsholt-Member *A. opercularis* (Johnson et al., 2009; Vignols et al., 2019), water values of −0.5, −0.2, +0.1 and +0.5‰ were used in conjunction with the calcite equation of O'Neil et al. (1969). The first two water values are minimum and maximum estimates of the Pliocene global seawater average (Buchardt and Simonarson, 2003) and are doubtfully appropriate for a shelf basin somewhat isolated from the North Atlantic (e.g. Dearing Crampton-Flood et al., 2020, fig. 1). The last two are minimum and maximum modelled values for seawater in the Pliocene at the specific location of the Ramsholt Member (Johnson et al., 2009). The minimum modelled value yields temperatures from the co-occurring bivalve *Arctica islandica* that are all below the upper tolerance limit of modern *A. islandica* in the North Sea (16°C; Witbaard and Bergman, 2003), while the maximum modelled value yields a temperature above this from one shell (Vignols et al., 2019). Of the four values previously considered, +0.1‰ is therefore the most credible and adopted here. It is worth noting that this value is almost identical to modern seafloor values in the western part of the southern North Sea (i.e. adjacent to the location of the Ramsholt Member), and that more centrally, within the area of influence of the rivers Rhine, Meuse and Scheldt, values are only 0.2‰ lower (Harwood et al., 2008). In both the western and central southern North Sea seasonal variation in salinity is only about 0.25 PSU (Howarth et al., 1993), which translates to a seasonal variation in water $\delta^{18}O$ of just 0.07‰ using the salinity-water $\delta^{18}O$ relationship for the North Sea of Harwood et al. (2008). It seems doubtful that the additional supply of freshwater from the Baltic region in the Pliocene (e.g. Dearing Crampton-

749 Flood et al., 2020, fig. 1) would have had much effect on salinity, and hence water $\delta^{18}O$, at the
750 location of the Ramsholt Member.
751
752 Table 3 about here - ? single column
753
754 We argued in Section 3.2 that the LL calcite equation of Bemis et al. (1998) is more appropriate
755 than the calcite equation of O'Neil et al. (1969) for calculation of temperatures from *A. opercularis*
756 shell $\delta^{18}O$. Using the former in conjunction with the minimum shell $\delta^{18}O$ values from the 10
757 Ramsholt-Member *A. opercularis* analysed to date, together with the water $\delta^{18}O$ value and (for surface
758 temperatures) stratification factors identified above, yields the summer seafloor and surface
759 temperature estimates set out in Table 3. All surface estimates with a stratification factor of 9°C are in
760 the warm temperate summer range (20°C or above), as are six with a stratification factor of 7°C, and
761 four with a stratification factor of 5°C. These temperatures are consistent with the dinoflagellate
762 evidence referred to above. Included in Table 3 are winter seafloor temperatures calculated from
763 maximum shell $\delta^{18}O$—all well within the cool temperate winter range (below 10°C). Contrary to
764 earlier speculation (Vignols et al., 2019) it is unlikely that surface temperatures were lower, since at
765 present in the North Sea winter seafloor and surface temperatures are identical (Fig. 1). Nevertheless,
766 these firmly cool temperate estimates for winter, combined with the warm temperate surface estimates
767 for summer, indicate that during Ramsholt Member deposition seasonal variation in surface
768 temperature (perhaps > 15°C) was higher than at present in the adjacent southern North Sea (12.4°C;
769 Fig. 1A) and much higher than in the central North Sea (7.5°C; Fig. 1B). As it is not significantly
770 affected by assumptions about water $\delta^{18}O$, this is a robust inference, with implications in its own right
771 for the early Pliocene climatology of NW Europe—e.g. possibly reduced oceanic heat supply
772 (Johnson, 2009; Vignols et al., 2019). It would be desirable, however, to obtain firm estimates of
773 absolute seasonal temperatures. The carbonate clumped isotope (Δ_{47}) technique provides a means of

774 determining water $\delta^{18}O$ and hence of translating shell $\delta^{18}O$ values into reliable temperatures (e.g.
775 Winkelstern et al., 2017; de Winter et al., 2018; Peral et al., 2020). Application of the technique to
776 early and also late Pliocene marine shells from NW Europe that have already supplied $\delta^{18}O$ data
777 (Johnson et al. 2009; Valentine et al., 2011; Vignols et al., 2019) should serve to settle current
778 conflicts over absolute seasonal temperatures in the marine realm and enable accurate comparison
779 with terrestrial absolute temperatures, which are presently at odds with marine temperatures over
780 some intervals (Dearing Crampton-Flood, 2018, 2020). Such an improvement in the marine database
781 would also assist evaluation of the roles of oceanic heat supply and radiative heating in determining
782 regional climate.
783
784 **7. Conclusions**
785
786 Modern *A. opercularis* individuals from (warm temperate) sub-thermocline settings are
787 characterised by high-amplitude variation in microgrowth-increment size over the course of ontogeny;
788 those from supra- (and intra-) thermocline settings show much less variation. In neither sub- nor
789 supra-thermocline settings is there a characteristic pattern of ontogenetic variation in $\delta^{13}C$ relative to
790 $\delta^{18}O$. Shell $\delta^{18}O$ affords a fairly accurate record of winter temperature in both settings and of summer
791 benthic temperature in supra-thermocline settings. It affords a fairly accurate record of summer
792 benthic temperature in sub-thermocline settings during relatively cool years, but in relatively warm
793 years temperature may be seriously underestimated.
794 On the basis of the findings from modern *A. opercularis*, early Pliocene specimens from the
795 Ramsholt Member of the Coralline Crag Formation (UK) can be interpreted as sub-thermocline
796 individuals by the evidence of their increment patterns. Subject to the accuracy of estimates of water
797 $\delta^{18}O$ and (for summer) the difference between maximum seafloor and surface temperatures, their shell
798 $\delta^{18}O$ indicates winter surface temperatures within the cool temperate range and summer surface

799 temperatures at least sometimes in the warm temperate range. There can be little doubt that the
800 seasonal range in surface temperature was higher than now in the area.
801
802 **Acknowledgements**
803
804 We thank L. Iveša and D. Skoko for collecting the set of Adriatic shells alongside their commercial
805 fishing activities, and M. Peharda (Institute of Oceanography and Fisheries, Split, Croatia) for
806 processing and forwarding the shells for investigation. S. Gofas and V. Héros kindly facilitated the
807 loan of French Mediterranean shells from the Muséum National d'Histoire Naturelle, Paris, and T.
808 White and J. Perera did likewise for English Channel shells from the Natural History Museum,
809 London. W. Austin (University of St Andrews) generously retrieved and supplied precise location and
810 depth information relating to the data in Figure 1. We are grateful to M. Maus for assistance with
811 isotopic analysis at the Institute of Geosciences, University of Mainz, and to the Alexander von
812 Humboldt Foundation for support of work there by ALAJ. We also appreciate the assistance of S.
813 Berry (College of Engineering and Technology, University of Derby) in rearranging the temperature-
814 $\delta^{18}O$ equation of O'Neil et al. (1969) to enable derivation of expected shell $\delta^{18}O$ values for given
815 temperatures and water $\delta^{18}O$ values. We thank the two anonymous reviewers for their close reading of
816 the manuscript and constructive comments, which led to significant improvements in the final version.
817
818 **Appendix A. Supplementary data**
819
820 Supplementary data to this article can be found online at https://doi.org/……
821
822 **References**
823

824 Arthur, M.A., Williams, D.F., Jones, D.S., 1983. Seasonal temperature-salinity changes and
825 thermocline development in the mid-Atlantic Bight as recorded by the isotopic composition of
826 bivalves. Geol. 11, 655–659. https://doi.org/10.1130/0091-
827 7613(1983)11<655:STCATD>2.0.CO;2.
828 Austin, W.E.N., Cage, A.G., Scourse, J.D. 2006. Mid-latitude shelf seas: a NW European perspective
829 on the seasonal dynamics of temperature, salinity and oxygen isotopes. The Holocene 16, 937–
830 947. https://doi.org/10.1177/0959683606hl985rp.
831 Bemis, B.E., Spero, H.J., Bijma, J., Lea, D.W., 1998. Reevaluation of the oxygen isotopic
832 composition of planktonic foraminifera: Experimental results and revised paleotemperature
833 equations. Paleoceanogr. 13, 150–160. https://doi.org/10.1029/98PA00070.
834 Broom, M.J., Mason, J., 1978. Growth and spawning in the pectinid *Chlamys opercularis* in relation
835 to temperature and phytoplankton concentration. Mar. Biol. 47, 277–285.
836 https://doi.org/10.1007/BF00541005.
837 Buchardt, B., Simonarson, L.A., 2003. Isotopic palaeotemperatiures from the Tjörnes Beds in Iceland:
838 evidence of Pliocene cooling. Palaeogeogr. Palaeoclimatol. Palaeoecol. 189, 71–95.
839 https://doi.org/10.1016/S0031-0182(02)00594-1.
840 Chauvaud, L., Thébault, J., Clavier, J., Lorrain, A., Strand, Ø., 2011. What's hiding behind
841 ontogenetic $\delta^{13}C$ variations in mollusk shells? New Insights from the Great Scallop (*Pecten*
842 *maximus*). Estuaries and Coasts 34, 20111–220. https://doi.org/10.1007/s12237-010-9267-4.
843 Chavanne, C., Janeković, I., Flament, P., Poulain, P.-M., Kuzmić, M., Gurgel, K.-W., 2007. Tidal
844 currents in the northwestern Adriatic: High- frequency radio observations and numerical
845 model predictions. J. Geophys. Res.—Oceans 112, eC03S21.
846 https://doi.org/10.1029/2006JC003523.
847 Dearing Crampton-Flood, E., Peterse, F., Munsterman, D., Sinninghe Damsté, J. S., 2018. Using
848 tetraether lipids archived in North Sea Basin sediments to extract North Western European

Pliocene continental air temperatures. Earth Planet. Sci. Lett. 490, 193–205. https://doi.org/10.1016/j.epsl.2018.03.030.

Dearing Crampton-Flood, E., Noorbergen, L.J., Smits, D., Boschman, R.C., Donders, T.H., Muns, D.K., 2020. A new age model for the Pliocene of the southern North Sea basin: a multi-proxy climate reconstruction. Clim. Past 16, 523–541. https://doi.org/10.5194/cp-16-523-2020.

De Winter, N.J., Vellekoop, J., Vorsselmans, R., Golreihan, A., Soete, J., Petersen, S.V., Meyer, K.W., Casadio, S., Speijer, R.P., Claeys, P., 2018. An assessment of latest Cretaceous *Pycnodonte vesicularis* (Lamarck, 1806) shells as records for palaeoseasonality: a multi-proxy investigation. Clim. Past 14, 725–749. https://doi.org/10.5194/cp-14-725-2018.

Djakovac, T., Supić, N., Bernardi Aubry, F., Degobbis, D., Giani, M., 2015. Mechanisms of hypoxia frequency changes in the northern Adriatic Sea during the period 1972–2012. J. Mar. Syst. 141, 179–189. https://doi.org/10.1016/j.jmarsys.2014.08.001.

Elliott, A.J., Li, Z., 1991. Thermocline depths and water temperature at selected sites in the N.W. European shelf seas. Mar. Pollut. Bull., 22, 282−286. https://doi.org/10.1016/0025-326X(91)90805-3.

Foster, L.C., Allison, N., Finch, A.A., Andersson, C., Ninnemann, U.S., 2009. Controls on $\delta^{18}O$ and $\delta^{13}C$ profiles within the aragonite bivalve *Arctica islandica*. The Holocene 19, 549–558, https://doi.org/10.1177/0959683609104028.

Gillikin, D.P., Wanamaker, A.D., Andrus, F.T., 2019. Chemical sclerochronology. Chem. Geol. 526, 1–6. https://doi.org/10.1016/j.chemgeo.2019.06.016.

Global Sea Temperature, 2020. Brighton sea temperature. https://www.seatemperature.org/europe/united-kingdom/brighton.htm (accessed 26 March 2020).

Gobler, C.J., Baumann H., 2016. Hypoxia and acidification in ocean ecosystems: coupled dynamics and effects on marine life. Biol. Lett. 12, e20150976. https://doi.org/10.1098/rsbl.2015.0976.

874 Gobler, C.J., DePasquale, E.L., Griffith, A.W., Baumann, H., 2014. Hypoxia and acidification have
875 additive and synergistic negative effects on the growth, survival, and metamorphosis of early
876 life stage bivalves. PLoS ONE 9, e83648. https://doi.org/10.1371/journal.pone.0083648.
877 Gonfiantini, R., Stichler, W., Rozanski,, K. 1995 Standards and intercomparison materials distributed
878 by the International Atomic Energy Agency for stable isotope measurements, in: International
879 Atomic Energy Agency, Reference and Intercomparison Materials for Stable Isotopes of Light
880 Elements: IAEA-TECDOC-825, Vienna, Austria, pp. 13–29.
881 Harwood, A.J.P., Dennis, P.F., Marca, A.D., Pilling, G.M., Millner, R.S., 2008. The oxygen isotope
882 composition of water masses within the North Sea. Estuar. Coast. Shelf Sci. 78, 353-359.
883 https://doi.org/10.1016/j.ecss.2007.12.010.
884 Head, M.J., 1997. Thermophilic dinoflagellate assemblages from the Mid-Pliocene of eastern
885 England. J. Paleontol. 71, 165–193. https://doi.org/10.1017/S0022336000039123.
886 Head, M.J., 1998. New goniodomacean dinoflagellates with a compound hypotractal archeopyle from
887 the late Cenozoic: Capisocysta Warny and Wrenn, emend. J. Paleontol. 72, 797–809.
888 https://doi.org/10.1017/S0022336000027153.
889 Heilmayer, O., Brey, T., Storch, D., Mackensen, A., Arntz, W.E., 2004. Population dynamics and
890 metabolism of *Aequipecten opercularis* (L.) from the western English Channel (Roscoff,
891 France). J. Sea Res. 52, 33–44. https://doi.org/10.1016/j.seares.2003.07.005.
892 Hickson, J.A., Johnson, A.L.A., Heaton, T.H.E., Balson, P.S., 1999. The shell of the Queen Scallop
893 *Aequipecten opercularis* (L.) as a promising tool for palaeoenvironmental reconstruction:
894 evidence and reasons for equilibrium stable-isotope incorporation. Palaeogeogr.
895 Palaeoclimatol. Palaeoecol. 154, 325–337. https://doi.org/10.1016/S0031-0182(99)00120-0.
896 Hickson, J.A., Johnson, A.L.A., Heaton, T.H.E., Balson, P.S., 2000. Late Holocene environment of the
897 southern North Sea from the stable isotopic composition of Queen Scallop shells.

898 Palaeontolog. Electron. 3, iss. 2, art. 3, 11 pp. http://palaeo-
899 electronica.org/2000_2/scallop/issue2_00.htm.
900 Howarth, M.J., Dyer, K.R., Joint, I.R., Hydes, D.J., Purdie, D.A., Edmunds, H., Jones, J.E., Lowry,
901 R.K., Moffat, T.J., Pomroy, A.J., Proctor, R. 1993. Seasonal cycles and their variability.
902 Philosophical Transactions R. Soc. A, 343, 383−403. https://doi.org/10.1098/rsta.1993.0054.
903 Janeković, I., Dutour Sikirić, M., Tomažić, I., Kuzmić, M., 2010. Hindcasting the Adriatic Sea surface
904 temperature and salinity: A recent modeling experience. Geofizika 27, 85–100.
905 Janeković, I., Mihanović, H., Vilibić, I., Tudor, M., 2014. Extreme cooling and dense water formation
906 estimates in open and coastal regions of the Adriatic Sea during the winter of 2012. J.
907 Geophys. Res.—Oceans 119, 3200–3218. https://doi.org/10.1002/2014JC009865.
908 Johnson, A.L.A., Hickson, J.A., Bird, A., Schöne, B.R., Balson, P.S., Heaton, T.H.E., Williams, M.,
909 2009. Comparative sclerochronology of modern and mid-Pliocene (c. 3.5 Ma) *Aequipecten*
910 *opercularis* (Mollusca, Bivalvia): an insight into past and future climate change in the north-
911 east Atlantic region. Palaeogeogr. Palaeoclimatol. Palaeoecol. 284, 164–179.
912 https://doi.org/10.1016/j.palaeo.2009.09.022.
913 Johnson, A.L.A., Valentine, A., Leng, M.J., Sloane, H.J., Schöne, B.R., Balson, P.S., 2017. Isotopic
914 temperatures from the Early and Mid-Pliocene of the US Middle Atlantic Coastal Plain, and
915 their implications for the cause of regional marine climate change. Palaios 32, 250–269.
916 https://doi.org/10.2110/palo.2016.080.
917 Johnson, A.L.A., Valentine, A.M., Leng, M.J., Schöne, B.R., Sloane, H.J., 2019. Life history,
918 environment and extinction of the scallop *Carolinapecten eboreus* (Conrad) in the Plio-
919 Pleistocene of the US eastern seaboard. Palaios 34, 49–70.
920 https://doi.org/10.2110/palo.2018.056.

921 Kim, S.-T., O'Neil, J.R., 1997. Equilibrium and nonequilibrium oxygen isotope effects in synthetic
922 carbonates. Geochim. Cosmochim. Acta 61, 3461–3475. https://doi.org/10.1016/S0016-
923 7037(97)00169-5.
924 Kralj, M., Lipizer, M., Čermelj, B., Celio, M., Fabbro, C., Brunetti, F., Francé, J., Mozetič, P., Giani,
925 M., 2019. Hypoxia and dissolved oxygen trends in the northeastern Adriatic Sea (Gulf of
926 Trieste). Deep Sea Res. Part II: Topical Stud. Oceanography, 164, 74−88.
927 https://doi.org/10.1016/j.dsr2.2019.06.002.
928 Krantz, D.E., 1990. Mollusk-isotope records of Plio-Pleistocene marine paleoclimate, U.S. Middle
929 Atlantic Coastal Plain. Palaios 5, 317–335. https://doi.org/10.2307/3514888.
930 Krantz, D.E., Jones, D.S., Williams, D.F., 1984. Growth rates of the sea scallop, *Placopecten*
931 *magellanicus*, determined from the $^{18}O/^{16}O$ record in shell calcite. Biol. Bull. 167, 186–199.
932 https://doi.org/10.2307/1541347.
933 Krantz, D.E., Williams, D.F., Jones, D.S., 1987. Ecological and paleoenvironmental information using
934 stable isotope profiles from living and fossil molluscs: Palaeogeogr. Palaeoclimatol.
935 Palaeoecol. 58, 249–266. https://doi.org/10.1016/0031-0182(87)90064-2.
936 Long, P.E., Zalasiewicz, J.A., 2011. The molluscan fauna of the Coralline Crag (Pliocene, Zanclean)
937 at Raydon Hall, Suffolk, UK: Palaeoecological significance reassessed. Palaeogeogr.
938 Palaeoclimatol. Palaeoecol. 309, 53–72. https://doi.org/10.1016/j.palaeo.2011.05.039.
939 Lorrain, A., Paulet, Y.M., Chauvaud, L., Dunbar, R., Mucciarone, D., Fontugne, M., 2004. $\delta^{13}C$
940 variation in scallop shells: Increasing metabolic carbon contribution with body size?
941 Geochim.Cosmochim. Acta 68, 3509–3519. https://doi.org/10.1016/j.gca.2004.01.025.
942 Marchais, V., Richard, J., Jolivet, A., Flye-Sainte-Marie, J., Thébault, J., Jean, F., Richard, P., Paulet,
943 Y.-M., Clavier, J., Chauvaud, L., 2015. Coupling experimental and field-based approaches to
944 decipher carbon sources in the shell of the great scallop, *Pecten maximus* (L.). Geoch.
945 Cosmochim. Acta 168, 58–69. https://doi.org/10.1016/j.gca.2015.07.010.

McConnaughey, T.A., Gillikin, D.P., 2008. Carbon isotopes in mollusk shell carbonates. Geo-Mar. Lett. 28, 287–299. https://doi.org/10.1007/s00367-008-0116-4.

Mook, W.G., Vogel, J.C., 1968. Isotopic equilibrium between shells and their environment. Science 159, 874–875. https://doi.org/10.1126/science.159.3817.874.

NOAA (US Department of Commerce, National Oceanic and Atmospheric Administration, 1994. NODC (Levitus) World Ocean Atlas: Ocean Temperature: Monthly Long Term Mean. https://www.esrl.noaa.gov/psd/cgi-bin/db_search/DBSearch.pl?Dataset=NODC+(Levitus)+World+Ocean+Atlas&Variable=Ocean+temperature (accessed 25 March 2020).

O'Neil, J.R., Clayton, R.N., Mayeda, T.K., 1969. Oxygen isotope fractionation in divalent metal carbonates. J. Chem. Phys. 51, 5547–5558. https://doi.org/10.1063/1.1671982.

Owen, R., Richardson, C., Kennedy, H., 2002. The influence of shell growth rate on striae deposition in the scallop *Pecten maximus.* J. Mar. Biol. Assoc. U. K. 82, 621–623. https://doi.org/10.1017/S0025315402005969.

Peharda, M., Thébault, J., Markulin, K., Schöne, B.R., Janeković, I., Chauvaud, L., 2019. Contrasting shell growth strategies in two Mediterranean bivalves revealed by oxygen-isotope ratio geochemistry: The case of *Pecten jacobaeus* and *Glycymeris pilosa*. Chem. Geol. 526, 23–35. https://doi.org/10.1016/j.chemgeo.2017.09.029.

Peral, M., Blamart, D., Bassinot, F., Daëron, M., Dewilde, F., Rebaubier, H, Nomade, S., Girone, A, Marino, M., Maiorano, P, Ciaranfi, N., 2020. Changes in temperature and oxygen isotopic composition of Mediterranean water during the Mid-Pleistocene transition in the Montalbano Jonico section (southern Italy) using the clumped-isotope thermometer. Palaeogeogr. Palaeoclimatol. Palaeoecol. 544, https://doi.org/10.1016/j.palaeo.2020.109603.

Pierre, C., 1999. The oxygen and carbon isotope distribution in the Mediterranean water masses. Mar. Geol. 153, 41–55. https://doi.org/10.1016/S0025-3227(98)00090-5.

971 Prendergast, A.L., Versteegh, E.A.A., Schöne, B.R., 2017. New research on the development of high-
972 resolution palaeoenvironmental proxies from geochemical properties of biogenic carbonates.
973 Palaeogeogr. Palaeoclimatol. Palaeoecol. 484, 1–6.
974 https://doi.org/10.1016/j.palaeo.2017.05.032.
975 Ren, J.S., Ross, A.H.. Schiel, D.R., 2000. Functional descriptions of feeding and energetics of the
976 Pacific oyster *Crassostrea gigas* in New Zealand. Mar. Ecol., Prog. Series 208, 119–130.
977 https://doi.org/10.3354/meps208119.
978 Schöne, B.R., Surge, D., 2005. Looking back over skeletal diaries — High-resolution environmental
979 reconstructions from accretionary hard parts of aquatic organisms. Palaeogeogr.
980 Palaeoclimatol. Palaeoecol. 228, 1–3. https://doi.org/10.1016/j.palaeo.2005.03.043.
981 Schöne, B.R., Fiebig, J., 2009. Seasonality in the North Sea during the Allerød and Late Medieval
982 Climate Optimum using bivalve sclerochronology. Int. J. Earth Sci. 98, 83–98.
983 https://doi.org/10.1007/s00531-008-0363-7.
984 Schöne, B.R., Gillikin, D.P., 2013. Unravelling environmental histories from skeletal diaries—
985 Advances in sclerochronology. Palaeogeogr. Palaeoclimatol. Palaeoecol. 373, 1–5.
986 https://doi.org/10.1016/j.palaeo.2012.11.026.
987 Schöne, B.R., Freyre Castro, A.D., Fiebig, J., Houk, S.D., Oschmann, W., Kröncke, I., 2004. Sea
988 surface water temperatures over the period 1884–1983 reconstructed from oxygen isotope
989 ratios of a bivalve mollusc shell (*Arctica islandica*, southern North Sea). Palaeogeogr.
990 Palaeoclimatol. Palaeoecol. 212, 215–232. https://doi.org/10.1016/j.palaeo.2004.05.024.
991 Schöne, B.R., Houk, S.D., Freyre Castro, A.D., Fiebig, J., Kröncke, I., Dreyer, W., Oschmann, W.,
992 2005a. Daily growth rates in shells of *Arctica islandica*: assessing subseasonal environmental
993 controls on a long-lived bivalve mollusk. Palaios 20, 78–92.
994 https://doi.org/10.2110/palo.2003.p03-101.

995 Schöne, B.R., Fiebig, J., Pfeiffer, M., Gleß, R., Hickson, J., Johnson, A.L.A., Dreyer, W., Oschmann,
996 W., 2005b. Climate records from a bivalved Methuselah (*Arctica islandica*, Mollusca;
997 Iceland). Palaeogeogr. Palaeoclimatol. Palaeoecol. 228, 130–148.
998 https://doi.org/10.1016/j.palaeo.2005.03.049.
999 Schöne, B.R., Schmitt, K., Maus, M., 2017. Effects of sample pretreatment and external
1000 contamination on bivalve shell and Carrara marble $\delta^{18}O$ and $\delta^{13}C$ signatures. Palaeogeogr.
1001 Palaeoclimatol. Palaeoecol. 484, 22–32. https://doi.org/10.1016/j.palaeo.2016.10.026.
1002 Stenni, B., Nichetto, P., Bregant, D., Scarazzato, P., Longinelli, A., 1995. The $\delta^{18}O$ signal of the
1003 northward flow of Mediterranean waters in the Adriatic Sea. Oceanol. Acta 18, 319–328.
1004 Taylor, A.C., Venn, T.J., 1978. Growth of the queen scallop, *Chlamys opercularis*, from the Clyde
1005 Sea area. J. Mar. Biol. Assoc. U. K. 58, 687–700.
1006 https://doi.org/10.1017/S0025315400041333.
1007 Valentine, A., Johnson, A.L.A., Leng, M.J., Sloane, H.J., Balson, P.S., 2011. Isotopic evidence of
1008 cool winter conditions in the mid-Piacenzian (Pliocene) of the southern North Sea Basin.
1009 Palaeogeogr. Palaeoclimatol. Palaeoecol. 309, 9–16.
1010 https://doi.org/10.1016/j.palaeo.2011.05.015.
1011 van Leeuwen, S., Tett, P., Mills, D., van der Molen, J., 2015. Stratified and nonstratified areas in the
1012 North Sea: Long-term variability and biological and policy implications, J. Geophys. Res.—
1013 Oceans 120, 4670–4686. https://doi.org/10.1002/2014JC010485.
1014 Vignols, R.M., Valentine, A.M., Finlayson, A.G., Harper, E.M., Schöne, B.R., Leng, M.J., Sloane,
1015 H.J., Johnson, A.L.A., 2019. Marine climate and hydrography of the Coralline Crag (early
1016 Pliocene, UK): isotopic evidence from 16 benthic invertebrate taxa. Chem. Geol. 536, 62–83.
1017 https://doi.org/doi:10.1016/j.chemgeo.2018.05.034.

VisitMyHarbour, 2012. Hourly tidal streams, English Channel East. https://www.visitmyharbour.com/articles/3173/hourly-tidal-streams-english-channel-east/ (accessed 26 March 2020).

Vilibić, I., Mihanović, H., Janeković, I., Šepić, J., 2016. Modelling the formation of dense water in the northern Adriatic: Sensitivity studies. Ocean Model. 101, 17–29. https:doi.org/10.1016/j.ocemod.2016.03.001.

Winkelstern, I. Z., Rowe, M.P., Lohmann, K.C., Defliese, W.F., Petersen, S.V., Brewer , A.W., 2017. Meltwater pulse recorded in Last Interglacial mollusk shells from Bermuda. Paleoceanogr. 32. https://doi.org/10.1002/2016PA003014.

Witbaard, R., Bergman, M.J.N., 2003. The distribution and population structure of the bivalve *Arctica islandica* L. in the North Sea: what possible factors are involved? J. Sea Res. 50, 11–25. https://doi.org/10.1016/S1385-1101(03)00039-X.

FIGURE CAPTIONS

Fig. 1. Profiles of monthly average surface (red line) and seafloor (blue line; red where identical with surface) temperature for locations in the southern (A) and central (B) North Sea (data from Austin et al., 2006, fig. 8). Note the almost identical summer surface and seafloor temperatures at the shallow (well-mixed) southern location and the strongly divergent summer temperatures at the deeper (seasonally stratified) northern location (see also Elliott and Li, 1991; van Leeuwen et al., 2015). Summer and winter surface temperatures are within the respective cool temperate ranges (< 20°C, < 10°C; Vignols et al., 2019) at both locations.

Fig. 2. Profiles of ontogenetic variation in $\delta^{13}C$ (grey), $\delta^{18}O$ (pink) and microgrowth-increment height (green; thicker, continuous line connects 5-point moving averages) in *Aequipecten opercularis* from:

(A) a supra-thermocline setting in the UK sector of the southern North Sea (macrotidal); (B) a sub-thermocline setting in the Gulf of Tunis, southern Mediterranean Sea (microtidal, 50 m depth); (C) the Ramsholt Member of the Coralline Crag Formation (early Pliocene), Suffolk, eastern England. Specimens represented are, respectively, British Geological Survey (BGS) Zt 9957, Muséum National d'Histoire Naturelle, Paris (MNHN), IM-2008-1537, and University of Derby, Geological Collections (UD) 52795 (illustrated in Fig. 3A). Data from Johnson et al. (2009), where further background information can be found. Specific location for BGS Zt 9957 given in Hickson et al. (2000); general location for all shells shown in Fig. 4. The isotopic axis has been reversed in each part so that lower values of shell $\delta^{18}O$ (corresponding to higher temperatures) plot towards the top. Note that data for BGS Zt 9957, a specimen from which the dorsal part had been broken off, are here correctly plotted (as by Hickson et al., 2000, fig. 4) in relation to height from the ventral margin, unlike in plots by Johnson et al. (2009, fig 4D; 2017, fig. 5B). Open triangles indicate the position of minor growth breaks. Value shown for variation in increment height is the difference between the maximum and minimum of smoothed (5-point moving average) data.

Fig. 3. Microgrowth increments in *Aequipecten opercularis.* A: the early Pliocene specimen (right valve) from which the measurements in Fig. 2C were obtained; B: the modern Adriatic specimen S3A4 (left valve) from which the measurements in Fig. 7C were obtained; C: the modern English Channel specimen EC1 (left valve) from which the measurements in Fig. 8A were obtained. Note the substantial variation in increment size in A and B, and the much more uniform increment size in C. Triangles indicate the positions of minor (open) and moderate–major (filled) growth breaks within the area of the enlargements. Scale bars = 10 mm; vertical for full-shell images, horizontal for enlargements. Microgrowth increments have been described as 'striae' in work on this and other scallop species (e.g. Broom and Mason, 1978; Owen et al., 2002; Peharda et al., 2019). They are bounded by commarginal lamellae, which on left valves (e.g. B, C) are commonly discontinuous

between the plicae ('ribs'), making it difficult to define increments there. In such circumstances measurements were made on the plicae.

Fig. 4. Collection locations of the Adriatic (1), English Channel (2) and French Mediterranean (3) shells, and of the shells represented in Fig. 2A (4), Fig. 2B (5) and Fig. 2C (6). See Section 2 and Table 1 for details.

Fig. 5. A: Profiles of daily temperature from 2008–2016 for the surface (red line) and seafloor (38 m depth; blue line) at the location of the Adriatic specimens, derived using the numerical ocean model ROMS. B: Profiles of daily salinity and water $\delta^{18}O$ at the seafloor for the same location and interval; salinity derived using ROMS and water $\delta^{18}O$ derived using the salinity-water $\delta^{18}O$ relationship of Peharda et al. (2019), based on the data of Stenni et al. (1995) from adjacent sites in the northern Adriatic. C: Predicted shell (calcite) $\delta^{18}O$ for the location and depth of the Adriatic specimens, derived using the seafloor temperature and water $\delta^{18}O$ data in A and B, and the LL equation of Bemis et al. (1998). Note that the $\delta^{18}O$ axis has been reversed in C (see Fig. 2 for explanation). Error estimates have been excluded for the sake of clarity but are included in the shorter profile of predicted shell $\delta^{18}O$ (2013–2016) in Fig. 10. All data available online (see Appendix A).

Fig. 6. Shell $\delta^{18}O$ values (filled circles) from Fig. 2A (supra-thermocline *A. opercularis* from 53°N in the North Sea) temporally aligned with a curve (pink line) of expected monthly shell (calcite) $\delta^{18}O$ for 53°N in the North Sea, derived using the LL equation of Bemis et al. (1998) and the monthly average seafloor temperature and water $\delta^{18}O$ data of Austin et al. (2006, fig. 8), replicated over four years (note that the $\delta^{18}O$ axis has been reversed; see Fig. 2 for explanation). Also included are curves based on the same data but derived using the calcite equations of O'Neil et al. (1969; lavender) and Kim and O'Neil (1997; gold). Minor growth breaks (open triangles) inserted in accordance with their position

1093 relative to measured $\delta^{18}O$ values (Fig. 2A). The decreasing completeness of the measured record over
1094 time probably reflects increasing time-averaging within samples due to ontogenetic decline in growth
1095 rate.
1096
1097 **Fig. 7.** Isotope and increment data for Adriatic shells S3A1 (A), S3A3 (B), S3A4 (C), S3A5 (D),
1098 S3A33 (E) and S3A36 (F), plotted as in Fig. 2, with a pale green background used to correspond with
1099 Fig. 2B (data also from a sub-thermocline setting). Isotope profiles link singleton or mean values
1100 (crosses indicate the values from which these were derived). Open and filled triangles indicate the
1101 position of minor and moderate–major growth breaks, respectively. S3A4 is illustrated in Fig. 3B.
1102
1103 **Fig. 8.** Isotope and increment data for English Channel shells EC1 (A) and EC2 (B), plotted as in Fig.
1104 2, with a pale blue background used to correspond with Fig. 2A (data also from a supra-thermocline
1105 setting). Isotope profiles link singleton or mean values (crosses indicate the values from which these
1106 were derived). Open and filled triangles indicate the position of minor and moderate–major growth
1107 breaks, respectively. EC1 is illustrated in Fig. 3C.
1108
1109 **Fig. 9.** Isotope and increment data for French Mediterranean shells FM1 (A) and FM2 (B), plotted as
1110 in Fig. 2, with a pale blue background used to correspond with Fig. 2A (data also from a supra-
1111 thermocline setting). Increment data from 55–60 mm height in FM2 have been excluded in the
1112 interests of clarity and comparability with other datasets; inclusion of these data (available online; see
1113 Appendix A) would not have increased the range of variation recorded. Open and filled triangles
1114 indicate the position of minor and moderate–major growth breaks, respectively.
1115
1116 **Fig. 10.** Values of $\delta^{18}O$ (circles; open for anomalous values) from Adriatic shells S3A1 (A), S3A3
1117 (B), S3A4 (C), S3A5 (D), S3A33 (E) and S3A36 (F), aligned with a curve of predicted daily values.

Note that the $\delta^{18}O$ axis has been reversed (see Fig. 2 for explanation). Measured values from Fig. 7 (individual values contributing to means excluded); predicted values from Fig. 5C, with added error estimates (dotted lines) based on 1σ values for modelled temperature and salinity. Minor and moderate–major growth breaks (open and filled triangles, respectively) inserted in accordance with their position relative to measured $\delta^{18}O$ values (Fig. 7). Vertical grey bars signify gaps of > 100 days in the sequence of measured $\delta^{18}O$ values. References in the text to winters in specific calendar years refer to the cold period (i.e. the interval of high $\delta^{18}O$) at the start of the year stated.

Fig. 11. Scatterplot showing the relatively low $\delta^{13}C$ values from Adriatic shells (open orange diamonds), the relatively high values from English Channel shells (filled teal diamonds), and the intermediate values from French Mediterranean shells (black crosses), independent of $\delta^{18}O$. Data from the profiles in Figs 7–9.

TABLE CAPTIONS

Table 1

Locational information and descriptive statistics for shell $\delta^{13}C$ and $\delta^{18}O$

Table 2

Modelled annual surface and seafloor temperature maxima in the northern Adriatic (Fig. 5A; Appendix A), and inferred surface maxima from accurate and underestimated (2015, 2016) seafloor data, using various stratification factors (see text for explanation of underestimation and stratification factors)

Table 3

1143 Seasonal seafloor and surface temperatures from $\delta^{18}O$ of Ramsholt Member *A. opercularis*, calculated

1144 using the LL equation of Bemis et al. (1998) and water $\delta^{18}O$ of +0.1‰

1145

1146 Total word-count: 14,159

Figure 1

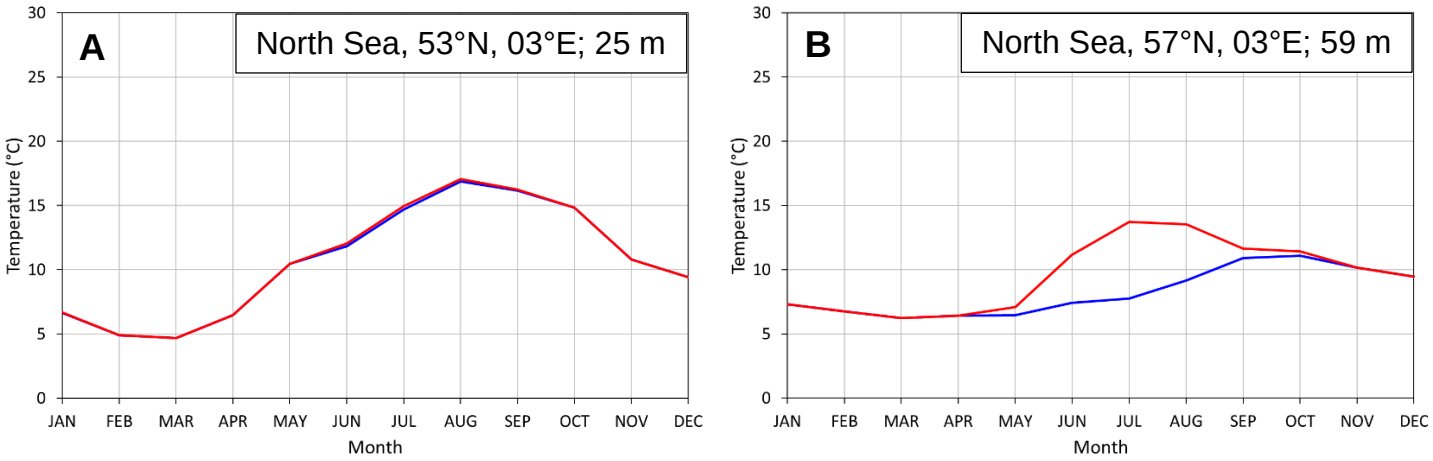

FIGURE 1 – double column

Figure 2

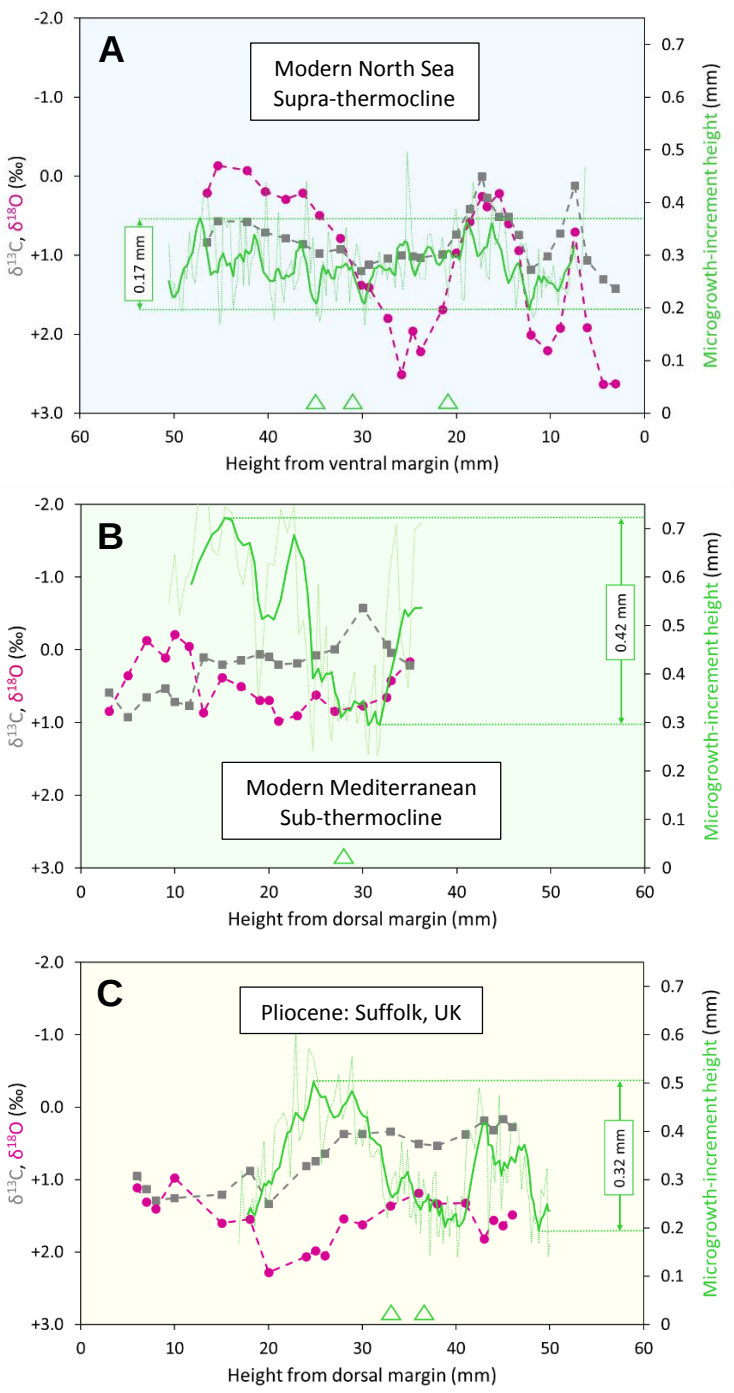

FIGURE 2 – single column

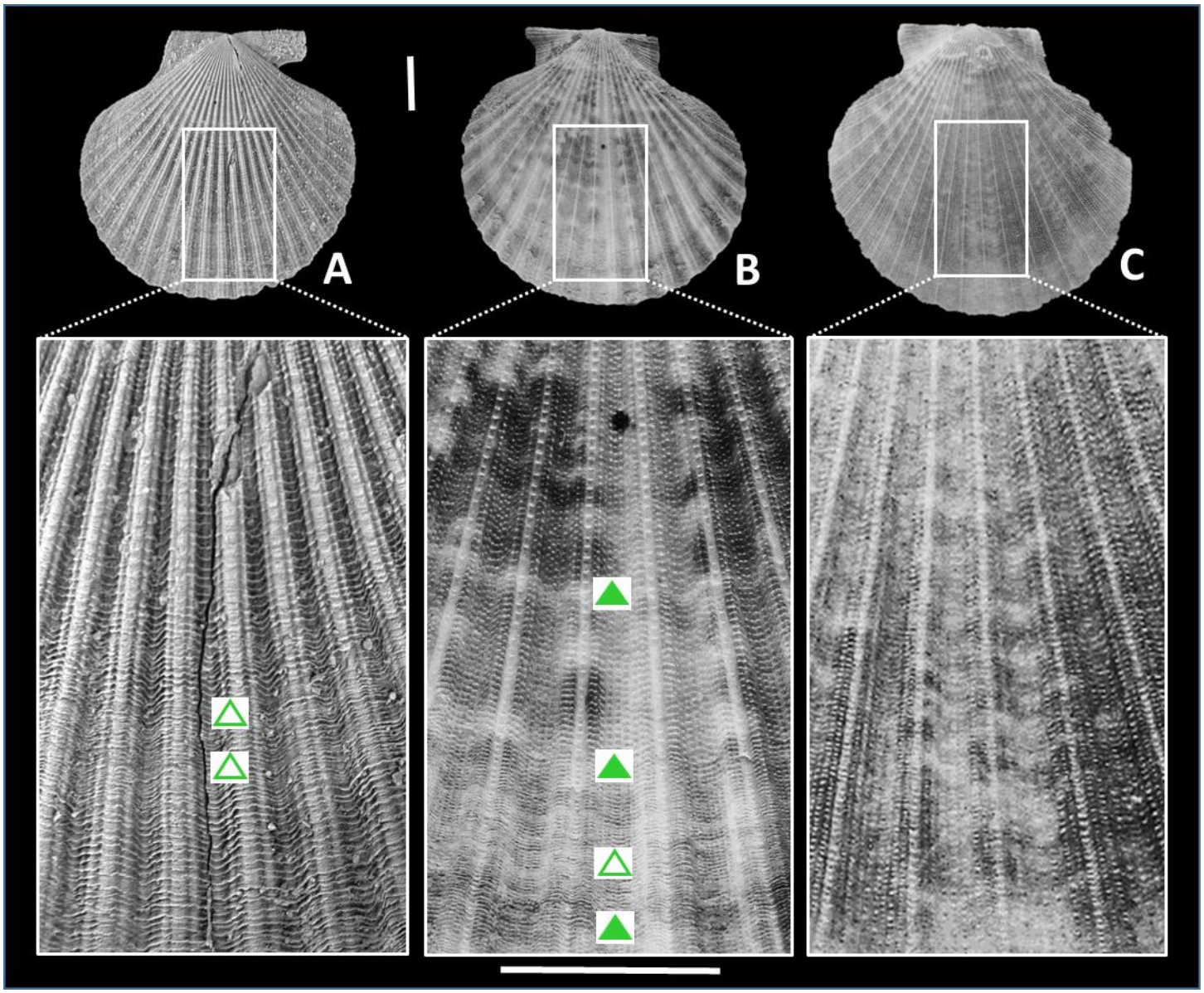

FIGURE 3 – double column

Figure 4

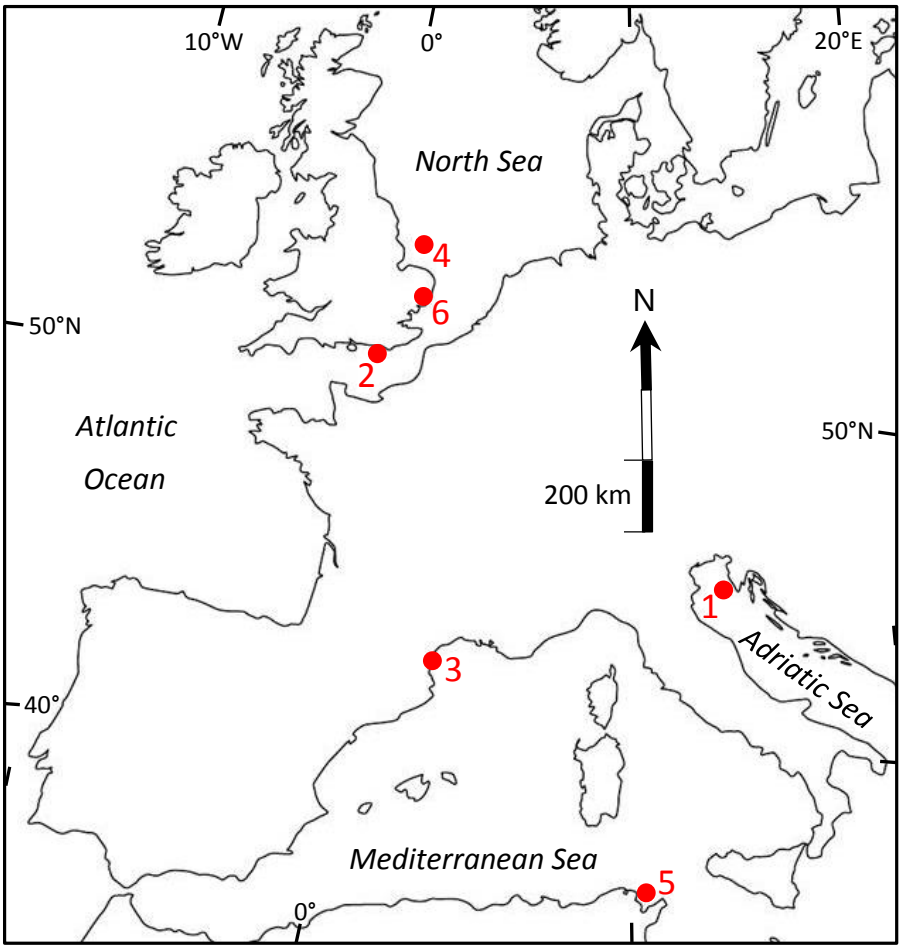

FIGURE 4 – single column

Figure 5

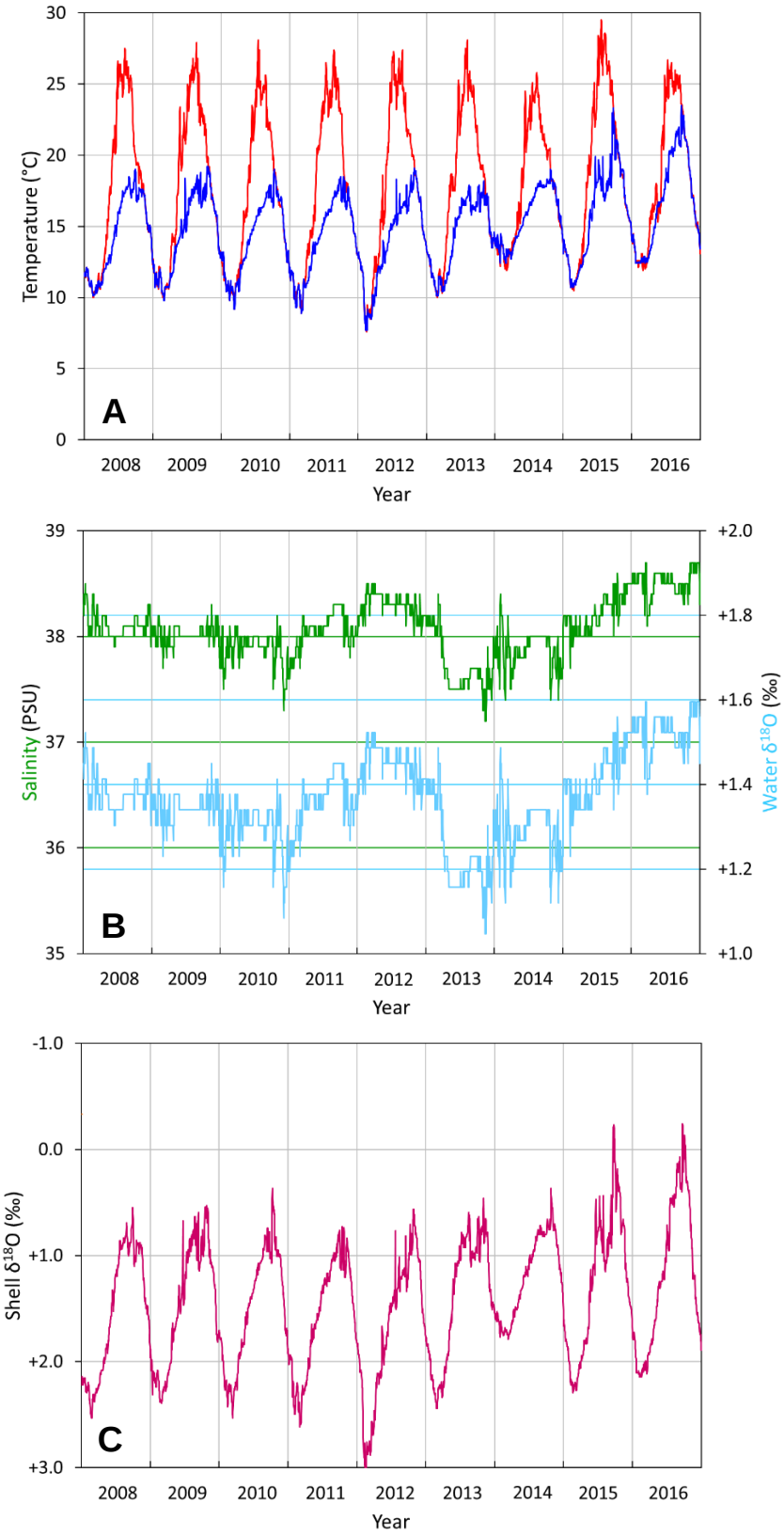

FIGURE 5 – single column

Figure 6

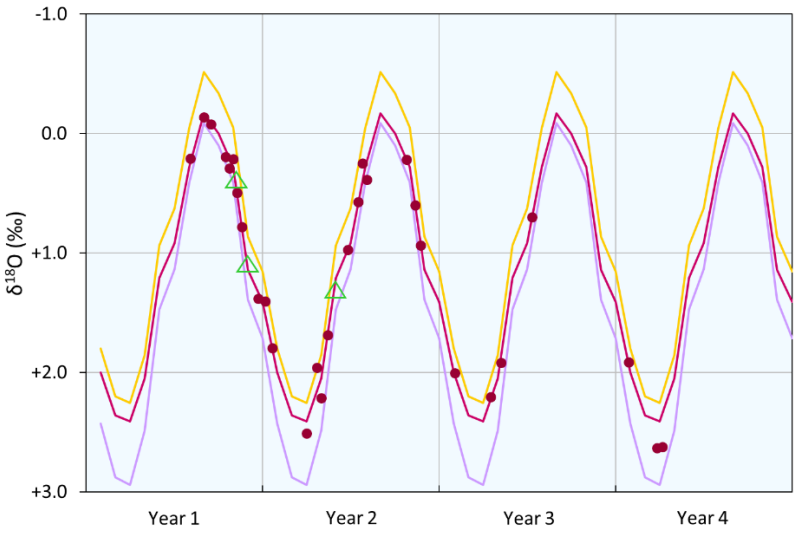

FIGURE 6 – single column

Figure 7

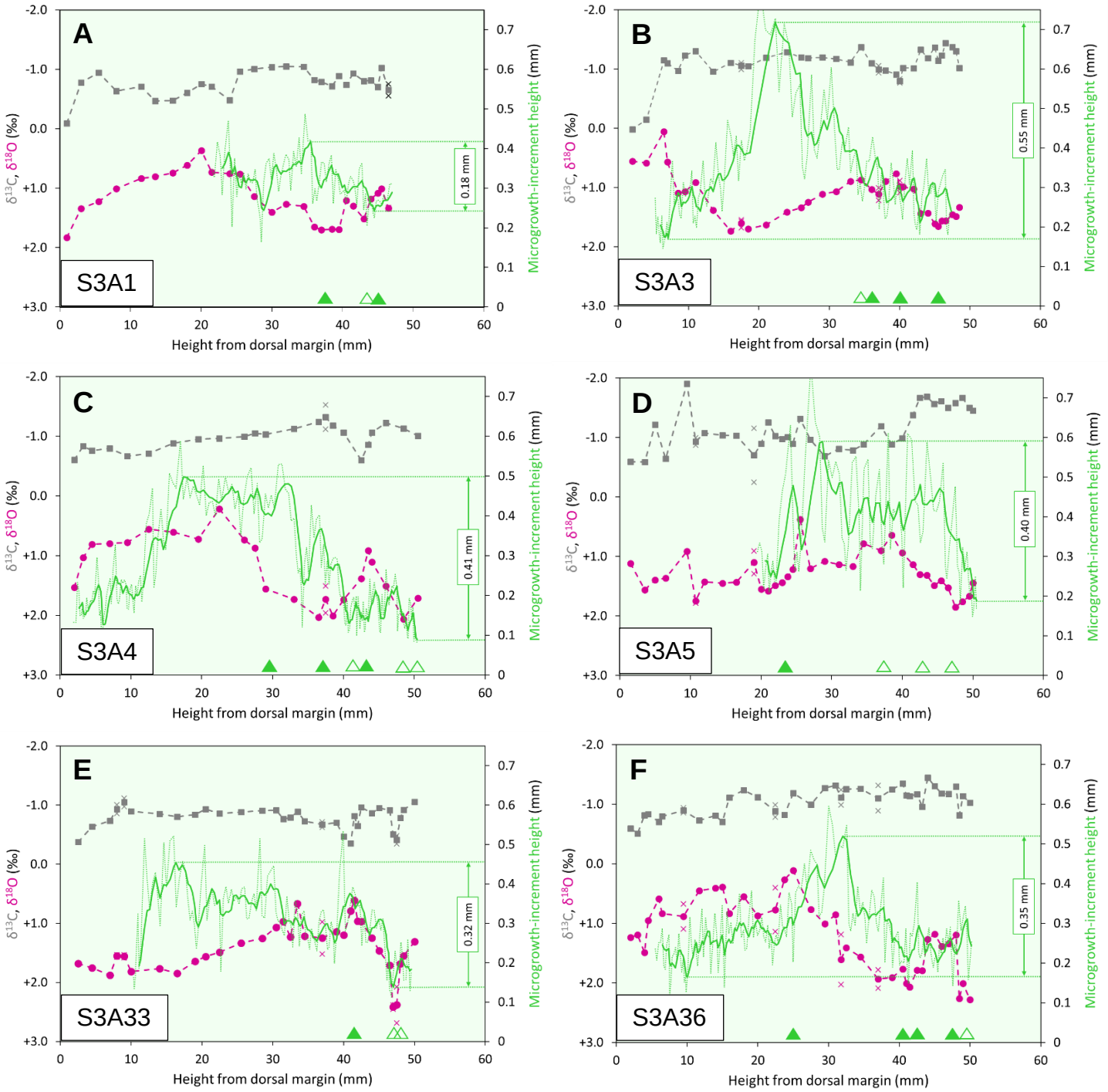

FIGURE 7 – double column

Figure 8

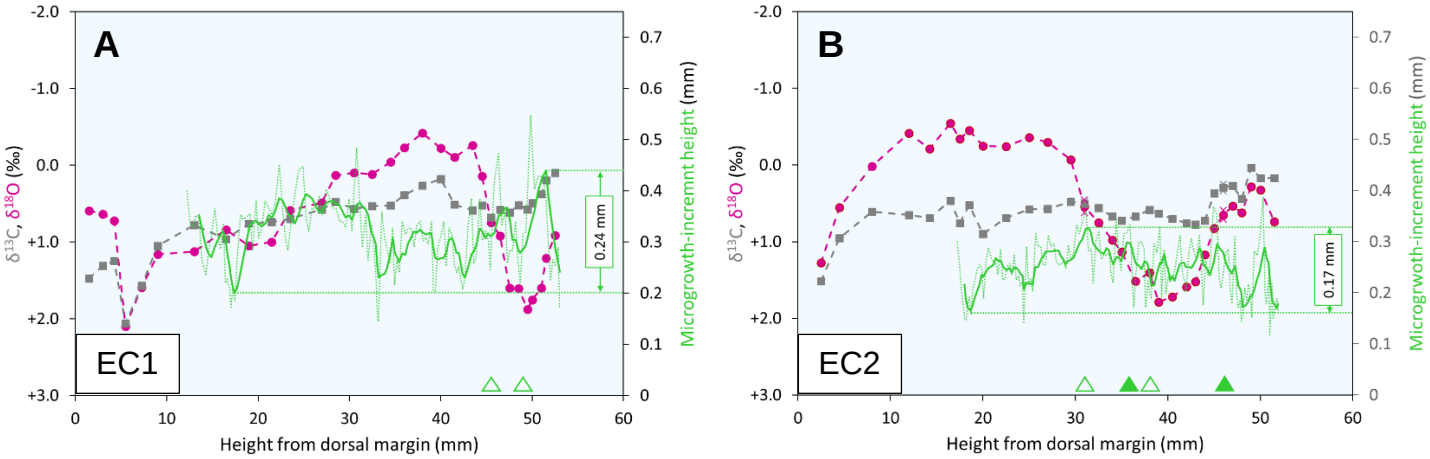

FIGURE 8 – double column

Figure 9

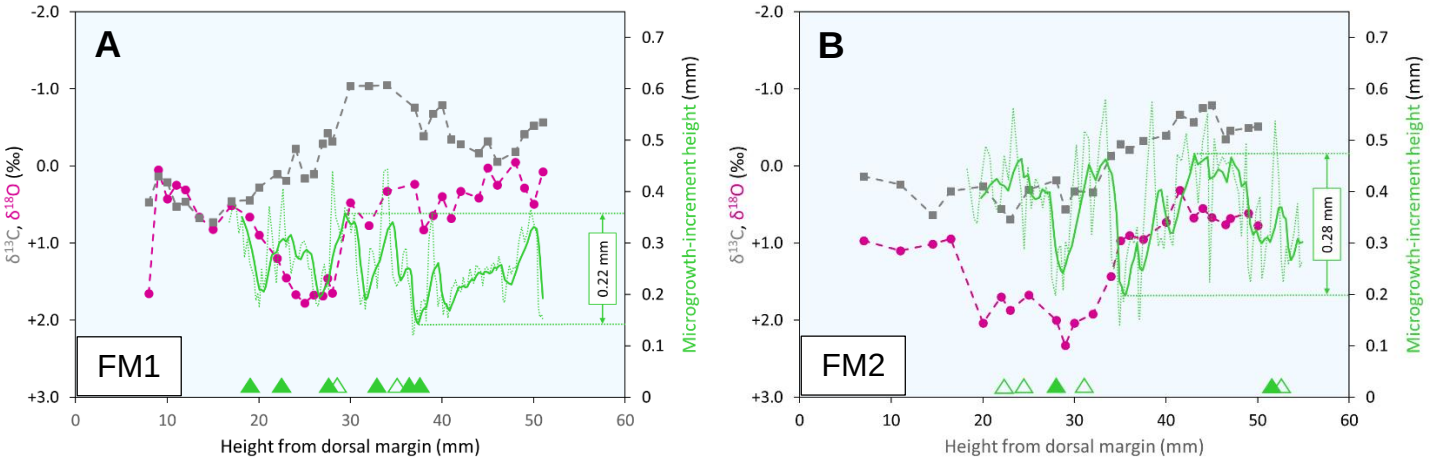

FIGURE 9 – double column

Figure 10

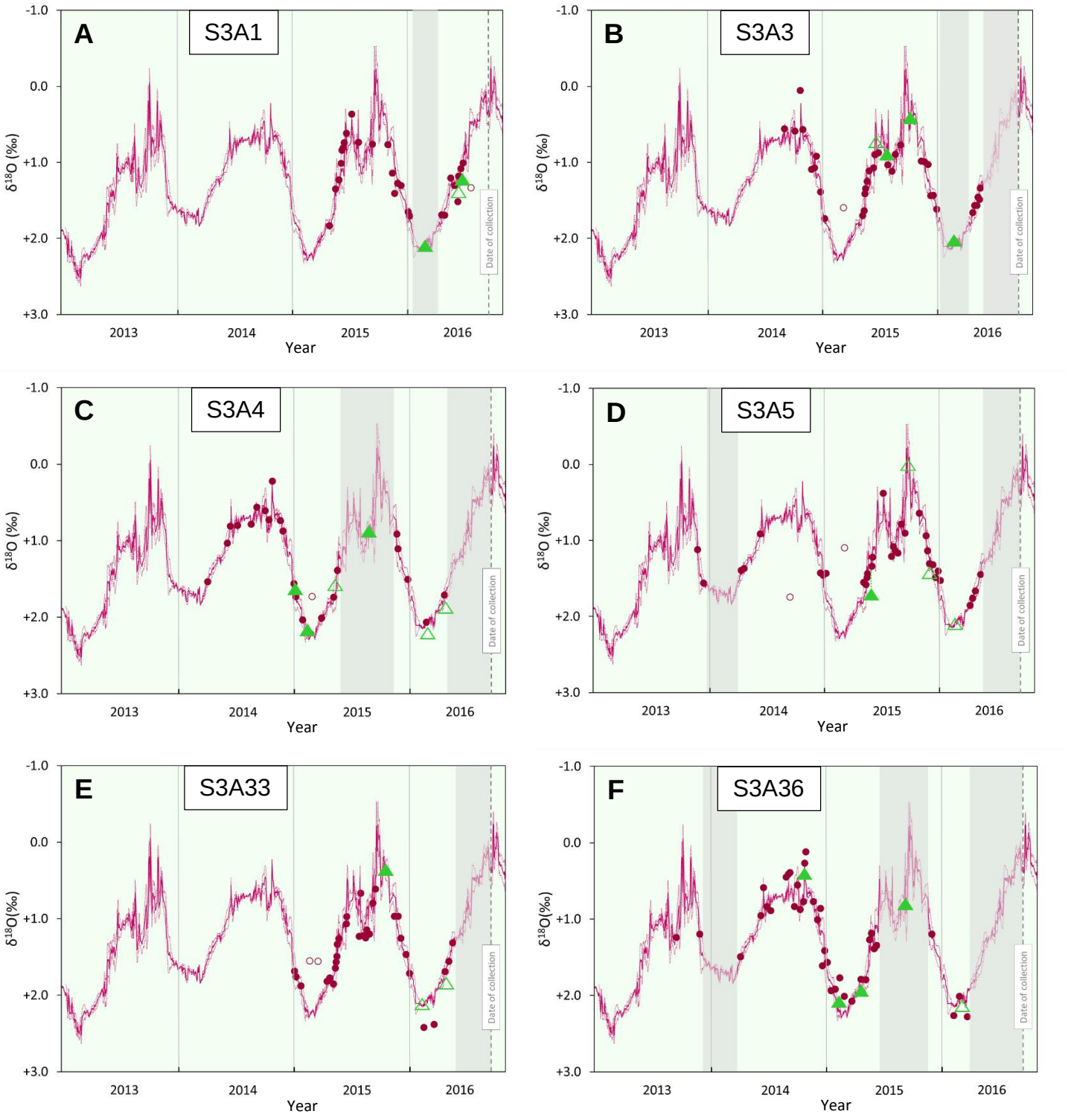

FIGURE 10 – double column

Figure 11

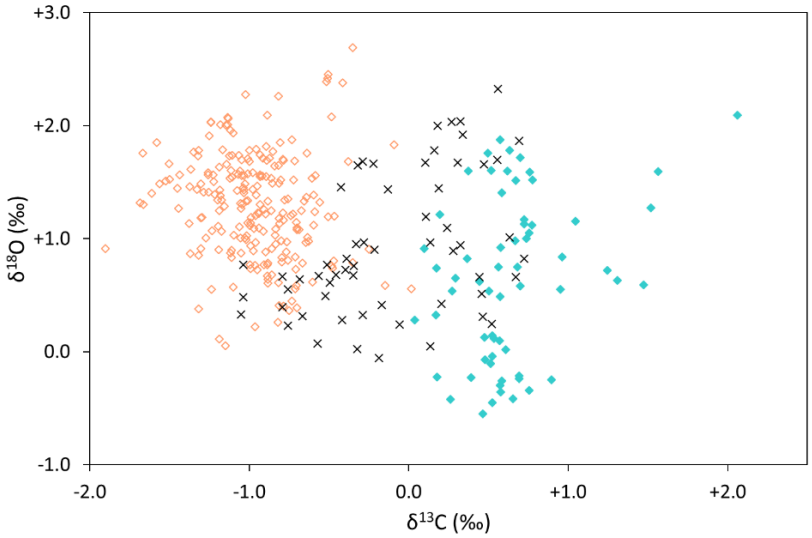

FIGURE 11 – single column

Click here to access/download
Table
Table 1 - Johnson et al..docx

Click here to access/download
Table
Table 2 - Johnson et al..docx

Click here to access/download
Table
Table 3 - Johnson et al..docx

Declaration of competing interest

The authors declare no conflict of interest.

Click here to access/download
Supplementary Material
Supplementary data - Johnson et al..xlsx